

**Performance evaluation of vegetable oil based hybrid nano
cutting fluids in turning of AISI 1040 steel**

*Submitted in partial fulfilment of the requirements
for the award of degree of*

**DOCTOR OF PHILOSOPHY
in
Mechanical Engineering**

by
SRINU GUGULOTHU

(Roll. No. 714125)

under the supervision of

Dr. P. Vamsi Krishna
Associate Professor
Department of Mechanical Engineering



**DEPARTMENT OF MECHANICAL ENGINEERING
NATIONAL INSTITUTE OF TECHNOLOGY
WARANGAL- 506 004, TELANGANA, INDIA.
DECEMBER-2019**



NATIONAL INSTITUTE OF TECHNOLOGY, WARANGAL – 506004

Mechanical Engineering Department

Approval Sheet

This Thesis entitled "**Performance evaluation of vegetable oil based hybrid nano cutting fluids in turning of AISI 1040 steel**" by **Mr. Srinu Gugulothu (Reg. No. 714125)** is approved for the degree of Doctor of Philosophy.

Examiner

Prof. Govind Sharan Dangayach

Supervisor

Dr. P. VAMSI KRISHNA

Chairman

Prof. N. SELVARAJ

Date: 30th December 2019



NATIONAL INSTITUTE OF TECHNOLOGY

WARANGAL – 506 004, Telangana State, INDIA

CERTIFICATE

This is to certify that the work presented in the thesis entitled "**Performance evaluation of vegetable oil based hybrid nano cutting fluids in turning of AISI 1040 steel**" which is being submitted by **Mr. Srinu Gugulothu (Roll No. 714125)**, is a bonafide work submitted to National Institute of Technology, Warangal in partial fulfillment of the requirement for the award of the degree of **Doctor of Philosophy in Mechanical Engineering**.

To the best of our knowledge, the work incorporated in the thesis has not been submitted to any other university or institute for the award of any other degree or diploma.

Dr. P. Vamsi Krishna
Supervisor
Associate Professor
Department of Mechanical Engineering
National Institute of Technology
Warangal-506 004, Telangana, India.

Prof. N. Selvaraj
Chairman-DSC
Head of the Department
Department of Mechanical Engineering
National Institute of Technology
Warangal-506 004, Telangana, India.



NATIONAL INSTITUTE OF TECHNOLOGY WARANGAL – 506 004, Telangana State, INDIA

Declaration

This is to certify that the work presented in the thesis entitled "**Performance evaluation of Vegetable oil based hybrid nano cutting fluids in turning of AISI 1040 steel**" is a bonafide work done by me under the supervision of **Dr. P. Vamsi Krishna**, Associate Professor, Department of Mechanical Engineering, NIT Warangal, India and was not submitted elsewhere for the award of any degree.

I declare that this written submission represents my ideas in my own words and where others' ideas or words have been included, i have adequately cited and referenced the original sources. I also declare that i have not misrepresented or fabricated or falsified any idea / data / fact / source in my submission. I understand that any violation of the above will be a cause for disciplinary action by the Institute and can also evoke penal action from the sources which have thus not been properly cited or from whom proper permission has not been taken when needed.

.....
(Signature)

.....
(Name of the student)

.....
(Roll No.)

Date:

Dedicated
To
My parents
My beloved wife Swapna
My Sweet Kids (Sai praneeth & Pratheekha)
&
All my teachers

ACKNOWLEDGEMENT

I would like to express my special appreciation and thanks to my supervisor **Dr. P. Vamsi Krishna**, Associate Professor, Department of Mechanical Engineering, NIT Warangal for suggesting the topic of my thesis and their ready and able guidance throughout the course of my work.

I express my sincere thanks to Director NIT Warangal **Prof. N. V. Ramana Rao** for providing all academic and administrative help during the course of my work.

I like to extend my sincere thanks to **Prof. N. Selvaraj**, Head of the Mechanical Engineering Department and to the members of DSC, **Prof. A. Venu Gopal**, Department of Mechanical Engineering, **Dr. P.V. Suresh**, Associate Professor, Department of Chemical Engineering, and **Dr. D. Jaya Krishna**, Associate Professor, Department of Mechanical Engineering, for all the support bestowed on me by suggesting and verifying the research work.

My sincere thanks also go to **Prof. C.S.P Rao**, **Prof. S. Srinivasa Rao** and **Prof. P. Bangaru Babu** former HoDs, Department of Mechanical Engineering, National Institute of Technology, Warangal, for their encouragement, for providing access to the laboratory and research facilities. Without their precious support it would not be possible to conduct this research.

I am thankful to all the faculty members of the Department of Mechanical Engineering and to all my well-wishers for their inspiration and help.

Non-teaching staff of Department of Mechanical Engineering have been instrumental in making arrangements during DSC meetings, and their help is acknowledged. Finally, I am extremely thankful to my friends and well-wishers who helped me directly and indirectly during my entire course.

This work is also the outcome of the blessing guidance and support of my father **Mr. Harilal Gugulothu**, my mother **Mrs. Hasili Gugulothu**. This work could have been a distant dream if I did not get the moral encouragement and help from my wife **Mrs. Swapna**.

(Srinu Gugulothu)

ABSTRACT

The survival of present day industry is decided by its ability to produce high quality cost effective products in order to meet the challenges. However, several factors that contribute to the idle and down times associated with production processes have been hindrances in realizing this dream.

Machining is one of the widely used processes in manufacturing industries due to its ability to produce components to precision. Enormous amount of heat is generated in deformation zones of machining due to friction and rubbing of tool and workpiece, which affects the accuracy of machined surface, tool life and surface finish. In this context application of cutting fluids in machining play an important role through cooling and lubrication. Lubrication minimizes heat generation by reducing the friction between chip-tool and tool-workpiece interfaces and cooling action control the temperature at chip -tool interface by dissipating the heat.

Metal working fluids are the type of lubricants, which improves the product quality and production rate in machining sectors by lubricating and cooling action. With that fact in machining Industries, consumption of metal working fluids is rising day to day. The wide use of cutting fluids in machining is due to the reasons, which prevents corrosion of the machined surface, flushing away the chips from cutting area, cool the workpiece, chip tool interface, avoids the built-up edge formation on cutting tool, increase the tool life and improve the surface integrity. But they do create several adverse effects such as environmental pollution, dermatitis to workers in machining industries etc. Alternatives to these cutting fluids are being searched for manufacturing industries by several investigators. In the present work, an attempt is made to assess the performance of vegetable oil based hybrid nano fluids as cutting fluids in turning of AISI 1040 steel.

In the present work, nanoparticles used are multi walled carbon nanotube (MWCNT) of 30 nm outer diameters, boric acid (BA) of 80 nm and molybdenum disulphide (MoS₂) of 30 nm respectively. Sesame oil, neem oil and mahua oils are used as base oil in preparation of vegetable oil based hybrid nano cutting fluids. Triton x100, Tween80 and SDS surfactants are used for dispersion of nanoparticles in vegetable oils. Different / various combinations of hybrid nano cutting fluids are prepared according to Taguchi's L₉ orthogonal array. The

nanoparticles combinations of CNT/BA and CNT/MoS₂ at 1 % weight in hybrid ratio (1:1; 1:2; 2:1) along with surfactant are dispersed in the above mentioned three oils. Stability test is performed for the prepared samples of CNT/BA and CNT/MoS₂ hybrid nano cutting fluid by using sedimentation method and zeta potential test. Machining experiments are conducted at constant cutting conditions during turning of AISI 1040 steel under MQL mode of CNT/MoS₂ hybrid nanofluid. Optimal factors for stable hybrid nano cutting fluids are found to be sesame oil, 15% content SDS surfactant and 1:2 hybrid ratio. Machining performance is improved with CNT/MoS₂ hybrid nano cutting fluid under MQL mode in terms of reduction in main cutting force, temperature, surface roughness and tool flank wear compared to dry and conventional cutting fluid respectively.

In the second stage, CNT/MoS₂ (1:2) hybrid nano cutting fluids are prepared by varying concentration of nanoparticle inclusion in sesame oil (i.e. 0.5%, 1%, 1.5%, 2%, 2.5% and 3%) by weight. Thus fluids are subjected to measurement of basic properties such as thermal conductivity, specific heat and dynamic viscosity to assess their performance in machining. Machining experiments are conducted in turning of AISI 1040 steel at constant cutting conditions by varying concentration of hybrid nano cutting fluids and machining performance are compared with dry and conventional cutting fluid. Coefficient of friction test was also performed for the same nanofluids by using Pin on disc apparatus. It is found that the thermal conductivity and dynamic viscosity are increased with increase in particle concentration. Dynamic viscosity is found to decrease with increase in temperature.

From the machining results, concentration 2wt% of CNT/MoS₂ hybrid nano cutting fluid has shown better performance in reducing forces, temperature, surface roughness and tool flank wear than that of dry and conventional cutting fluid. Subsequently, comparative assessment of machining performance is made in terms of main cutting force, cutting temperature, surface roughness and tool flank wear in turning of AISI 1040 steel using the concentration 2 wt% of vegetable oil based pure CNT, pure MoS₂ nanofluids and CNT/MoS₂ hybrid nano cutting fluid at constant cutting conditions. The significant reduction in main cutting force is observed to be 22% and 17.3%, cutting temperature is observed to be 8% and 12.5%, surface roughness is observed to be 13% and 9% and tool flank wear is observed to be 63% and 68% with use of 2 wt% of hybrid nano cutting fluid than that of pure CNT and Pure MoS₂ nanofluids.

Finally, turning experiments are conducted by varying cutting conditions in turning of AISI 1040 steel with use of only 2wt% of CNT/MoS₂ (1:2) hybrid nanofluid under MQL condition. Experiments are designed using response surface methodology by taking three factors at each 3 levels and analysis of variance (ANOVA) is performed to study the significant effect of each individual factor on machining responses. Optimization is performed for multiple responses by using desirability function which converts multi objective into single objective and optimal setting parameters for single objective is found. Cutting force F_z is found to increase with increase in cutting speed, feed and depth of cut and then slightly decrease with cutting speed of 100 m/min. Cutting temperature and tool flank wear are observed to increase with increase in cutting speed, feed and depth of cut. Surface roughness value is found to decrease with increase in cutting speed and it increased with increase in feed and depth of cut. Desirability approach confirms that single combination of optimal setting parameters for cutting force, cutting temperature, surface roughness and tool flank wear is 70.25 m/min, 0.13 mm/rev and 0.5 mm at desirability value of 0.907.

List of contents

<i>Acknowledgement</i>	i
<i>Abstract</i>	ii
<i>Table of Figures</i>	ix
<i>List of Tables</i>	xii
<i>List of Abbreviations</i>	xiii
<i>List of English alphabets and Greek symbols</i>	xv
Chapter - 1. Introduction	1-18
1.1 Machining processes	1
1.2 Cutting forces	2
1.3 Cutting temperature	3
1.4 Surface roughness (Ra)	4
1.5 Tool wear	5
1.5.1 Tool wear mechanisms	5
1.5.2 Forms of Tool wear	6
1.6 Cutting fluids	7
1.7 Alternatives to Conventional Cutting fluids	8
1.7.1 Dry Machining	8
1.7.2 Cryogenic coolant	9
1.7.3 Minimum Quantity Lubrication	9
1.7.4 Solid Lubricants	10
1.7.5 Vegetable oils	14
1.7.6 Nanofluids	16
1.7.7 Hybrid nanofluids	17
1.8 Organization of the thesis	18
Chapter - 2 Literature review	19-33
2.1 Introduction	19
2.2 Cutting fluids	19
2.3 Alternatives to Conventional Cutting fluids	20
2.3.1 Dry machining and machining with coated tools	20
2.3.2 Cryogenic coolant	21
2.3.3 Minimum Quantity Lubrication	21
2.3.4 Solid Lubricants	23

2.3.5 Vegetable oils	24
2.3.6 Nanofluids	25
2.3.7 Hybrid nanofluids	28
2.4 Optimization	30
2.5 Present work	31
2.6 Summary	33
Chapter-3. Experimental setup and Experimentation	34-51
3.1 Introduction	34
3.2 Nanoparticles	34
3.3 Formulation of hybrid nano cutting fluids	36
3.4 Evaluation of hybrid nano cutting fluids composition for stability	38
3.4.1 Sedimentation test	38
3.4.2 Zeta potential test	38
3.5 Evaluation of basic properties	38
3.5.1 Density	39
3.5.2 Dynamic viscosity	39
3.5.3 Kinematic viscosity	40
3.5.4 Thermal conductivity	41
3.5.5 Volumetric heat capacity	41
3.6 Coefficient of friction	42
3.7 Machining experimental setup	43
3.7.1 Machine Tool	43
3.7.2 Workpiece material	44
3.7.3 Tool holder and Cutting tool inserts	45
3.7.4 Lubricant environment and cutting conditions	46
3.7.5 Supply of hybrid nano cutting fluids in MQL	46
3.8 Measurement of machining performance	47
3.8.1 Cutting forces	47
3.8.2 Cutting temperature	48
3.8.3 Surface roughness (R_a)	49
3.8.4 Tool flank wear	49
3.9 Summary	51

Chapter-4. Formulation of hybrid nano cutting fluids with optimum composition for stability (base oil, surfactant, hybrid ratio and content of surfactant)	52-73
4.1 Introduction	52
4.2 Selection of vegetable oils	52
4.3 Experimental design	54
4.4 Basic properties	55
4.5 Stability of hybrid nano cutting fluid	57
4.6 Selection of cutting fluids	63
4.7 Machining performance	63
4.7.1 Cutting force (F_z)	64
4.7.2 Cutting temperature	66
4.7.3 Surface Roughness (R_a)	69
4.7.4 Tool flank wear	70
4.8 Summary	73
Chapter- 5. Evaluation of basic properties and machining performance of hybrid nano cutting fluids in varying concentration of nanoparticle for machining	74-90
5.1 Introduction	74
5.2 Sedimentation test results	74
5.3 Basic properties of CNT/MoS ₂ hybrid nanofluid	75
5.3.1 Dynamic viscosity	75
5.3.2 Thermal conductivity	76
5.3.3 Volumetric heat capacity	77
5.4 Coefficient of friction	78
5.5 Machining performance	80
5.5.1 Cutting forces	80
5.5.2 Cutting temperature	82
5.5.3 Surface Roughness (R_a)	83
5.5.4 Tool flank wear	85
5.6 Comparing machining performance of HNCF with nanofluids at (2 wt %.)	86
5.6.1 Main Cutting force (F_z)	86

5.6.2 Cutting temperature	87
5.6.3 Surface Roughness (R_a)	88
5.6.4 Tool flank wear	88
5.7 Summary	89
Chapter- 6. Evaluation of optimal machining parameters using hybrid nano cutting fluids for better performance in turning	91-106
6.1 Introduction	91
6.2 Design of experiments	91
6.3 Optimization using desirability approach	92
6.4 Machining performance with variable cutting conditions	93
6.4.1 Effect of cutting parameters on main cutting force (F_z)	94
6.4.2 Effect of cutting parameters on cutting temperature ($T^{\circ}C$)	96
6.4.3 Effect of cutting parameters on surface roughness (R_a)	97
6.4.4 Effect of cutting parameters on tool flank wear (V_b)	99
6.5 Optimization using desirability function	101
6.6 Machining performance obtained with optimal cutting parameters	103
6.6.1 Main Cutting force (F_z)	103
6.6.2 Cutting temperature	104
6.6.3 Surface Roughness (R_a)	104
6.6.4 Tool flank wear	105
6.7 Summary	106
Chapter-7.Conclusion	107-121
7.1 Conclusions	107
7.2 Future scope	109
References	110
Publications from the present work	121

List of figures

Fig. No.	Description of Figure	Page No.
1.1	Sources of heat generation during turning	2
1.2	Cutting forces in turning	3
1.3	Pictorial view of crater wear and tool flank wear on single point cutting tool	7
1.4	Crystal structure of graphite	11
1.5	Structure of Hexagonal boron nitride	12
1.6	Structure of Molybdenum di sulphide	12
1.7	Structure of Boric acid	13
1.8	Structure of carbon nanotube	14
1.9	Chemical structure of glycerides of a vegetable oil	15
3.1	X-Ray Diffraction machine	35
3.2	Crystal structure of the boric acid nanoparticle	35
3.3	SEM image of CNT	36
3.4	TEM image of MoS ₂	36
3.5	Ultrosonicator	37
3.6	Nano partica SZ100 series nanoparticle analyzer	38
3.7	Hydrometer	39
3.8	Rheometer	40
3.9	Redwood viscometer-I	40
3.10	Hot disc thermal conductivity analyzer	41
3.11	Pin on disc Tribometer	42
3.12	Machining experimental setup	44
3.13	AISI1040 steel workpiece material	44
3.14	Tool holder and tool insert	45
3.15	Minimum Quantity Lubrication system	47
3.16	Multi components dynamometer	47
3.17	Setup for temperature measurement	48
3.18	Surface roughness tester	49
3.19	Tool maker's microscope	50
3.20	Schematic representation of experimentation	50

Fig. No.	Description of Figure	Page No.
4.1	Structure of vegetable oil	54
4.2	Schematic representation of sedimentation of nanofluid over time	59
4.3	Main effect plot for zeta potential values of CNT/MoS ₂ hybrid nano cutting fluid	62
4.4	(a) Zeta potential report of CNT/MoS ₂ hybrid nano cutting fluid (b) Sedimentation of confirmation sample after 156 hours of sedimentation time	63
4.5	Variation of Main cutting force in dry, conventional and hybrid nano cutting fluid	65
4.6	Structures of various types of fatty acids	65
4.7	Mechanism of MoS ₂	66
4.8	Variation of cutting temperature in dry, conventional and hybrid nano cutting fluid	68
4.9	(a) Synergistic effect of CNT/ MoS ₂ hybrid nanoparticles (b) Rolling effect of MoS ₂	68
4.10	Physical encapsulation of CNT and MoS ₂ nanoparticle	69
4.11	Variation of surface roughness in dry, conventional and hybrid nano cutting fluid	70
4.12	Variation of tool flank wears in dry, conventional and hybrid nano cutting fluid.	71
4.13	Synergistic effect of CNT and MoS ₂ and ball bearing effect of MoS ₂ nanoparticles	72
4.14	MQL nanomechanism	72
5.1	Sedimentation test results after 72 hours	75
5.2	Viscosity of nanofluids with respect to temperature	76
5.3	Thermal conductivity versus temperature	77
5.4	Volumetric heat capacity of CNT/MoS ₂ hybrid nano cutting fluids with variation in temperature	78
5.5	Coefficient of friction with respect to nanoparticles concentration	79

Fig. No.	Description of Figure	Page No.
5.6	Thin Tribo film between sliding surfaces	80
5.7	Variation of cutting forces in different lubrication environment	82
5.8	Variation of cutting temperature in different lubrication environment	83
5.9	Variation of surface roughness in different lubrication environment	84
5.10	Variation of tool flank wear in different lubrication environment	85
5.11	Variation of main cutting force with different lubrication environment	86
5.12	Variation of cutting temperature with different lubrication environment	87
5.13	Variation of surface roughness (R_a) with different lubrication environment	88
5.14	Variation of tool flank wear with different lubrication environment	89
6.1	Esteemed response surface plot for main cutting force (F_z)	94
6.2	Esteemed response surface plot for cutting temperature ($T^{\circ}C$)	96
6.3	Esteemed response surface plot for surface roughness (R_a)	98
6.4	Esteemed response surface plot for tool flank wear	100
6.5	Ramp function graph of desirability	102
6.6	Variation of main cutting force with different lubrication environment	103
6.7	Variation of cutting temperature with different lubrication environment	104
6.8	Variation of surface roughness (R_a) with different lubrication environment	105
6.9	Variation of tool flank wear with different lubrication environment	105

List of Tables

Table No.	Description of Table	Page No.
3.1	Composition of AISI 1040 steel	44
3.2	Cutting conditions and lubrication environment	46
4.1	Composition and structure of vegetable oil	53
4.2	Factors and levels	55
4.3	Kinematic viscosity and density of CNT/BA hybrid nanofluid	56
4.4	Kinematic viscosity and density of CNT/MoS ₂ hybrid nano cutting fluid	56
4.5	Results of sedimentation test for CNT/BA hybrid nano cutting fluid (156 hr)	59
4.6	Zeta potential values of CNT/BA hybrid nano cutting fluid	60
4.7	Results of sedimentation test for CNT/BA hybrid nano cutting fluid (156 hr)	60
4.8	Zeta potential values of CNT/MoS ₂ hybrid nano cutting fluid	61
4.9	Analysis of mean for S/N ratios for Zeta potential value of CNT/MoS ₂ hybrid nano cutting fluid	61
4.10	ANOVA for Zeta potential values (S/N data) of CNT/MoS ₂ hybrid nano cutting fluid	62
6.1	Factors and levels chosen	92
6.2	Machining input cutting conditions and four response parameters	93
6.3	ANOVA for main cutting force (F _z)	95
6.4	ANOVA table for cutting temperature (T° C)	97
6.5	ANOVA table for surface roughness (R _a)	99
6.6	ANOVA table for tool flank wear (V _b)	101
6.7	Optimized and experimental values	102

List of Abbreviations

S No.	Abbreviation	Description
1	AISI	American Iron and Steel Institute
2	ANOM	Analysis of mean
3	ANOVA	Analysis of variance
4	ASTM	American Society for Testing and Materials
5	BA	Boric acid
6	BO	Base oil
7	BUE	Built up edge
8	CaF ₂	Calcium fluoride
9	CAPB	Cocamidopropylbetaine
10	CBN	Cubic boron nitride
11	CCF	Conventional cutting fluid
12	CFRPs	carbon fiber-reinforced plastics
13	CMC	carboxymethyl cellulose
14	CNF	Carbon nano fiber
15	CNT	Carbon nanotube
16	Con. Of SF	Concentration of surfactant
17	Cu	Copper
18	DF	Degrees of Freedom
19	DWCNT	double wall carbon nanotube
20	EP	Extreme pressure
21	HBN	Hexagonal boron nitride
22	HNCF	Hybrid nano cutting fluid
23	HNF	Hybrid nanofluid
24	Hp	Horse power
25	HRC	Rockwell Hardness scale
26	LCFA	Long chain fatty acid
27	MCFA	Medium chain fatty acid
28	mL	Milli litre

S No.	Abbreviation	Description.
30	MoS ₂	Molybdenum Di Sulphide
31	MQL	Minimum quantity lubrication
32	MS	Mean square
33	Mv	Milli volt
34	MWCNT	Multi walled Carbon nanotube
35	NCF	Nano cutting fluid
36	NF	Nanofluid
37	Nm	Nanometer
38	Np	Nanoparticle
39	Npi	Nanoparticle inclusion
40	OA	Orthogonal array
41	OD	Overall desirability
42	PVD	Physical vapor deposition
43	RPM	Revolution per minute
44	RSM	Response surface methodology
45	SAE	Society of Automotive Engineers
46	SDS	Sodium dodecyl sulfate
47	SF	Surfactant
48	SFA	Saturated fatty acid
49	SiC	Silicon carbide
50	S/N	Signal to noise
51	SS	Sesame
52	SWCNT	single wall carbon nanotube
53	USFA	Unsaturated fatty acid
54	VOBHNCF	Vegetable oil based hybrid nano cutting fluid
55	VOBNCF	Vegetable oil based nano cutting fluid
56	WS ₂	Tungsten di sulfide
57	Wt	Weight
58	xGnp	Graphene Nanoplatelets
59	XRD	X-Ray Diffraction
60	Zn	Zink

List of English alphabets and Greek symbols

English Alphabets

Symbol	Description of Symbol
A	Ampere
C	Centigrade
D	Length of specimen
d	Depth of cut (mm)
D(x)	Desirability function
f	Feed rate (mm/rev)
F	Cutting force (N)
F _x	Axial force (N)
F _y	Radial force/ feed force (N)
F _z	Main cutting force/ tangential force (N)
H	Height of specimen
K	Kelvin
L	Litre
L ₉	Length of the orthogonal array
m	Meter
M _x	Moment about X axis (N. m)
M _y	Moment about Y axis (N. m)
M _z	Moment about Z axis (N. m)
N	Newton
n	Number of replications
R _a	Surface roughness (micrometers)
s	Second
t	Time required to collect the sample (seconds)
T	Cutting temperature (° C)
V	Cutting speed (m/min)
V _b	Tool flank wear (micrometers)
W	Width of specimen
y	Response parameter

Greek Symbols

Symbol	:	Description
ϕ	:	Diameter of workpiece
η	:	Signal to noise ratio
ρ	:	Density in gram/ cubic centimeter
κ	:	No. of response parameters
$\%$:	Percentage
μ	:	Microns
wt. %	:	Weight percentage
$^{\circ}\text{C}$:	Degree centigrade

Chapter-1

1. Introduction

In the present scenario of severe competition, the sustainability of any industry depends on its ability to produce high quality products at economical rates. However, the idle time and overhead associated with the production process prevent to achieve this goal.

Machining is a key manufacturing process, often suffers due to frequent interruptions during tool change as cutting tools wear prolonging the production time, thus hike the cost of product. Further excessive wear of the cutting tool results in poor surface finish and dimensional inaccuracy, consequently reducing product quality. Cutting parameters, lubrication environment, material of workpiece and cutting tool affects the surface finish and dimensional accuracy of the machined component.

1.1. Machining processes

Machining can be defined as the process of removing unwanted material from parent material of workpiece in the form of chips by employing diverse metal removal tool for diverse machining process to get desired shape, size and finishing of end product. Some of the traditional machining processes are turning, milling, grinding, broaching, drilling, shaping, planning, honing and lapping etc. Mostly machining has least set-up cost compared to forming, moulding, and casting processes. Though, machining is much more expensive for high volumes, still it is very essential for tight tolerances on dimensions and finishing. Qualities of a workpiece material for machining would be lower shear strength, shock resistant, material must not have a tendency to stick to the tool and with ease of material removal from the workpiece.

Turning operation is one of the manufacturing processes to produce the high quality of cylindrical workpiece with single point cutting tool. Single point cutting tool play a key role in metal cutting operation by removing unwanted material from the workpiece in the form of chips. During turning operation 80 to 85 % of heat is generated in primary deformation zone, 15 to 20 % in secondary deformation zone and 1 to 3 % of heat is generated in tertiary deformation zone due to shearing and friction in chip-tool interface. The sources of heat generation during turning operation are shown in Fig. 1.1. The enormous amount of heat in

machining affects the accuracy of machined surface, tool life and surface finish [1]. Hence, the main purpose of the machining is to produce a component with good surface finish and dimensional accuracy. In this context, types of cutting fluids and their application methods affects surface quality of machining through cooling and lubrication. Lubrication reduces the heat generation by reducing the friction between contacting surfaces and cooling action helps to reduce the temperature by dissipating the heat [2]. In order to judge the quality of the machining, cutting forces, cutting temperature, surface roughness and tool flank wear are examined in general.

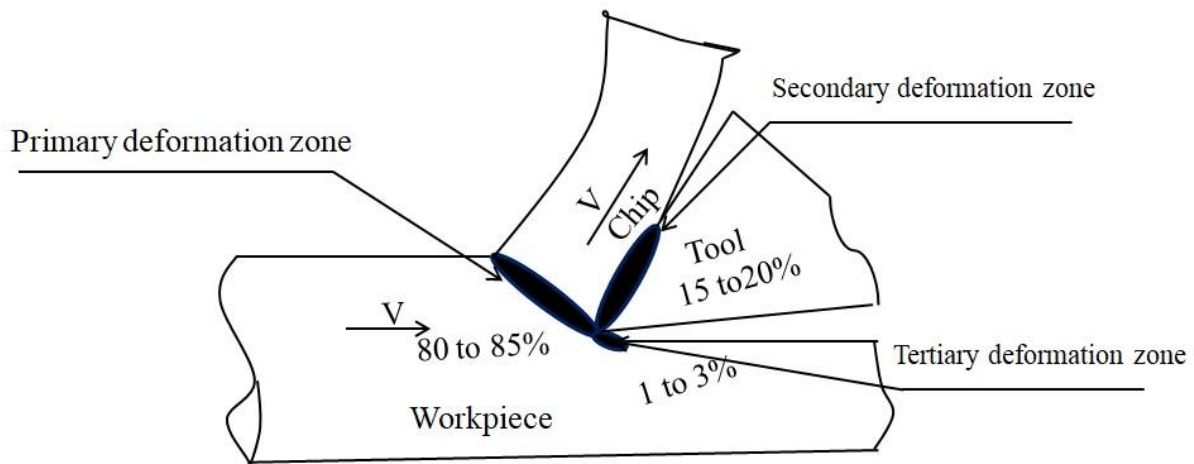


Fig. 1.1 Sources of heat generation during turning [3]

1.2 Cutting forces

During turning with a single point cutting tool, plastic deformation occurs and excessive stresses are induced on cutting zone. Because of high compressive and frictional stresses at the tool face, the cutting force 'F' acts in oblique direction. Hence the proper selection of workpiece, cutting tool, cutting conditions and fixtures to hold the work material and evaluation of power consumption during machining to be done. In cutting operation total force in contact zone is resolved into three components of axial force (F_x), Radial force (F_y) and main cutting force (F_z). The direction of components of forces are mutually perpendicular to each other which are shown in Fig. 1.2. F_z is also termed as tangential component of the force acting along the direction of primary motion. This contains 70% to 80% of total cutting force and used in calculating power consumption during machining operation. The Force F_x acts along the tool traverse direction and which is least significant for power consumption.

The component of force F_y acts along the tool shank direction and does not contribute for power consumption.

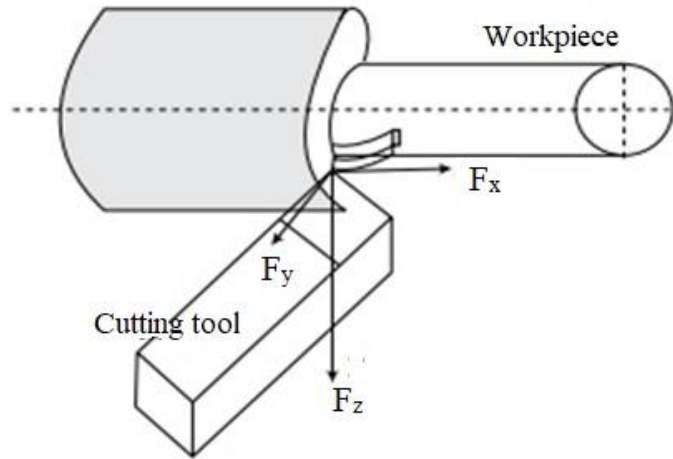


Fig. 1.2 Cutting forces in turning [4]

1.3 Cutting temperature

A source of heat generation in machining causes for development of temperature in cutting zone is shown in Fig 1.1.

- Primary deformation zone - where maximum amount of energy is converted into heat due to shear.
- Secondary deformation zone-at a point of chip-tool interfaces due to friction.
- Tertiary deformation zone- where least amount of energy is converted into heat due to rubbing between tool and machined part.

Under normal cutting conditions, the largest portion of the work is done during the formation of the chip at the shear plane. Most of the heat resulting from this work remains in the chip and is carried away by it, while only small percentage is conducted into the workpiece. Work done at shear plane to form the chip does not make any significant contribution to the heating of the cutting tool.

At the chip-tool interface, the heat generation is normally attributed to friction between chip and tool. The tool rake face is continuously heated by the generating heat in this zone resulting in development of high temperature. The temperature at the chip-tool interface increases with cutting speed which sets the ultimate limit to cutting speed for any tool materials. The distribution of this chip-tool interface temperature is non uniform along the path of contact of the chip with tool face. This non uniform temperature distribution on rake face causes the initial crater wear at some distance from the cutting edge.

In the tool-workpiece interface, only a small amount of work converts into heat. However, as the flank wear increases, generating heat in contacting zone also increases. This results in a further increase in flank wear when worn surface is long enough, this region becomes a serious heat source which leads to the sudden failure of the tool. The detrimental effects of rise in cutting temperature on tool are tool wear which reduces tool life and built up edge formation on cutting tool. The possible detrimental effects of rise in cutting temperature on workpiece are dimensional inaccuracy and surface damage due to oxidation.

Cutting temperature is measured by using two ways such as analytical models and experimental techniques. Experimental techniques for measurement of cutting temperature in machining are contact type and non contact type. Contact type techniques include tool - work thermo couple method, colorimetric method and embedded thermocouple technique [5, 6]. Non contact type technique is use of infrared sensor in measuring the temperature.

1.4 Surface roughness (R_a)

The vertical deviation of the real surface from its ideal is called surface texture and measurement of these textures of surface is the surface roughness. High rough surface is obtained by high vertical deviations, whereas low vertical deviation gives smooth surface. Rough surface may wear out and gives highest coefficient of friction. The surface roughness (R_a) plays a major role on quality of the machined product. R_a is the arithmetic average of roughness values of absolute ordinates. It is also called as centerline average. Quality of the machined part is judged by measuring surface roughness (R_a) after machining operation. The factors which influence surface roughness are properties of work material, cutting tool variable, cutting parameters and type of lubrication.

Cutting tool variables such as tool material and tool geometry have a significant affect on surface quality. Different tool materials can have the different hardness, toughness and frictional effect. High hardness enables the tool to be used in high cutting speeds, high toughness of tool material may help to provision for the larger rake angles and relief angles without risk of cutting edge. Larger rake angle decreases the cutting forces, which decrease the waviness height on workpiece surface. Side and end cutting edge of the tool have the little effect on surface roughness.

Workpiece variables such as chemical composition, hardness and microstructure affect the surface roughness. Cutting conditions including cutting speed, feed rate and depth of cut

affects the surface roughness. At low cutting speeds, the cutting forces are high and tendency of workpiece material to form built up edge on tool rake face is greater. At high cutting speeds, tendency towards built up edge formation is less due to increase in temperature and decrease in frictional effects. Both the conditions favor the surface quality of the machined parts. Feed rate has large affect on surface roughness than depth of cut. Height of the peak and depth of valleys are proportional to square of the feed per revolution. Depth of cut changes the cutting force and deflection. Waviness height is increased with increase in dept of cut which causes for dimensional inaccuracy. Machine tool rigidity and accuracy can affect surface roughness.

Supply of lubricants in machining is the indirect way to improve surface roughness. By acting as lubricants and coolant, cutting fluids reduces the friction in chip-tool interface and tool wear thus improves surface quality of machined surface and tool life.

1.5 Tool wear

Tool wear is the loss of material from surfaces which occur in sliding contact with each other. The variation in original shape of tool and failure of tool attributed to phenomenon of tool wear. Quality of the machining is attained with sharpness of the tool. In order to maintain qualitative machined product, cutting tool require a re-sharpening after attaining certain degree of wear.

1.5.1. Tool wear mechanisms

The categories of tool wear mechanisms are adhesion wear, abrasion wear, diffusion wear and fatigue wear.

Adhesion wear: It occurs when chips are sticking on tool face in the form of microscopic fragments. Under high temperature and pressure at cutting edge, the chip-tool interface form metallic bond in the form of spot weld. This spot weld results in an irregular flow of chips over tool face and results in formation of built up edge. Sliding of chips over the built up edge causes fracture of the spot weld and small amount of material is carried by them. This phenomenon is called adhesion wear. This wear is reduced by use of cutting fluid.

Abrasion wear: This is the most common type of wear mechanisms. It occurs when the hard particles present on the chips which passes over tool face. Steel alloys contain compositions of hard particle such as oxides, nitrides and other non metallic inclusion. Having sharp edges

of hard particle inclusion on workpiece removes material on cutting tool due to abrasion action.

Diffusion wear: It occurs due to diffusion of atomic attraction between tool and work material, the atoms of tool material will get diffused and deposited over workpiece is called diffusion wear. This diffusion process weakens the surface structure of cutting tool and leads to tool failure.

Fatigue wear: It occurs when two surfaces are sliding one over the other with the application of higher pressure. It interlocks the roughness of one surface over the other while sliding due to friction and induces the cyclic loading thus resulting in surface crack. These tool wear mechanisms may cause of tool failure in terms of flank wear and crater wear.

1.5.2 Forms of Tool wear

Crater wear: It occurs on rake face of single point cutting tool in the form of pit is called crater wear. The crater is formed at some distance from the cutting edge. Crater wear occurs due to friction between chip-tool interface, abrasion action of microchips present on tool and diffusion of atoms between tool and workpiece.

Tool flank wear: The wear taking place on flank face of a single point cutting tool is called tool flank wear. This wear produces wear land on the side and end flanks of cutting tool due to rubbing. The pictorial view of crater wear and tool flank wear is shown in Fig. 1.3. Tool flank wear and crater wear are reduced by using cutting fluid.

Nose wear: It occurs out the corner of tool as a result of friction between nose and workpiece material being machined. It is the matting part of flank and face which is combination effect of crater wear and flank wear. It is considered as separate wear because the tool corners are very important for proper cutting of workpiece.

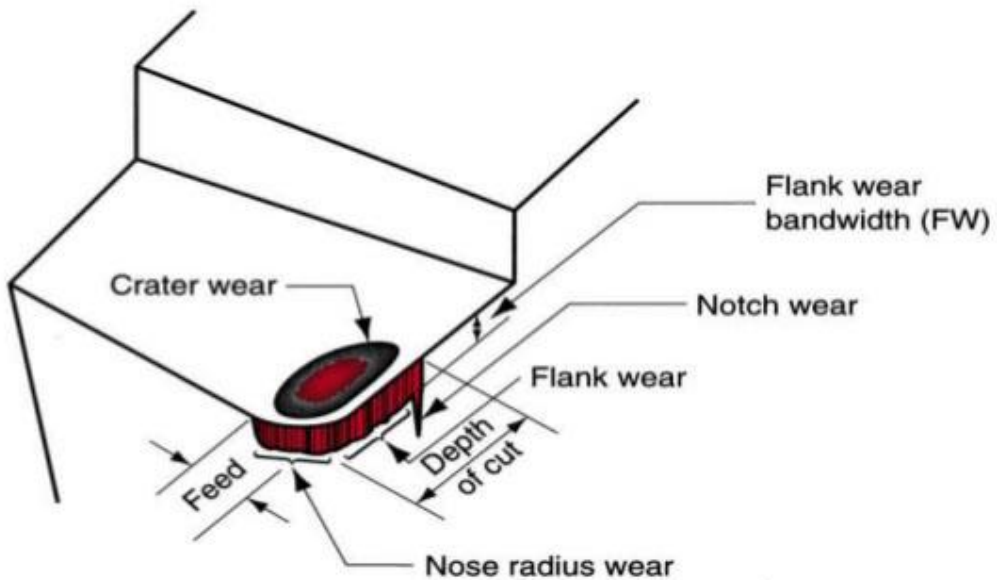


Fig.1.3 Pictorial view of crater wear and tool flank wear on single point cutting tool [7]

1.6 Cutting fluids

In order to obtain a machined product with desired dimensional accuracy and good surface finish, cutting fluids have been conventional choice for manufacturer in machining industry. These fluids are reducing the friction between contacting surfaces and removing heat in cutting zone by lubrication and cooling action. The wide use of cutting fluids in machining is due to the reasons which prevents corrosion on the machined surface, flushing away the chips from cutting area, cool the workpiece and improve the surface integrity, avoid the built-up edge formation on the cutting tool, increase the tool life and improve the surface finish.

Cutting fluids include straight cutting oils, synthetic oils, semi synthetic oils and soluble oils. Mineral oils and fatty oils come under the category of straight cutting oils. These oils have high lubricating properties but poor heat absorption capacity. Beneficial effect of mineral oils can be improved with the help of additives which are generally compounds of sulphur and chlorine. Addition of sulphur compounds reduces chances of chip welding on the tool rake face. Other additives may be used to improve stability and antirust properties. Biocides may be added to prevent any organic growth. Fatty oils may be added to improve lubricity of these oils. Synthetic oils are oils which don't constitute mineral oil instead of that they contains some chemicals as additives. Main advantages of these synthetic oils are not to affect the bacterial growth with increase in storage time and capable of acting as emulsion in

hard water. Limitations are poor lubricity and have a tendency to foam. If the flow rate of fluid for particular requirement is high, excessive foaming can be results in poor surface finish and reduced tool life. Semi synthetic oils are the coolant contains mineral oil partially and synthetic chemicals. It constitutes the advantages of synthetic oils and not to 100% disadvantages of synthetics. The ideal applications of semi synthetic oils are the combinations with additive packages. Soluble oils are also called water-based cutting fluids. These are mineral oils, fat mixtures and emulsifier added to water. The oil is held in the form of microscopic droplets in water which assumes a white milky appearance. Because of water these fluids have excellent cooling effects.

Along with the beneficial effect, some cutting fluids may produce harmful effects on machine operator and environments. Use of cutting fluids in machining may produce toxic vapor which is very dangerous to health of machine operator. It may damage surface of workpiece due to chemical action. These fluids are degrading in quality over a period of time with increased usage time. This promotes bacterial growth and results in contamination with time. Hence the disposal of conventional cutting fluid (CCF) is necessary, which impact the environment negatively. In addition, CCFs have several limitations such as environmental pollution, dermatitis to the machinist, water pollution, high cost of disposal and soil contamination after disposal [8].

In order to realize the beneficial effect and harmless, desirable properties of cutting fluids are good lubricity property, high heat absorption capacity, high flash and fire point, stable fluid and harmless to work surface.

1.7 Alternatives to Conventional Cutting fluids

To minimize the use of CCFs in machining and to reduce their adverse effects, researchers have started investigations with various alternatives. Dry machining, cryogenic cooling, minimum quantity lubrication (MQL), solid lubricants, vegetable oils, and nanofluids are some of the alternatives to CCFs [9].

1.7.1 Dry machining

The need for machining with higher cutting speed and also difficult-to-machined materials is imposing pressure for tool materials. The research on area of dry machining has lead to improve the mechanical properties of the tool material by making them more refractory or generating less heat during machining. There has been a continuous development

in the field of cutting tool material starting with HSS, cobalt alloys, cemented tungsten carbide coated carbide and coated HSS, cubic boron nitride and diamond. However, dry machining has causes for high tool wear, poor surface quality and accuracy of outcome from machining due to generating heat and friction in cutting zone [4]. Hence, lubricants were the conventional choice for improving surface quality and decreasing tooling cost.

1.7.2 Cryogenic coolant

Cryogenics is the study and use of the materials at very low temperature which is less than -150°C . The Liquid nitrogen is mostly used cryogenic coolant in machining because of widely available and posse's characteristics of colorless, odorless and non toxic [10].

Cryogenic cooling is classified into four types which are pre cooling the workpiece, indirect cryogenic cooling, cryogenic spraying, jet cooling and cryogenic treatment.

Pre cooling the workpiece: It is the process of cooling the workpiece at temperature below -150°C , aim is to change the properties of the material from ductile material to brittle at lower temperature.

Indirect cryogenic cooling: It is also termed as tool cooling process. It cools the tool before starting of machining process and improves the machining performance.

Cryogenic spraying and jet cooling: It is the process of cooling the chip tool interface by supplying cryogenic coolant to exact chip tool interface through nozzle or jet.

Cryogenic treatment: this process is similar to heat treatment to cool the workpiece for longer time and heated back to room temperature to improve the dimensional stability and wear resistance.

1.7.3 Minimum Quantity Lubrication (MQL)

To minimize the excessive coolant, MQL play a major role for improving tool life and surface quality of machined parts. MQL is the most versatile technique in machining industry, which supplies the minimum volume of fluid in the machining process, typically in the flow rate of 5-10 mL/min, which are about ten thousand of cutting fluid used in flood cooling machining [11]. The concept of MQL also known as near dry machining or “extremely low quantity lubricant”, is regarded as a solution to negative impact of the cutting fluids on the environment. MQL has attracted great notice since mid 1990's.

1.7.4 Solid Lubricants

Being a solid phase of dry lubricants can able to reduce friction between the contacting surfaces sliding against to each other without any fluids. The most applications of dry lubricants are in locks and dry lubricated bearing. These lubricants can operate up to 350°C in oxidizing environment even more in non oxidizing environments. The low coefficient of friction property of these solid or dry lubricants is due to layered structure on molecular level with strong covalent bond within layer and weak bonding between the layers. Such layers are made them to achieve low friction properties to sliding against each other with minimum load. The use of solid lubricants in machining is in trend as lubricants to improve the machining performance either individually or as additives along with fluids. Calcium fluoride (CaF₂), Graphite, Molybdenum Di Sulphide (MoS₂), Boric acid (BA) and Hexagonal boron nitride (HBN) etc., are some of the solid lubricants used in machining [1].

Graphite

Graphite is a layered or planner structure. The individual layers are called graphene. Each layer is arranged with carbon atoms in the form of hexagonal or triangular lattice separation of 0.1415 nm with strong covalent bond. The distance between atomic layers is 0.335nm at room temperature [12]. The weaker Van der waals bonding between the planes of graphite allow to easily slide past to each other and minimize the shear strength, thus exhibit good tribological properties of coefficient of friction and wear. The coefficient of friction value for graphite is in ranges between 0.007 to 0.15 depending upon sliding conditions, form of graphite used and type of machine. Graphite can be act as effective lubricant up to about 300°C beyond that the value of coefficient of friction is tends to rise. Therefore it is best suited for an effective lubricant in regular atmosphere. The crystal structure of the graphite is shown in Fig. 1. 4.

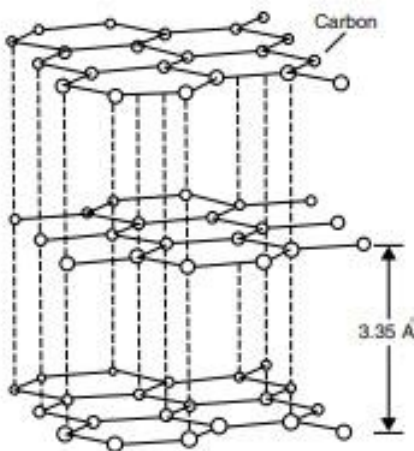


Fig. 1.4 Crystal structure of graphite [12]

Calcium fluoride

Calcium fluoride is an inorganic compound of calcium and fluoride elements occurs naturally as a mineral fluorite with chemical formula CaF_2 . It is in white colour and insoluble solid with cubic fluorite type structure. Calcium is synchronized to eight fluoride ions and each fluoride ion is bounded by four Ca^{2+} ions. CaF_2 solid lubricant reacts with silicate ingredients at high temperature and produce weak bond structure [13]. Properties of CaF_2 are melting point 1423°C ; boiling point 2500°C ; density 3.18 g/cc at 25°C .

Hexagonal Boron nitride

It is solid lubricant of synthetic type with high refractory and good lubricity characteristics at elevated temperature. Oxidation is negligible below the 1000°C . B_2O_3 reacts chemically with ammonia or urea at high temperature and produced HBN in powder form. It is in white colour and cubic configuration (cubic boron nitride). Like diamond it is also hard and resistant to wear. Crystal structure of hexagonal boron nitride is similar to graphite as shown in Fig. 1.5. Its atomic planes are made up of 2D boron and nitrogen atom. Similar to graphite bonding between the interatomic planes are weak Van der Waals and strong covalent bonding within a layer. Coefficient of friction in an air is 0.2 to 0.3 around 700°C . Typical application of HBN is under self lubricated, high load carrying and high temperature sliding conditions [14].

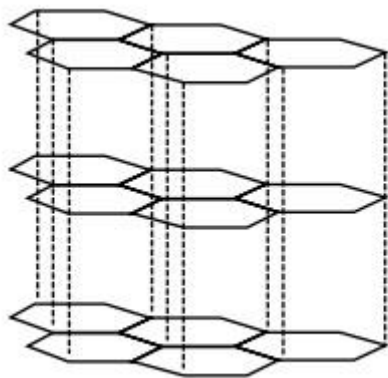


Fig. 1.5 Structure of Hexagonal boron nitride [12]

Molybdenum di sulphide

Molybdenum di sulphide is proved as best lubricant among other solid lubricants due to layered structure and low coefficient of friction. Appearance of MoS_2 is like graphite, but crystal structure is slightly diverse. It is widely used as solid lubricant due to low friction properties. In MoS_2 structure, each trigonal prismatic Mo atom is sandwiched between six sulfide ligands of hexagonal pattern as shown in Fig. 1.6. The weaker Van der Waals bonding between sulphur layer and strong covalent bonding within the layer of sulphur imparts better friction properties. Layered structure of nano or micron sized MoS_2 additive in oil or any other base fluid helps to reduce the coefficient of friction on contact surfaces when used as lubricant in sliding movement.

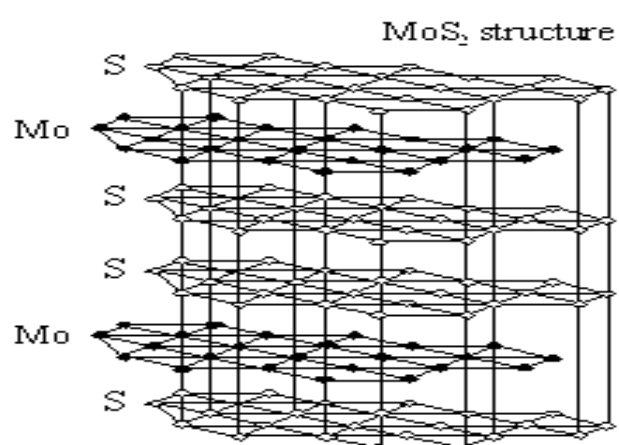


Fig. 1.6 Structure of Molybdenum di sulphide

Boric acid

Boric acid is a lamellar type of promising solid lubricant with crystal structure similar to HBN and graphite. In which boron, oxygen and hydrogen atoms are connected like triclinic unit cell as shown in Fig. 1.7. Bonding within a layer of atom is strong covalent/ionic, hydrogen type and distances between the layers are 0.312 nm. The planes of layers are held together by weak Van der Waals force of attraction. Boric acid is existing in Meta boric acid (HBO_2) and orthoboric acid (H_3BO_3). In addition, meta boric acid have different forms: orthorhombic, monoclinic and cubic. Among all these orthorhombic and orthoboric acid are having layered crystal structure thus enable to offer low friction and wear properties. Besides, high load carrying capacity and low coefficient of friction (0.02) in steady state condition, boric acid also act as good remarkable lubricant when used as additive in vegetable oil or petroleum based oil.

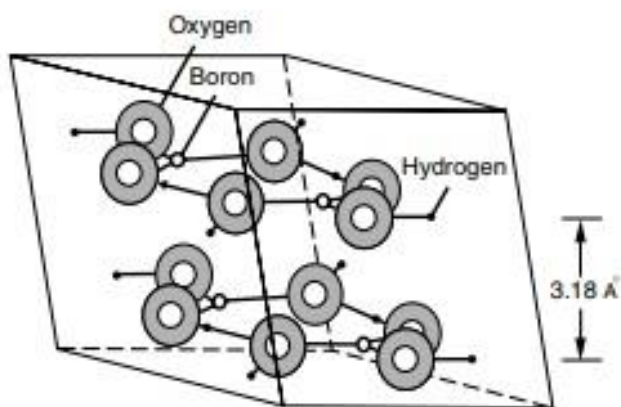


Fig. 1.7 Structure of Boric acid [12]

Carbon nanotube (CNT)

CNT is belonging to structure of fullerene family which is in the form of carbon with diameter in nanometer sized and micrometer length of tube. One end of CNT is open to atmosphere and other end is closed with fullerene cap. Carbon nanotubes are categorized as single wall carbon nanotube (SWCNT), double wall carbon nanotube (DWCNT) and multi walled carbon nanotube (MWCNT) based on concentric walls. SWCNT and MWCNT are almost similar to fullerene related structure, but striking small differences.

SWCNT is rolled up to a graphene sheet on a seamless cylinder and the allotropy of SP² hybridization with six carbon rings are attached together in the form of hexagon like

graphite. MWCNT is a tubal structure includes several concentric cylinders as shown in Fig. 1.8. CNT has a high strength, hardness and young's modulus due to large number of carbon in their structure and high aspect ratio (length to diameter ratio). Furthermore, carbon atom in CNT adopt SP^2 hybridization which include more number of S path ways than SP^3 hybridization and this helps to strengthen CNT.

Thermal conductivity value of CNT (averagely 3000W /m.K) is 1000 times higher than the thermal conductivity of base oil. When small content of CNT is used as additive in vegetable oil/ mineral oil, CNT could act as independent micro tube and serve as similar bearing effect that reduce friction in cutting zone by improving heat transfer rate. This may improves the lubrication effect of nanofluid in machining.

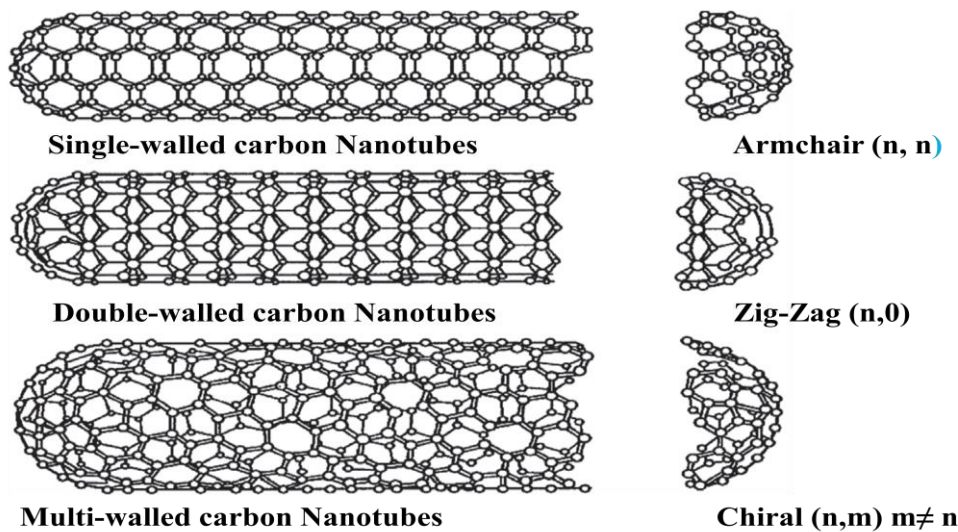


Fig. 1.8 Structure of carbon nanotube [15]

1.7.5 Vegetable Oils

Vegetable oils are composed of triglyceride structure which is extracted from a seeds of plant. Any oil that comes from plants is known as vegetable oil. Typical glycerol structure of vegetable oil is shown in Fig. 1. 9. Where R_1 , R_2 and R_3 are the long chain atoms of carbon and hydrogen, another words termed as fatty acids chain. Lubricants derived from vegetable oils are replacing the conventional oils due to their added advantages. Since the industries require a material with properties similar to the conventional lubricants that had to be environmental friendly. Vegetable oils became the lubricant of choice for many operations.

Nowadays, Vegetable oils like coconut oil, sunflower oil, soybeans oil, sesame oil, mahua oil, neem oil and mustard oils are being used in various metal cutting operations. Some of this is due to their eco-friendly nature and rest due to their efficiency but most of them are a combination of both. The unique property of vegetable oils which is responsible for their use is ‘Polarity’. Polarity is the alignment of atoms between two metallic surfaces or substances in such a way that friction is reduced by about 50% compared to mineral and animal based lubricants. This unique property is due to the seeds exposure to oxygen during its development. Another property responsible for wide applications is the flash point. Flash point of vegetable oils is around 400°C whereas flash point of mineral oils is 200°C .

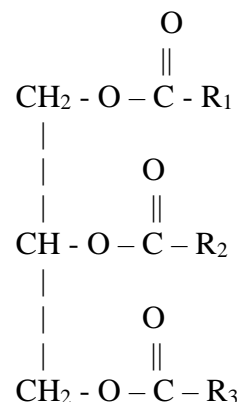


Fig. 1.9 Chemical structure of glycerides of a vegetable oil [16]

The property of oxidation is a barrier for the use of vegetable oils. Oxidation of the oil causes it to be sticky which causes the chips to stick to each other, tools, parts, fixtures etc. This property causes a ‘Varnish’ to build up in undesirable areas. But this can be easily removed by a hammer and chisel.

Vegetable oils are suitable for machining applications because of their nontoxicity, renewability, biodegradability and high viscosity index. They contain triglycerides through which three long chain fatty acids are connected to the hydroxyl groups via ester linkages. The glycerol structure with long chain fatty acids and presence of polar groups in vegetable oils impart lubricating properties to these oils [17]. The basic reason behind the performance of vegetable oils as cutting fluids is their chemical compositions and fatty acid profiles. The fatty acids in vegetable oils are of two types saturated and unsaturated .Saturated fatty acid(SFA) contains all single bonds, where as un saturated fatty acid (USFA) at least one double bond. The length of carbon chain is different in different fatty acids. Less than 8

carbons are present in short chain fatty acid (SCFA). Similarly, 8 to 14 carbons and 16 or more carbons contain in medium and long chain fatty acids respectively. Some of the most commonly used vegetable oil as base oil in machining are coconut oil, sesame oil, soybean oil, palm oil, rapeseed oil, canola oil, neem oil, mahua oil and mustered oil etc.

Sesame oil

Sesame oil is edible oil which is extracted from sesame seeds. Besides, being used in cooking purpose, it is also used as lubricants in some of the metal cutting industries due its chemical structure. Sesame oil is composed of various saturated and unsaturated fatty acids. Some of them to help in film forming characteristics of unsaturated long chain fatty acids in sesame oil are oleic C_{18:1} (35.9 -43.7%) and Linoleic C_{18:2} (38.6-48.9%) [18].

Mahua oil

Mahua oil is the non edible oil in India which is extracted from the madhuca tree seeds. In some countries it is used as edible oil for preparing ghee. Mahua seed contains 30 to 40% fatty oil. Hence, one Lakh eighty thousand tons of mahua oil is annually produced [19]. Mahua oil is used in preparing biodiesel as blends and applied as lubricants due to high viscosity, flash and fire point temperature. Mahua oil constitutes saturated long chain fatty acids of palmitic acid C_{16:0} (23.7% -24.7%), stearic acid C_{18:0} (19.3% - 29%) and arachidic acid C_{20:0} (2%). Unsaturated long chain fatty acids in mahua oil are oleic acid C_{18:1}(36.3% - 43.3%) and linoleic acid C_{18:2}(11.6%- 15.8%) [20].

Neem oil

Neem oil is also nano edible oil extracted from fruits, seeds of the neem. Neem oil is used in preparing soaps, body hygiene and hair oil. Neem oil is also used in manufacturing sectors as lubricants owing to fatty acids and chemical structure which enable to forming consistent film on contacting surfaces. The fatty acids profiles and chemical composition of neem oil are palmitic acid C_{16:0} (16-33%), stearic acid C_{18:0} (9-24%), oleic acid C_{18:1} (25-54%) and linoleic acid C_{18:2} (6-16%).

1.7.6 Nanofluid

Nanofluids are obtained by dispersing nanoparticles of size less than 100 nm (nanowires, nanorods, nanotubes, and nanodroplet) in the base fluids (water, oil and glycol etc.). The fluid in which nanoparticles are dispersed is called as base fluid. The particles

which are in nanometer size used for dispersion in base fluid are called nanoparticles. Since solids are better carriers of heat than liquids, dispersing them in a fluid, enhances the thermo-physical properties like viscosity, thermal conductivity, thermal diffusivity and heat transfer coefficient owing to their high surface to volume ratio. The phenomenon like abrasion or blocking of the coolant supply system is caused by millimeter or micrometer sized particles which get settled rapidly in fluids. The large surface to volume ratio of nanometer scale particle helps it to remain stable and sustain for a longer period of time.

Different types of nanoparticles used in formulation of nanofluids are Al_2O_3 , SiC , SiO_2 , CuO , TiO_2 Cu , Fe , Au , Ag , SWCNT and MWCNT etc. Mostly spherical shaped nanoparticles are used as additive in machining and various industrial applications. Cylindrical shaped, rod shaped nanoparticle also used industrial application. Nano materials are synthesized using top down and bottom up approaches [21].

Top down approach: Top down approach is the method of reduction of bulk material into nano dimensions. Mechanical milling, nanolithography, laser ablation, thermal decomposition and sputtering are process of producing nanometerials using top down approach.

Bottom up approach: It is the method to build up the material from atom to cluster and cluster to nanometerials. Sol-gel process, chemical vapor deposition, spinning, pyrolysis and bio synthesis are the process of build up the nanometerials using bottom up approach.

Nanofluids are prepared using one step and two step method [1]. One-step method deals with production as well as dispersion of nanoparticles in base fluid. In two-step method production and dispersion are done separately, which is advantageous to produce nanoparticles at large scale. A probe type or chamber type sonicator is normally used to formulate nanofluids.

1.7.7 Hybrid Nanofluids

Besides single nanoparticle enriched cutting fluids, the combination of dissimilar with different shaped nano-materials suspending in base fluid resulted in more improved properties like thermal conductivity, viscosity, antifriction and antiwear properties. The suspension of the dissimilar nano materials in base fluid either in the form of composite or mixture is termed as hybrid nanofluids (HNF), which offers excellent thermo-physical properties than single nanoparticle enriched cutting fluid. HNFs offered improved machining performance in terms of reduction in cutting force, cutting temperature, surface roughness and tool flank wear when used in machining [22, 23].

1.8. Organization of the Thesis

Chapter-1 is the introduction section which deals in detail about machining aspects and cutting fluids. A brief introduction about various lubrication environment and nanofluids are discussed.

Chapter-2 presents the extensive review of literature on machining and various alternatives of CCF in machining. A spectrum of previous literature on vegetable oil, solid lubricants and nanofluids in machining applications are presented as well.

Chapter-III focuses on description of experimental setup for machining, stability evaluation and characterization of HNCFs. A brief introduction about cutting tools, work materials and MQL system which are used while carrying out various experiments in the present work are also discussed.

Detailed discussion about deciding the HNCF compositions for stability are presented in **Chapter-IV**. Comparative assessment of machining performance in terms of main cutting force, cutting temperature, surface roughness and tool flank wear under dry, CCF and HNCFs environment are also explored in this chapter as well.

Chapter-V presents detailed discussion about thermo physical properties and tribology property of CNT/MoS₂ (1:2) nanofluid by varying concentration (i.e. 0.5, 1, 1.5, 2, 2.5 and 3 wt.%). Results of applicability of CNT/ MoS₂ (1:2) nanofluid in machining by varying concentration has been presented.

Chapter-VI dealt with modeling and optimization of cutting parameters. In this section minimization of cutting force, cutting temperature, surface roughness and tool flank wear using Box-Behnken design of response surface methodology has been discussed. Optimal combination of multiple responses is presented.

Chapter-VII presents the overall conclusion of the present work and followed by future scope of the work and references.

Chapter-2

Literature review

2.1 Introduction

Product quality has received much concern due to accelerating competition in production industries. For survival of fittest industry, quality is a benchmark. Quality of any machined product is characterized by several parameters, in which surface roughness and dimensional accuracy are prominent. Surface roughness is focus for growth of quality consciousness. It has ever been an important design feature and quality measure in machining process and a critical constraint for cutting parameters selection. The factors affected on surface roughness are workpiece, tool geometry and cutting conditions. Cutting forces generated during machining and rise in temperature in cutting zone due to enormous amount of generated heat in chip-tool interface are influence the tool wear; dimensional accuracy and surface finish of machined surface in turn affect the quality of machined surface.

This chapter describes previous investigations on machining and machining performance of cutting force, cutting temperature, surface roughness and tool wear. Brief literature review of various elements which were considered in the present work also discussed.

2.2 Cutting fluids

Cutting fluids were the conventional choice for improving surface quality of workpiece and productivity through cooling and lubrication action. Lubrication reduces the heat generation by reducing the friction between contacting surfaces and cooling action reduces the temperature by dissipating the heat [2]. Most of the industries were utilizing lubricants for lubricating their machines or substance, among them 85% of the lubricants adopted throughout the world are petroleum based [24]. Furthermore, metal working fluids are the type of lubricants, which improves the product quality and production rate in machining sectors by lubricating and cooling action. With that fact, in machining industries consumption of metal working fluids is rising day to day. These Metal working fluids being consumed by the European union was approximately 3,20, 000 tons/year, out of that 2/3 were

need to be disposed [24]. But they do create several negative effects on environment after disposal. These effects include ground water contamination, air pollution, soil and food contamination [25]. Furthermore, due to widespread use metal working fluids were exposed to health issues and skin related diseases like mechanical trauma to the skin, infection and allergic dermatitis. Dry machining, solid lubricants, Minimum Quantity Lubrication (MQL), cryogenic coolant, vegetable oil and nanofluids were the various alternatives to the conventional cutting fluids for minimizing such adverse effects on environment and operator health [1].

2.3 Alternatives to conventional cutting fluids

To minimize the adverse effects with CCFs in machining, researchers have shown several alternatives. These include dry machining with coated tools, cryogenic coolant, Minimum Quantity Lubrication, solid lubricants, vegetable oils, nanofluids, vegetable oil based nanofluids and hybrid nanofluids.

2.3.1 Dry machining and machining with coated tools

The researchers conducted machining experiments under dry cutting environment in turning of AISI1040 steel by varying cutting speed, feed rate and depth of cut. The results revealed that consumption of the power during dry cutting gives very less and obtained good surface finish compared to wet machining [26]. Diniz et al .[27] carried out several experiments by varying parameters of cutting speed, feed rate , depth of cut and tool material in machining of ABNT 1045 steel in dry and wet turning. They inferred that the wet turning incurs better tool life compared to machining with dry condition and dry cutting is used only for smaller depth of cut (less than 1 mm). Alok et al. [28] assessed the machining performance in terms of cutting force, surface roughness and tool flank wear by conducting turning experiments on AISI 52100 steel with newly developed HSN² coated carbide insert using RSM. The PVD coated HSN² carbide inserts were more effective in terms of achieved lower value of flank wear and cutting forces for dry hard turning within the selected range of process parameters.

Coated tools constitute the structure of compound materials which is deposited on substrate with a thermal isolating layer of thickness one to three micrometers thus improves wear resistant property of the tools and enhance tool life and wear. Some of the researchers inferred that through their studies on surface coating tool and improvement in wear resistant of tool by changing contact conditions at chip and tool interface. To avoid the usage of

cutting fluids in machining, coated tools are used due to the reason that coated tools have low thermal conductivity so that it can prevent the heat into bulk material of the cutting tool. It should have good resistance to abrasion wear and must possess high thermal and chemical stability.

2.3.2 Cryogenic coolant

Cryogenic is a process of working with materials at very low temperature below - 150°C/123K. It is environmental secure and one of the alternatives to conventional cutting fluid. The cryogenic coolant is used in machining as lubricant in cutting zone where enormous amount of heat is generated in deformation zones. Thus applied coolant could take in the generated heat on tool and reduces maximum temperature thus improves tool life. The normal boiling point of gases such as helium, nitrogen, neon, hydrogen, oxygen and air as cryogens lies below -180 °C. Cryogenic gases have several applications in industry such as health, electronics, manufacturing, automotive and aerospace industry for cooling purposes. Liquid nitrogen is the commonly used lubricant in machining due to its characteristics such as colorless, non-toxic and odorless [29].

The main purpose of cryogenic coolant in metal cutting operation is removing the heat from machining zone and reducing the cutting temperature as well as modifying frictional characteristics in chip-tool interface [30]. Wang and Rajurkar [31] studied the wear behavior of CBN tool in turning of silicon nitride with and without cryogenic coolant. In order to control the temperature in cutting zone they designed a cooling system to circulate cryogenic coolant from top of arranged reservoir on to cutting tool. The experimental results showed that tool wear was found to be reduced with Liquid nitrogen cryogenic coolant. Yildiz et al. [10] investigated the performance of Liquid nitrogen cryogenic coolant in metal removal process by measuring cutting forces, cutting temperature, tool wear, tool life, surface finish and accuracy of machined part. They inferred that cryogenic cooling was the most preferred technique for reducing cutting temperature, cutting forces and improving tool life and surface finish.

2.3.3 Minimum quantity Lubrication

MQL is the most promising technique in which very low quantity of cutting fluid preferably (5-10mL/min) is supplied to machining area through the nozzle in the form of an aerosol (mist generation) or drop wise [1]. Thakur et al. [32] studied the effect of MQL and

optimized MQL parameters by using optimization technique during high-speed turning of inconel718 alloy. They reported that MQL pulse jet was the effective approach while machining of inconel718 alloy. They also explored that MQL technique protects the machinist health, prevents environmental hazards. Behera et al. [33] deigned and fabricated twin fluid MQL system and delivered the cutting fluid in machining to initial, middle and far field region with different flow rates (i.e 60, 125, 250 mL/hr). They observed the maximum decrease in tool flank wear, cutting forces and chip curling during machining with 125 mL/hr MQL flow rate. Uysal et al.[34] investigated the effect of MQL at 20 mL/h and 40 mL/h flow rates while milling of AISI420 steel. Better results were achieved in MQL at flow rate of 40 mL/h compared to dry and 20 mL/h conditions. Surface quality was improved and tool flank wear was diminished with MQL.

Pervaiz et al. [35] applied air and vegetable oil in MQL during turning of Ti6Al4V alloy. The flow rate of MQL was maintained constant at 240 mL/h for all the experiments and reported that affirmative machining results in terms of reduced cutting force, improved surface quality and tool life compared to dry condition. Setti et al. [36] studied the effect of MQL during surface grinding of Ti6Al4V and revealed that MQL showed the superior performance than dry and wet conditions in terms of reduced coefficient of friction, grinding force, surface roughness, and temperature in grinding zone. Kedare et al. [37] studied the effect of cutting speed, feed rate and depth of cut upon surface roughness during end milling of 15HRC mild steel under MQL mode of 900 mL/hr and results were compared with flood coolant of flow rate 2 L/min. They inferred that surface finish was enhanced by 27% with MQL compared to flood coolant.

Hadi and Atefi [11] observed the effect of MQL on surface roughness by dispersing γ -Al₂O₃ nano particle in vegetable oil during milling of AISI D3 steel. They inferred that the surface roughness was improved to an extent of 15% than pure MQL. Amritha et al. [38] investigated the performance of nanographite adding in water miscible cutting fluid with different supplying systems to cutting zone during machining. In System A, nanofluid was supplied through MQL device with high pressure and 1mL/min flow rate. In System B, coolant was supplied with low pressure and 5 mL/min MQL flow rate. The cutting force (F_z) and cutting temperature (T) were found to be high for both the systems compared to flood machining. The lowest surface roughness (R_a) and tool flank wear (V_b) were obtained with both the systems compared to flood cooling and dry machining. Marques et al. [39] found

improvement in surface quality and tool life with the inclusion of graphite in neat oil compared to (molybdenum di sulphide) MoS_2 , in machining of Inconel 718 under MQL conditions. Roy et al. [40] focused on effectiveness of small quantity twin jet lubrication system with nanofluid in turning of AISI4140 steel with a coated carbide insert. The turning experiments were conducted in varying cutting speed and feed rate with conventional cutting fluid and nanofluid. Significant R_a value was observed with small quantity of twin jet lubrication system than single jet.

2.3.4 Solid Lubricants

Nowadays all manufacturing industries focus their attention to solid lubricants as additives in base oils, because of their echo friendly nature, structure and excellent tribological properties. Some of the solid lubricants were calcium fluoride (CaF_2), tungsten di sulphide (WS_2), titanium nitride (TiN), molybdenum di sulfide (MoS_2) and boric acid (BA) etc. which can control heat generation and allow minimum frictional effect on rubbing surfaces [1]. Shaji and Radhakrishnan [41] studied the performance of solid lubricants CAF_2 , BaF_2 and MoS_2 in grinding and inferred that the tangential force and surface roughness have decreased. The considered solid lubricants have a layered structure, where the layers can slide over each other. This reduces the sliding friction, which is dominant in machining.

In a similar work, Venugopal and Rao [42] evaluated the performance of graphite as a solid lubricant in grinding. Paturi et al. [43] investigated the effect of WS_2 solid lubricant on surface finish by adding in emulsifier oil with 0.5% by weight and used in machining under MQL condition. The results revealed that much improvement in surface finish of work material by about 35% than pure MQL. Rahamati et al. [44] studied the performance of nano MoS_2 (20-60nm) enriched with oil in various concentrations (0, 0.2, 0.5 and 1wt %). Thus fluids were tested for applicability in milling under MQL condition. The experimental results explored the 0.5% nano MoS_2 in oil improved the surface quality of work part compared to other concentration. Kumar et al. [45] found the performance of boron nitride solid lubricant was better than Zns during hard turning of AISI4340 steel. Gunda et al. [46] studied the performance of MoS_2 in SAE oil in pin on disc test. The 20 wt % of MoS_2 in SAE oil has given superior performance in terms of reduction in coefficient of friction and temperature in sliding zone. Krishna et al. [47] reported the significant reduction in cutting temperature, surface roughness and tool flank wear by using boric acid solid lubricants during turning of

AISI 1040 steel. Similar kind of solid lubricants assisted machining studies were performed by researches [48, 49].

2.3.5 Vegetable oils

Vegetable oils are the better substitutes for mineral oils as cutting fluids in machining applications due to prominent characteristics such as high biodegradability, renewability, high viscosity index and flash point. Ojolo et al. [50] carried out experiments on turning of mild steel, aluminum and copper workpiece materials and studied the effect of different vegetable oils on cutting force during machining in varying cutting conditions. Experimental results showed that vegetable oils are best suitable as metalworking fluids and their relative effect is improving surface quality and reduction in cutting force is dependent on workpiece material. Xavior and Adithan [51] studied the effect of coconut oil, emulsion oil and neat cutting oil immiscible with water on tool wear and surface roughness for cylindrical turning of AISI304 austenite stainless steel using carbide tool. The experimental study revealed that the coconut oil had the greatest effect followed by neat cutting oil and emulsion oil was the least efficient for reduction in tool wear and surface roughness.

Cetin et al. [52] studied the performance of six cutting fluids that were formulated using sunflower and canola oils and had different ratios of extreme pressure (EP) additives. The authors compared the performance, with two commercial cutting fluids (semi-synthetic and mineral). The fluids were used while machining AISI 304L austenitic stainless steel with carbide inserts and it was reported that surface roughness and forces were decreased with the application of vegetable oils. Kumar et al. [53] investigated the efficacy of coconut oil with EP additives in MQL. It was reported that cutting forces, temperatures, wear and surface roughness were reduced with the application of coconut oil compared to the conventional lubricant. Wang et al. [54] studied lubrication properties of seven vegetable oils (i.e. maize, palm oil, soybean, peanut, caster, sunflower and rapeseed) under MQL condition and flood cooling technique in grinding. The experimental results were indicated that all vegetable oils with MQL grinding showed lower coefficient of friction, specific energy of grinding and grinding ratio than flood cooling. Among all vegetable oil castor oil achieved a lower specific grinding energy and coefficient of friction 73.47 J/mm^3 and 0.30 respectively.

Srikant et al. [55] examined the effect of vegetable oil based emulsifier (Cocamidopropylbetaine (CAPB)+ sesame oil) in machining by varying volume fraction

(5%,10%,15%, 20% and 25%) in water miscible oil. Found the 10% CAPB in water miscible oil performed better than other volume fraction for reduced nodal temperature, cutting forces, tool flank wear and thus improved surface quality. Ozcelik et al. [56] examined the performance of the various vegetable oils with (8% and 12%) include extreme pressure additives on cutting force ,surface roughness and tool flank wear in turning of AISI304L. The 8% EP included in canola oil performed better than other condition in terms of reducing F_z , R_a and V_b . Elmunafi et al. [57] used castor oil in machining of hardened steel and reported the considerable improvement in tool life, surface finish and reduction in cutting force. This may be due to cooling ability of castor oil during machining.

2.3.6 Nanofluids

Dispersing the colloidal suspension of nanometer scale solid particles in base fluids (oil, water and ethylene glycol) are termed as nanofluids (NFs). NFs are prepared by adding nanometer sized metallic or non metallic solid powder particles CaF_2 , Al_2O_3 , SiC , MoS_2 , graphite, fiber and nano rods etc. in liquids by using one step or two step method. The solid nanoparticles conduct heat better than liquids, and hence nanofluids have attained enhanced basic properties like viscosity, thermal diffusivity, thermal conductivity and convective heat transfer [58]. NFs posses improved stability over the conventional fluid with micron or millimeter sized solid particle. The reason for this is size effect and Brownian motion of the particle in liquids [59]. In past few decades several experimental and numerical investigations were processed and in progress by developing nanofluids for heat transfer and machining applications.

The enhancement in thermal conductivity of nanofluids is influenced by particle type, size, shape, structure, surfactant and temperature. The enhanced thermal conductivity of nanofluids results in better tool life and surface quality by reducing the force and temperature in machining. Turgut et al. [60] measured the thermal conductivity of diverse vegetable oils at 25°, 40°, 60°and 80°C temperature. The results were found to decrease with increase in temperature. The highest and lowest thermal conductivity was reported as 0.168 W/m.K for sunflower oil at 25°C and 0.152 W/m.K for corn oil at 80°C. Wei et al. [61] evaluated the thermal conductivity of TiO_2 nanofluid with thermal property analyzer KD 2 pro. Thermal conductivity was increased with augment in volume fraction and temperature. Amritha et al. [2] prepared nanofluids by adding suspensions of nanographite in base fluid (95% water+ 5% of mineral oil) in variation of concentration (0%,0.1%,0.3% and 0.5%) by weight. Thus,

prepared nanofluids were used for measurement of thermal conductivity, kinematic viscosity in range of temperature 25°C to 60°C. It is noticed that thermal conductivity and kinematic viscosity of nanofluids were increased with increase in concentration of nanoparticles in base fluid. Improvement in thermal conductivity and viscosity was found by the application of nanofluid compared to that of base fluids.

Yu et al. [62] analyzed thermal conductivity and viscosity of Aluminum nitride nanofluid. Thermal conductivity was measured with transient hotwire method and viscosity was measured with Brookfield programmable Viscometer. Both thermal conductivity and viscosity measurements were carried out in the temperature range of 10 to 60°C. They reported the enhancement in thermal conductivity at an extent of 38.71% and 40.2% for Ethylene glycol and propylene glycol base fluids. Viscosity was decreased with increase in temperature. Krajnik et al. [63] examined thermal and tribological properties of the nanofluids and tested their application in machining. They inferred that the enhancement in performance of nanofluids in terms of thermal conductivity, convective heat transfer coefficient, heat flux and viscosity when compared to CCF. Yu et al. [64] prepared two nanofluids by suspending nano MoS₂ in water and LB2000 oil at different mass concentration and tested their stability, thermal conductivity and surface tension. They inferred that stability of MoS₂- LB2000 oil nanofluid at 0.01% mass concentration was better than that of MoS₂- LB2000 nanofluid at mass concentration of 0.005%. In comparison to base fluid water based and oil based nanofluid show's improved thermal conductivity. The thermal conductivity and surface tension initially increased and then decreased with the increase of mass concentration.

Naik et al. [65] studied the rheological property and effective thermal conductivity by preparing carboxymethyl cellulose (CMC) based non Newtonian nanofluid with Fe₂O₃, γAl₂O₃ and CuO nanoparticle in Carboxymethyl Cellulose base fluid with different concentration. Viscosity and Thermal conductivity test were conducted by Rheometer and transient hotwire technique. Both the experiments were performed in the temperature range of 30° -50°C. As concentration and temperature rise, the effective thermal conductivity was found to increase and viscosity was observed to be decrease with respect to temperature. Similar findings were reported by researchers [66–69].

The friction between tool and work contact surface is the major parameter for generating heat in cutting zone. It affects tool life and surface quality of the machined parts with increasing tool tip temperature, which in turn leads to decrease in sharpness of cutting

edge. Kalita and Ajay [70] investigated the performance of nano MoS₂ (<100 nm) by dispersing in soyabean oil at 20% concentration by weight. Friction tests were conducted by using Pin on disc Tribometer with variation of sliding speeds. They reported the reduction in coefficient of friction by the application of nanofluid when compared to dry condition. Several researchers were performed machining operations by using different nanofluids as coolant and reported that the concentration of nanoparticle in base fluid, type of nanoparticle and flow rate play a significant role in the performance. Zhang et al. [71] observed the performance of nano MoS₂ in soybean, palm and rapeseed oil during MQL grinding of 45 steel. The comparison of experimental results were made with dry and flood cooling environment. They inferred that nano MoS₂ in vegetable oils under MQL condition performed better than dry and flood lubrication in terms of reduction in coefficient of friction and specific grinding energy. The application of palm oil based nanofluid is found to have minimum coefficient of friction (0.3) and specific grinding energy 0.65 J/mm³.

Khandekar et al. [72] reported that reduction in cutting force about 50% and 30% during turning operation by adding 1% of Al₂O₃ in CCF when compared to dry condition and machining with CCF. Raju al. [73] investigated the performance of the multi-walled carbon nanotubes (MWCNT) in distilled water and sodium dodecyl sulfate surfactant by using MQL technique in turning of EN31 steel for cutting force, tool wear and surface roughness. Surface roughness and tool life were improved compared to machining in dry condition and conventional cutting fluid, whereas cutting force was reduced with MWCNT nanofluid. Amritha et al. [8] investigated the affects of nanographite inclusion in soluble oil through MQL (10 ml/min and 15 ml/min) by varying concentration on cutting force, tool wear and chip-tool interface temperature during turning operation. Minimum cutting forces and tool wear were obtained at 15 mL/min with cemented carbide tool and HSS tools at a mass concentration of 0.45wt%.

Padmini et al.[9] formulated nanofluids by adding nano boric acid and nano MoS₂ in diverse vegetable oils in varying concentration. Thus prepared fluids were used in machining during turning of AISI1040 steel using MQL technique. The experimental results were signified 0.25% and 0.5% of nano MoS₂ in coconut oil outperformed than sesame oil based nanofluids in terms of reduction in cutting force, cutting temperature and surface roughness. Padmini et al. [18] prepared nanofluid by dispersing nano MoS₂ at varying concentrations in coconut oil, canola oil and sesame oil. The formulated fluids were used in machining AISI

1040 steel using MQL conditions. It was reported that cutting temperatures and tool flank wear were decreased significantly with 0.5% nano boric acid suspensions in vegetable oils. Among the considered oils, coconut oil based nanoparticle suspensions exhibited enhanced performance compared to other vegetable oil-based nanofluids (VOBNFs). Jia et al. [74] investigated the performance of castor oil and different vegetable oils as mixtures in grinding. They studied the rheological property and tested their applicability in MQL grinding with different vegetable oils and castor oil mixture at 1:1 proportion. Further they investigated the performance of nano MoS_2 in (castor + soybean oil) mixture at 1:1 proportion in varying concentrations (0, 2, 4, 6, 8 and 10 wt. %). It was noticed that from first set of experiments, the mixture of (castor oil + soybean) oil was performed better than other mixed vegetable oils (palm, maize, sunflower, rapeseed and peanut) at same proportion with castor oil in terms of reduction in specific grinding ratio, specific grinding energy and R_a . From second set of experiments the optimal concentration of nano MoS_2 in (Castor +Soybean) mixture oil was found to be 8% in terms of reducing grinding force, specific grinding energy, grinding ratio.

Sharma et al. [75] prepared the nanofluid by adding 0.5wt% of multi walled carbon nanotube (MWCNT) in SAE40W40 oil and used in MQL turning of AISI D2 steel. The experimental results were shown reduction in cutting temperature, tool flank wear and surface roughness. Nam et al. [76] formulated nanofluid by suspending nano diamond particles in vegetable oil and paraffin oil and used in machining under MQL mode. Results were revealed that vegetable oil based nanofluid with MQL condition significantly improve the quality of the drilled holes and reduces the forces in drilling. Park et al. [77] studied effect of xGnP in VOBNFs through wetting angle measurement, tribology test and milling of AISI 1045 steel with TiAlN coated tool. They reported the xGnP enriched vegetable oil based nanofluids performed better in terms of reducing coefficient of friction, central wear and flank wear than that of dry and CCF respectively. Vasu and Reddy [78] examined the performance of vegetable oil based Al_2O_3 nanofluids by turning of Inconel 600 alloy under dry, vegetable oil with MQL and nanofluid with MQL condition. They inferred that the use of 6 vol% of Al_2O_3 vegetable oil based nano fluid under MQL mode gave reduced cutting force, temperature, surface roughness and tool wear than dry and MQL.

2.3.7 Hybrid nanofluids

The suspension of the dissimilar nano materials in base fluid either in the form of composite or mixture is termed as hybrid nanofluids (HNFs), which offers excellent thermo-

physical properties than single nanoparticle enriched cutting fluids. Besides single nanoparticle enriched cutting fluids, the combination of dissimilar with different shaped nano-materials suspending in base fluid resulted in more improved properties like thermal conductivity, viscosity, antifriction and antiwear properties.

Recently very few researchers have started investigation on hybrid nanofluids. Zareie et al. [79] prepared hybrid nanofluid by suspending Mgo (40nm) and MWCNT (outer diameter:5-15 nm & inner diameter:3-5 nm) in equal proportion in water and Ethylene glycol. Thus HNFs were prepared in (0.025, 0.05, 0.1, 0.2, 0.4, 0.6, and 0.8%) volume fractions and measured dynamic viscosity with various shear rate at 25-60°C temperature. They reported that an increase in dynamic viscosity was observed with increase in vol% and it was noticed to decrease with increase in temperature. Tanshen et al. [80] reported enhancement in heat transfer properties of HNFs by adding small quantity of MWCNT -in water along with alumina nanoparticle compared to water. Singh et al.[22] prepared the HNF by adding alumina-graphene nanoparticles (90:10) in base fluid (5% servocut oil and 95% Di-ionized water) in 0.25, 0.75 and 1.25 vol%. Thermal conductivity and wear properties were measured for these HNFs and tested their applicability in machining. Results showed that increase in nanoparticle concentration enhanced the thermal conductivity property of HNF. Tribological tests confirms the decrease in wear with increase in concentration of hybrid nanoparticle. They reported the Al_2O_3 –graphene hybrid nanofluid performed better than Al_2O_3 nanofluid for reducing cutting force and surface roughness. Zhang et al. [81] prepared pure Al_2O_3 , pure SiC and Al_2O_3 –SiC HNF by varying the hybrid mixing ratio (1:1,1:2 and 2:1) at concentration of 6% and used in grinding. The results revealed that hybrid nanofluid performed better than pure Al_2O_3 and SiC nanofluid in reducing grinding force, coefficient friction and specific grinding energy.

Sharma et al. [75] prepared hybrid nanofluid by suspending Al_2O_3 - MWCNT (90:10) nanoparticles in (5% vol. of vegetable oil + distilled water) in concentration of 0.25, 0.75 and 1.25 vol%. The property of the thermal conductivity was measured with KD2 pro and tribological behavior of prepared fluids was tested with pin-on disc tribometer. Machining performance are examined by conducting turning experiments using RSM technique after characterization. Experimental results revealed that thermal conductivity was increased and coefficient of friction was decreased with increase in concentration of Al_2O_3 - MWCNT. Tool flank wear and cutting temperature were found to reduce by 11% and 27.36% compared to

alumina-based nanofluids respectively. Mechiri et al. [68] prepared nanofluid by adding the Cu-Zn hybrid nanoparticle with the combination of (0:100,75:25,50:50,25:75 and 100:0) in vegetable oils. Thermal conductivity was measured at various concentration of hybrid nanoparticles at different temperatures. The experimental results revealed that the thermal conductivity of the nanofluid was increased with increase in temperature and hybrid nanoparticle concentration.

2.4 Optimization

Optimization is a process for finding a best solution when more number of feasible solutions is available. Few investigations were also in processes for finding the optimal solution in combination of different cutting parameters for machining response variable. Sarikaya and gallu [82] carried out the optimization of MQL parameters using Taguchi-based grey relational analysis in turning. The process parameters include cutting fluid, fluid flow rate and cutting speed are optimized for tool flank wear, and surface roughness. The combination of optimal process parameters was found to be vegetable oil based cutting fluid, 180mL/h fluid flow rate and 30m/min cutting speed. Johnson et al. [83] conducted the turning experiments as per Taguchi's L_{27} orthogonal array by taking seven factors, which are cutting conditions and fluid application parameters at each three levels and measured surface roughness (R_a). From taguchi analysis, they found the optimal values of cutting speed, feed rate and depth of cut were in the order of 148.44 m/min, 0.06 mm/rev, 0.5 mm and injecting pressure 100 bar, pulsing frequency 500 pulse/min, fluid flow rate 6 mL/min and cutting fluid composition 20% respectively. Rapeti et al. [84] conducted the turning experiments using L_{27} orthogonal array by taking four factors (base fluid, speed, feed, and nanoparticle inclusion) each at 3 levels and measured four machining responses. The final optimum setting parameters for minimizing cutting force, cutting temperature, surface roughness and tool flank wear were found to be coconut oil, 40 m/min, 0.14 mm/rev and 0.5% nanoparticle inclusion.

Pasam et al. [85] conducted the experiments during wire electrical discharge machining of titanium alloy (Ti6Al4V) using taguchi L_{27} orthogonal array by taking 8 factors at each three levels. Regression models were developed for prediction of surface roughness and optimal values were found in range by using genetic algorythem approach. Leiw et al. [86] investigation was on optimization for tool flank wear and surface roughness in turning of AISI D2 Steel using RSM technique. The optimal combination of tool flank wear and surface roughness was found to be cutting speed of 144.58 m/min, feed rate of 0.14 mm/rev

with carbon nano fiber (CNF) nanofluid as a coolant. Rao et al. [87] studied an effect of cutting parameters on cutting force in turning of AISI 1045 steel with Al_2O_3 +TiC coated ceramic tool. They reported that cutting speed, feed rate and depth of cut are significantly influence on cutting forces and interaction of speed, feed and depth of cut also statistically significant on main cutting force.

Esfe et al. [88] investigated thermal and rheological properties of Al_2O_3 - EG/Water (20%:80%) nanofluid using a three level factorial design in RSM. In this investigation, factors such as temperature, solid particle volume fraction and their combined effect on thermal conductivity and viscosity were studied. They inferred that both the factors have positive effect on thermal conductivity, predicted and experimental results were in good agreement. Montazer et al. [89] examined the influence of process parameters on density of MWCNT-COOH and F-GNP nanofluids for different mass concentration and temperature range (20° to 40°C) using RSM. The quadratic model generated by RSM was used for prediction of density for both the nanofluids. Their experimental results revealed that density of both the nanofluids were increased with increase in mass concentration and reduced with temperature. Esfe et al. [90] investigated the thermo physical properties of thermal conductivity and viscosity of Al_2O_3 -water, CuO -water, SiO_2 -water and ZnO - water nanofluids using RSM and particle swarm optimization technique. They concluded that RSM was the best method for prediction of the thermal conductivity and viscosity compared to particle swarm optimization technique.

Gupta et al. [91] estimated the optimal cutting parameters for three surface roughness values of R_a , R_q and R_z in machining of titanium alloy under nanofluid MQL conditions by applying RSM. The prediction model for the surface roughness was developed with cutting speed, feed rate, approach angle and type of nanofluid as input parameters and machining response of surface roughness as output parameters. They reported that optimum parameters for minimum surface roughness were cutting speed 253 m/min, feed rate 0.14 mm/rev, approach angle 87° and graphite based nanofluid.

2.5 Present Work

In the view of above extensive research work, which is in progress to explore the machining performance in terms of reduction in cutting force, cutting temperature, surface roughness and tool flank wear by using MQL technique. It was shown that vegetable oil based

nano cutting fluid (VOBNCF) have prominent characteristics than CCF and dry machining. In addition to that some of the studies were revealed that HNFs performed well in antifriction, anti-wear properties than nanofluid. However, very few studies were reported by researchers on evaluation of stability for HNFs and application of HNFs in machining. The present work is motivated by the enhanced thermophysical properties, anti-friction and antiwear properties of HNCFs and an attempt is made to understand the performance of HNCFs in turning AISI1040 steel.

Initially HNCFs are prepared by dispersing 1% weight of CNT/BA, CNT/MoS₂ nanoparticles in three vegetable oils (sesame, neem and mahua oil). Three surfactants SDS, TritonX100 and Tween80 are used in preparation of the different HNCFs. The content of surfactant also varied in terms of % weight of nanoparticles in different samples. Hybrid ratio's of (1:1; 1:2; 2:1) are taken in the preparation of these HNCFs. Stability is evaluated by using sedimentation test and Zeta potential test. The best composition of the HNCF is selected based on stability using Taguchi method. Machining performance is also evaluated using the same stable HNCF under constant cutting condition (Cutting speed: 80m/min; feed rate: 0.161mm/rev; depth of cut: 0.5mm) and compared with dry, CCF. MQL flow rate for supplying cutting fluid in machining zone is 10mL/min, later; the preparation of HNCFs is carried out by dispersing CNT/MoS₂ nano sized particles in sesame oil at hybrid ratio of 1:2 in 0.5%, 1%, 1.5%, 2%, 2.5% and 3% (wt.) concentrations. The surfactant sodium dodecyl sulphate (SDS) is used in preparation of HNCFs. The content of SDS is taken as 15% weight of nanoparticles in all concentrations. Stability of prepared HNCFs is evaluated using sedimentation technique. The basic properties such as dynamic viscosity, volumetric heat capacity and thermal conductivity in varying concentration of prepared HNCFs are evaluated. After examining the basic properties, their applicability is tested in machining with AISI1040 steel at constant cutting conditions [92]. The optimal concentration of CNT/MoS₂ is found for lowest coefficient of friction and improving machining performance in terms of reducing cutting forces, temperature, surface roughness and tool flank wear.

Finally, to assess the performance of HNCFs in machining of AISI 1040steel, turning experiments are conducted by varying cutting conditions. Experiments are designed by using RSM technique. Analysis of variance (ANOVA) is performed using Design expert software. Regression models are developed for multiple responses of cutting force (F_z), cutting temperature (T), surface roughness (R_a) and tool flank wear (V_b). Optimization is performed

for multiple responses by using desirability function which converts multi objective into single objective and optimal setting parameters for single objective is found.

Thus the objectives of present work are:

- i. Formulation of hybrid nano cutting fluids with optimum composition for stability. (Base oil, surfactant, hybrid ratio and content of surfactant).
- ii. Evaluation of basic properties of hybrid nanofluids in varying concentration of nanoparticle.
- iii. Evaluation of machining performance using hybrid nano cutting fluids with varying concentration of nanoparticle for machining.
- iv. Evaluation of optimal machining parameters using hybrid nano cutting fluids for better performance in turning.

2.6 Summary

In this chapter influence of cutting conditions on machining performance are reviewed. Adverse effects of CCFs are discussed. Influences of basic properties on machining performance also reviewed. Alternatives to the CCFs, Antiwear and antifriction properties, optimization method and mathematical modeling techniques are discussed. It is observed from the literature that, VOBHNCFs through MQL technique resulted the improved machining performances of different machining process. Thus present work is motivated by enhanced thermo physical properties, antifriction properties of HNFs. Hence, an attempt is made to understand the performance of VOBHNCFs in turning of AISI1040 steel.

Chapter-3

Experimental setup and Experimentation

3.1 Introduction

The Aim of this chapter is to present the details of entire experimental setup and machining experiments used in the present work. In order to check the viability of HNCFs as cutting fluid in machining stability analysis and basic properties are evaluated by using various techniques. Diagrammatic illustration of various equipments, instruments, tools and consumable materials used are presented in detail. The procedure for online and offline measurement of machining responses during and after turning operation is discussed.

3.2 Nanoparticles

Multi walled carbon nanotube and nano powder of molybdenum di sulphide (MoS_2) were procured from the Ishu international (New Delhi) and nano boric acid particles were synthesized in-house from micron size to nanometer scale by using mini ball mill.

Size of the boric acid nanoparticle is calculated with Scherer equation at highest peak of X-Ray Diffraction (XRD) analysis. XRD analysis for the boric acid nanoparticle was performed with (Make: PANALYTICAL) as shown in Fig. 3.1. The sample scanning angle (2θ) and wavelength (λ) used were (6° - 130°) and 1.540598 \AA respectively. The data obtained from the XRD is shown in Fig. 3.2. Highest peak was obtained for boric acid nanoparticle at Two Theta (28.001°) at crystal structure (0 0 2). Particle size was obtained as 80 nm which is approximately $< 100 \text{ nm}$.

Scherer equation:

$$D_p = \frac{0.94 \times \lambda}{B_{\frac{1}{2}} \times \cos \theta} \quad (3.1)$$

Where D_p = Average particle size in mm

$B_{\frac{1}{2}}$ = Line broadening in radianc (FWHM)



Fig. 3.1 X-Ray Diffraction machine

Specifications

Make: PANALYTICAL

Wavelength (λ): 1.540598 Å

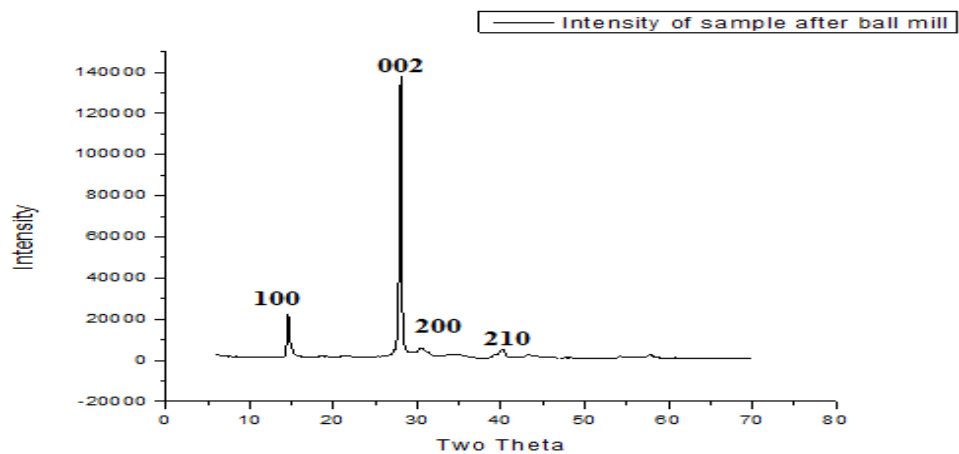


Fig. 3.2 Crystal structure of the boric acid nanoparticle

Size of the outer diameter of CNT is 30 nm as shown in Fig. 3.3 and size of the MoS₂ nanoparticle is 30 nm as shown in Fig. 3.4.

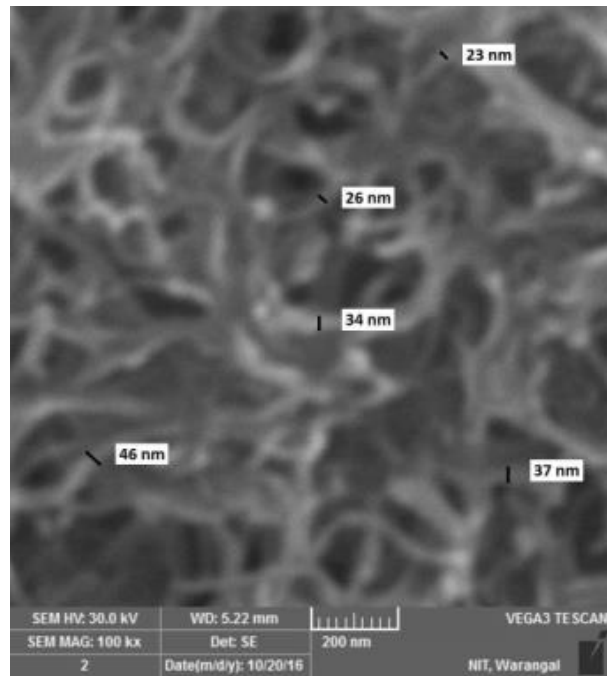


Fig. 3.3 SEM image of CNT

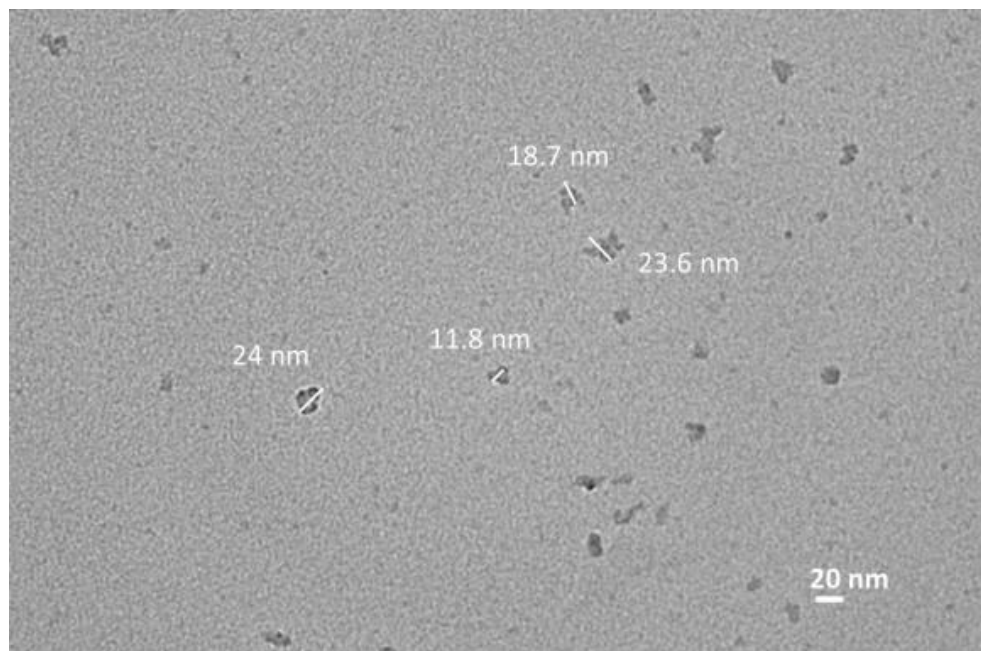


Fig. 3.4 TEM image of MoS₂

3.3 Formulation of hybrid nano cutting fluids

Vegetable oils required for formulation of vegetable oil based nanofluids in present work were procured from local market. Tritonx100, SDS and Tween80 with 5%, 10% and 15% weight of nanoparticles were used as surfactants in formulating VOBHNCFs to enhance the stability of suspensions [2]. In the present work, different VOBHNCFs were formulated

by dispersing CNT/BA, CNT/MoS₂ nanoparticles in sesame, neem and mahua oils at 1% weight along with surfactant in hybrid ratio's of (1:1; 1:2; 2:1). Three different surfactants SDS, TritonX100 and Tween80 were used in preparation of the different hybrid nano cutting fluids samples each at 150 mL. All the samples of hybrid nano cutting fluids were prepared based on Taguchi's L₉ orthogonal array to identify the optimum combination of elements for better stability. Thus prepared hybrid nano cutting fluids were performed manual mixing followed by ultrasonication for 3 hours by using (Piezo-U-sonic, 100W, Ultrasonic processor at 22.54 KHz) to get sable suspensions. These fluids were used for stability analysis for checking the agglomeration of nanoparticle/ sedimentation. After obtaining hybrid nano cutting fluids composition from sedimentation test, prepared six samples of hybrid nano cutting fluids with same method and characterization has been done. Each sample at 50 mL and 100 mL were prepared by varying concentration of CNT/MoS₂ (0.5%, 1%, 1.5%, 2%, 2.5% and 3%) by weight at 1:2 hybrid ratio. 50 mL quantity was taken for testing of basic properties such as thermal conductivity, specific heat and viscosity and 100mL was taken for measurement of coefficient of friction and machining experiments separately. Ultrosonicator used for formulation of HNCFs is shown in Fig. 3.5.



Fig. 3.5 Ultrosonicator

Specifications

Make: Piezo-U-sonic

Power capacity: 100 W

Processor frequency: 22.54 KHz

3.4 Evaluation of hybrid nano cutting fluids composition for stability

3.4.1 Sedimentation test

Dispersion analysis of HNCFs were carried out by using conventional sedimentation test and the results were verified through zeta potential analysis. All the experiments of both CNT/BA and CNT/MoS₂ HNCFs were sonicated thoroughly for at least 1 hour. 150 mL of nanofluid was poured in beakers and then all the samples were allowed to deposit for 156 hours. The status of all the samples was observed for every 12 hour and observations were noted.

3.4.2 Zeta potential test

The Zeta potential test was conducted by collecting 2 to 5 mL of suspensions in measuring cell, then zeta potential value was measured by using nano partica SZ100 series nanoparticle analyzer (Horiba scientific make) ASTM D4185-82 as shown in Fig. 3.6. The measurement was performed at electrode voltage of 3.9 V, temperature of 20°C and measuring time is 50 sec. Each experiment was repeated 3 times and the average value is reported. A solution containing zeta potential in 0 to ± 30 mv range is unstable and rapidly coagulates, ± 30 to ± 40 mv is moderate stability, and ± 40 to ± 60 mV is good stability. When it is more than ± 60 mv the solution is excellent stability [93].



Specifications

Make	: Horiba
Model	: SZ 100
Power supply	: AC 100-240 V, 50/60 Hz, 150 VA

Fig. 3.6 Nano partica SZ100 series nanoparticle analyzer

3.5 Evaluation of basic properties

Measuring the basic properties such as density, thermal conductivity, volumetric heat capacity and viscosity helps in understanding the behavior of the nanofluids or hybrid

nanofluids when apply as cutting fluid in machining. Hybrid nano cutting fluids were prepared and subjected to testing of basic properties like density, thermal conductivity, volumetric heat capacity and viscosity as per ASTM standards.

3.5.1 Density

Density of the base oils and HNCFs was measured with hydrometer (ASTMD4052-96). To ensure the accuracy of the measurements, this instrument was calibrated by measuring the density of the water and then measured the density of the base oils followed by density of the HNCFs. Hydrometer used for measurement of density for the HNCFs is shown in Fig. 3.7.



Specifications

Make : Leimco

Measuring density range: 0.9 to 0.95 g/cc

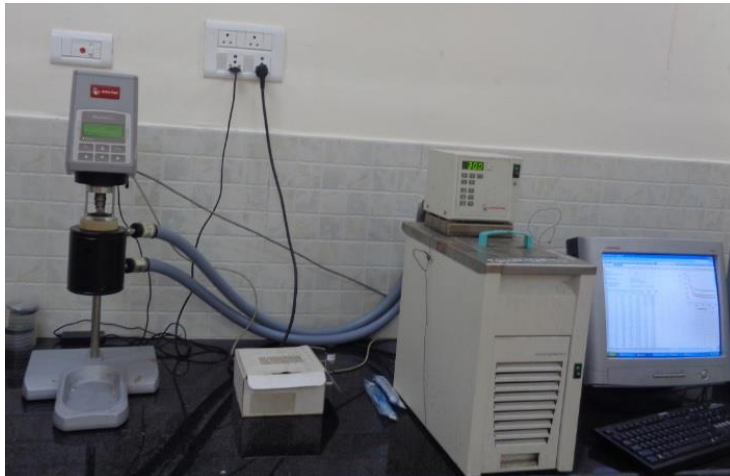
Fig. 3.7 Hydrometer

3.5.2 Dynamic viscosity

Viscosity is the property of the fluid which shows its lubricity. The friction between tool and workpiece influences the cutting forces, while friction between chip-tool interfaces causes the generation of heat in secondary deformation zone. Applying high viscous fluid as cutting fluid in machining can lower the friction due to good lubricity.

Dynamic viscosity of all the samples of the HNCFs was measured with Rheometer (Make: Anton Paar, Model: Rheolab QC, ASTMD440) in temperature range of 30° to 60° in a parallel plate configuration under controlled temperature which is shown in Fig. 3.8. The diameter of the plates is 50 mm and gap is 0.5 mm. The sample was loaded in the gap between the plates and the temperature was controlled with peltier temperature control device which is located below the lower plate. Reading was taken at controlled temperature and

repeated same procedure for rest of the samples with increase in temperature. Rheometer interconnected to the computer which constitutes Rheolab software for obtaining the dynamic viscosity results. The average value of three trials was considered for indicating the measured value.



Specifications

Make : Anton Paar

Model : Rheolab QC

Fig. 3.8 Rheometer

3.5.3 Kinematic viscosity

Kinematic viscosity of the base oil and HNCF was measured with Redwood viscometer-I (ASTMD445) shown in Fig. 3.9. The property of the kinematic viscosity is calculated by using following empirical relation:

$$K_v = A \times t - B / t \quad (3.2)$$

Where $A = 0.026$; $B = 1.72$; t = time required to collect 50 mL sample



Fig. 3.9 Redwood viscometer-I

3.5.4 Thermal conductivity

The property by virtue of which material conducts heat is called as thermal conductivity. The enhancement in thermal conductivity of the fluid imparts good thermal activity when applied as coolant in machining. Dispersion of smaller amount of nanoparticles which is less than 5% by volume in base oil enhances the thermal conductivity of the base fluid to a great extent [94–96]. Enhancement in thermal conductivity of nano fluid helps in extracting heat in machining zone when applied as cutting fluid and gives affirmative machining responses. In the present work, thermal conductivity of base oil and hybrid nano cutting fluids was measured by using Hot disc thermal conductivity analyzer (Make: Hot disk, Model: TPS500, ASTM (D2717) at three temperatures 30°, 40° and 50°. Approximately 50 mL of each sample was taken in beaker and loaded into the sample holder. Sample holder was inserted into the thermal conductivity measurement chamber through a pipe. It was ensured that no air bubbles are stuck while loading the sample of fluid in sample holder. The process of measurement of the thermal conductivity was started after attaining the steady state temperature. Experimental setup for thermal conductivity measurement is shown in Fig. 3.10.



Specifications

Make	: Hot disk
Model	: TPS500
Measuring range	: 0.03 to 100 W/mK (Thermal conductivity)
Measurement Time	: 2.5 to 2560 seconds
Sensor	: Kapton sensor 5465

Fig. 3.10 Hot disc thermal conductivity analyzer

3.5.5 Volumetric heat capacity

The volumetric heat capacity is the heat capacity of a sample of the substance divided by the volume of the sample. Volumetric heat capacity of the base oil and hybrid nano cutting fluid samples was measured with Hot disc thermal conductivity analyzer (Make: Hot disk, Model: TPS500, ASTM (D2717) at three temperatures 30°, 40° and 50° by varying concentrations. It may be useful to calculate specific heat of the hybrid nano cutting fluid by dividing the volumetric heat capacity to density.

3.6 Coefficient of friction

To understand the tribological behavior of HNCF, coefficient of friction was evaluated with pin-on-disc apparatus [22]. Series of experiments were performed by using Pin on disc Tribometer (make: Magnum Engineers, ASTM G 99). The maximum load and speed used in friction test were 200N and 2000rpm. The pin (28 mm length and 10 mm diameter) and disc (165 mm pitch circle diameter and 8 mm thickness) were made up of AISI1040 steel and EN31 steel respectively. During the friction test, the load, speed of disc and measuring time were maintained constant at 40N, 212 rpm and 5min respectively. The wear debris on disc was removed after each experiment with 1000 no. carbon emery paper. The whole experimental setup was cleaned with acetone after each test. The experimental setup for coefficient of friction test is shown in Fig. 3.11.



Fig. 3.11 Pin on disc Tribometer

Specifications

1. Normal load range – up to 200N
2. Sliding speed – 0.26 to 10m/s (disc speed 100 to 3000rpm)
3. Wear disc diameter –160mm (En31 disc 55-60 HRC)
4. Specimen pin diameter/diagonal –dia. 3mm to 12mm
5. Pin length-25 to 30 mm

3.7 Machining experimental setup

Machining was carried out by using lathe under dry, CCF, nanofluid and HNCF lubrication environment respectively. The comparative assessment of the entire lubrication environments was performed at constant cutting conditions in terms of main cutting force, cutting temperature, surface roughness (R_a) and tool flank wear. Cutting conditions were chosen to befit the combinations of tool and workpiece in addition to the availability of machine tool in machine shop for conducting experiment.

3.7.1 Machine Tool

Turning experiments were conducted on variable speed precision lathe machine at constant and variable cutting conditions. This precision Lathe machine was equipped with automatic feed rate and variable spindle speeds. The experimental setup for turning operation is shown in Fig. 3.12.

Specifications of the precision lathe

Make	:	Magnum
Type of the Bed	:	Straight
Swing over the Bed	:	350 mm
Swing over the Carriage	:	200 mm
Distance between centers	:	750 mm
Variable spindle speeds	:	45-1800RPM
Motor capacity	:	10h.p
Type of Chuck	:	Four jaw
Tool post	:	Square headed

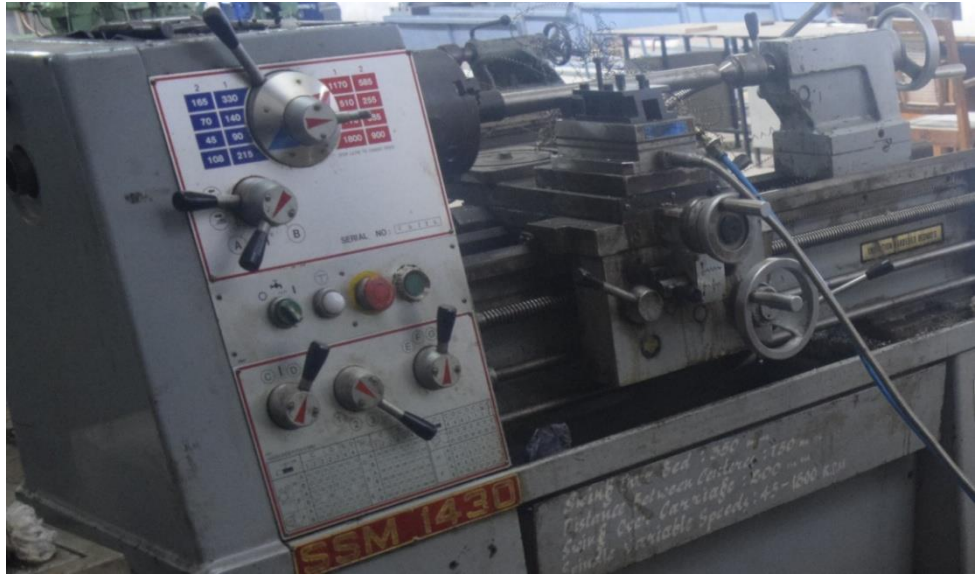


Fig. 3.12 Machining experimental setup for turning

3.7.2 Workpiece material

Turning experiments were performed on lathe with AISI1040 steel of uniform dimensions. The chemical composition and dimensions of AISI1040 steel is depicted in Table 3.1 and machined workpiece is shown in Fig. 3.13.

Table 3.1: Composition of AISI 1040 steel [18]

Composition:				
C%	Mn%	Si%	S%	P%
0.36-0.45	0.6-1.0	0.2-0.3	0.025	0.015
Dimensions and hardness of the material				
(Ø40 mm & 475.2mm length, Hardness: 30±2 HRC, heat treated)				



Fig. 3.13 AISI1040 steel workpiece material

3.7.3 Tool holder and Cutting tool inserts

To conduct the turning experiments on lathe, tool holder and cutting tool inserts were selected based on hardness of the workpiece material and cutting conditions. The tool holder has a thermocouple provision to measure the temperature in cutting zone. Tool holder and inserts are presented with Fig. 3.14.

Specifications of tool holder and tool inserts

Tool holder

Designation : PCLNR 2525M12

Make : Widia

Tool insert

Designation : CNMG 120408 uncoated carbide

Inclination angle : -6°

Orthogonal rake angle : 6°

Orthogonal clearance angle : 6°

Auxiliary cutting edge angle : 15°

Principle cutting edge angle : 75°

Nose radius : 0.8 mm

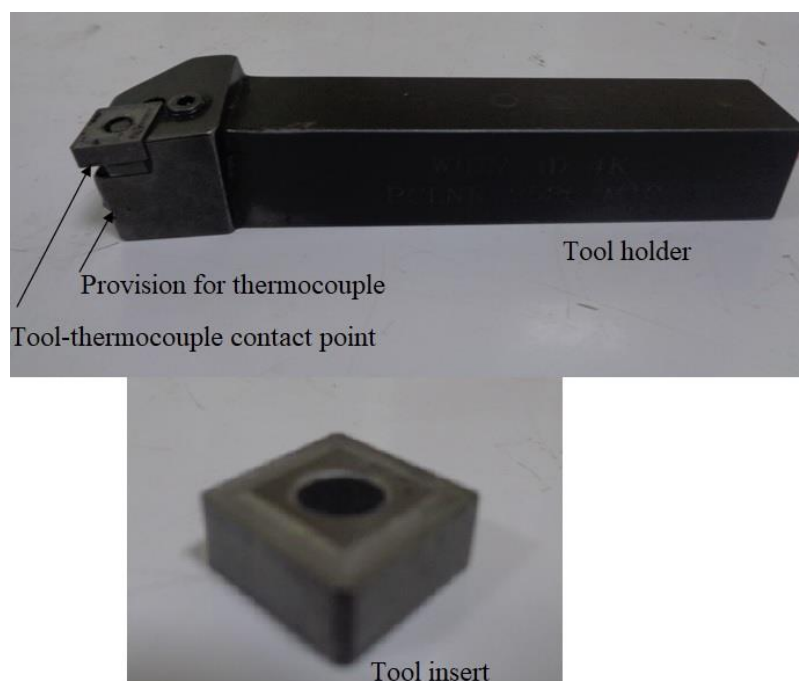


Fig. 3.14 Tool holder and tool insert

3.7.4 Lubricant environment and cutting conditions

In order to assess the performance of the HNCFs, comparative assessment is made by conducting turning experiments at same cutting conditions with dry, conventional cutting fluids, nanofluids and hybrid nano cutting fluid environment. In order to assess the machining performance with HNCF, the turning experiments were conducted in varying cutting conditions. Lubrication environment, constant and variable cutting conditions are presented in Table 3.2.

Table 3.2 Cutting conditions and lubrication environment [97]

Lubrication environment	Dry, conventional cutting fluid, nanofluid, hybrid nano cutting fluid
Constant cutting conditions	
Cutting speed (m/min)	80
Feed rate(mm/rev)	0.161
Depth of cut(mm)	0.5
Variable cutting conditions	
Cutting speed (m/min)	60, 80, 100
Feed rate(mm/rev)	0.131, 0.16, 0.191
Depth of cut(mm)	0.5, 0.75, 1

3.7.5 Supply of hybrid nano cutting fluids in MQL

In the current study initially turning experiments were conducted under dry condition, followed by conventional cutting fluid. The performance of nanofluid and hybrid HNCFs was tested in machining by supplying with MQL unit which is shown in Fig. 3.15. MQL is the most versatile technique, which supplies the minimum volume of fluid to exact cutting area through nozzle with pressurized compressed air [11]. The flow rate of MQL employed is 10 mL/min for supplying combination of vegetable oil and air in cutting area, so that the fluid can be sprayed on metal workpiece by mist generation for providing effective cooling and lubrication [47]. Each turning operation is performed approximately 3-5 minutes and three trials were run with each lubricant condition.

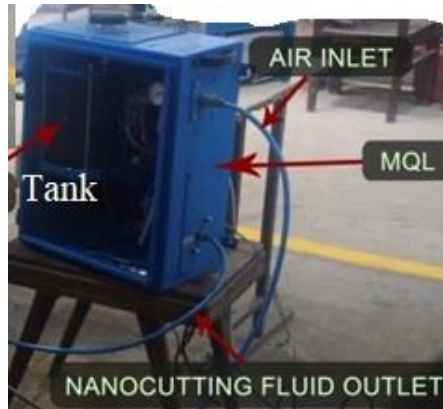


Fig. 3.15 Minimum Quantity Lubrication system

3.8 Measurement of machining performance

Cutting forces, cutting temperature, surface roughness and tool flank wear were measured with various equipments online and offline during and after turning operation at constant and variable cutting conditions in different lubrication environments.

3.8.1 Cutting forces

In the present work cutting forces were measured online by using kistler make piezo electric dynamo meter as shown in Fig. 3.16 which is fixed to lathe machine. The forces obtained along x, y and z directions are represented by F_x , F_y and F_z which were tracked by Dynoware software. A charge amplifier of 5070 type was employed to display the values of the forces which indicate the status of force measurement for a time period of regular interval in seconds.



Fig. 3.16 Multi components dynamometer

Specifications

Make : Kistler
Type : 9257B
No. of components: $F_x, F_y, F_z, M_x, M_y, M_z$
Charge Amplifier : Type 5070
Dimension : 140 mm X 170 mm X 60

3.8.2 Cutting temperature

Generated heat during machining influences the cutting temperature. To assess the temperature in cutting zone, K-type embedded thermocouple with a range of (0-1200°C) was used to measure the temperature of insert at a nodal point. Digital indicator was used to display hot junction temperature of thermocouple. Since it is challenging task to measure the exact temperature in cutting zone during machining, nodal temperature was measured at a remote point (Fig 3.14) at a distance of 5 mm from the tool tip. These are only representative of nodal temperature but not exact cutting tip temperature. Each experiment was repeated in 3 times and average value is considered. Setup for temperature measurement is shown in Fig.

3.17.

Specifications

Make: Industrial furnace & control
Digital temperature indicator with 02 points
Range: (0 to 1200°C)

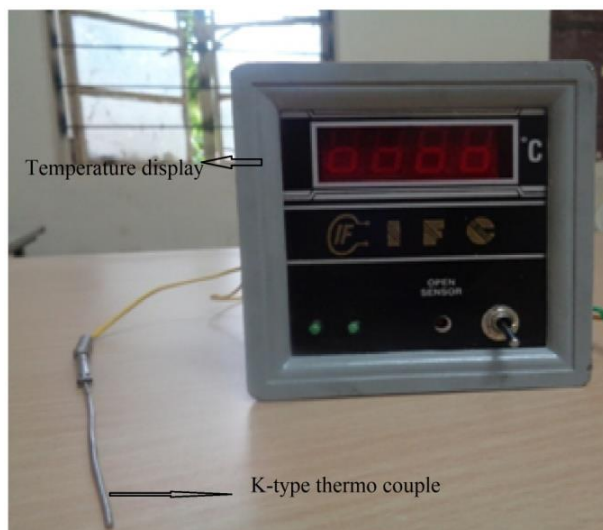


Fig. 3.17 Setup for temperature measurement

3.8.3 Surface roughness (R_a)

Taylor Hobson portable surface roughness tester was used to measure the surface roughness of the machined parts at different locations around the circumference of the machined surface. This is contact type measurement equipment, as the stylus moves along the surface; transducer converts the movements into a signal which is then displayed and further converts to any of the roughness parameter. The Taylor Hobson portable surface roughness tester is shown in Fig. 3.18.

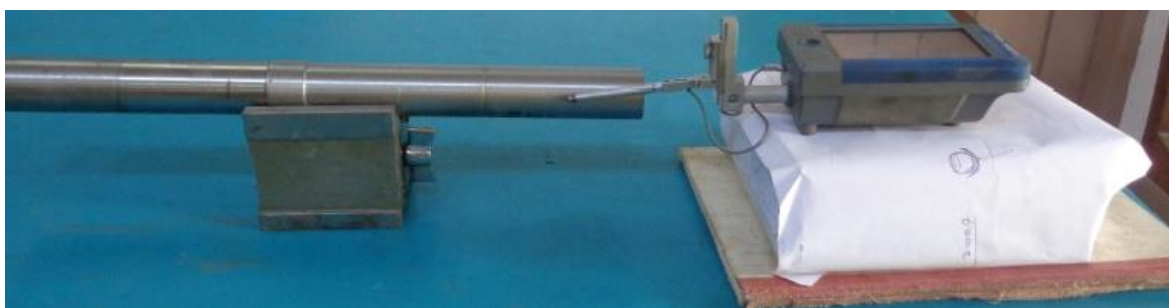


Fig. 3.18 Surface roughness tester

Specifications

Model no	: Surtronics128
Stylus tip radius	: 5 μm
Cutoff length	: 5 mm

3.8.4 Tool flank wear

After each and every turning operation cutting tool undergoes loss of material it is called as wear. The loss of the materials just below the cutting edge and on flank face is said to be tool flank wear which is measured offline by using tool maker's microscope (Mitutoyo make). The tool insert is placed on sample table of tool maker's microscope and marked the wear land on flank face which gives precise value of tool flank wear [98]. Tool maker's microscope is shown in Fig. 3.19.

Specifications

Make	: Mitutoya
Model	: TM505
Glass Stage Size	: 190 mm x 160 mm
Measurement method	: Digimatic Micrometer Head
Max. Workpiece height	: 120 mm



Fig. 3.19 Tool maker's microscope

The schematic representation of the experimentation in the present study is shown in Fig.3.20.

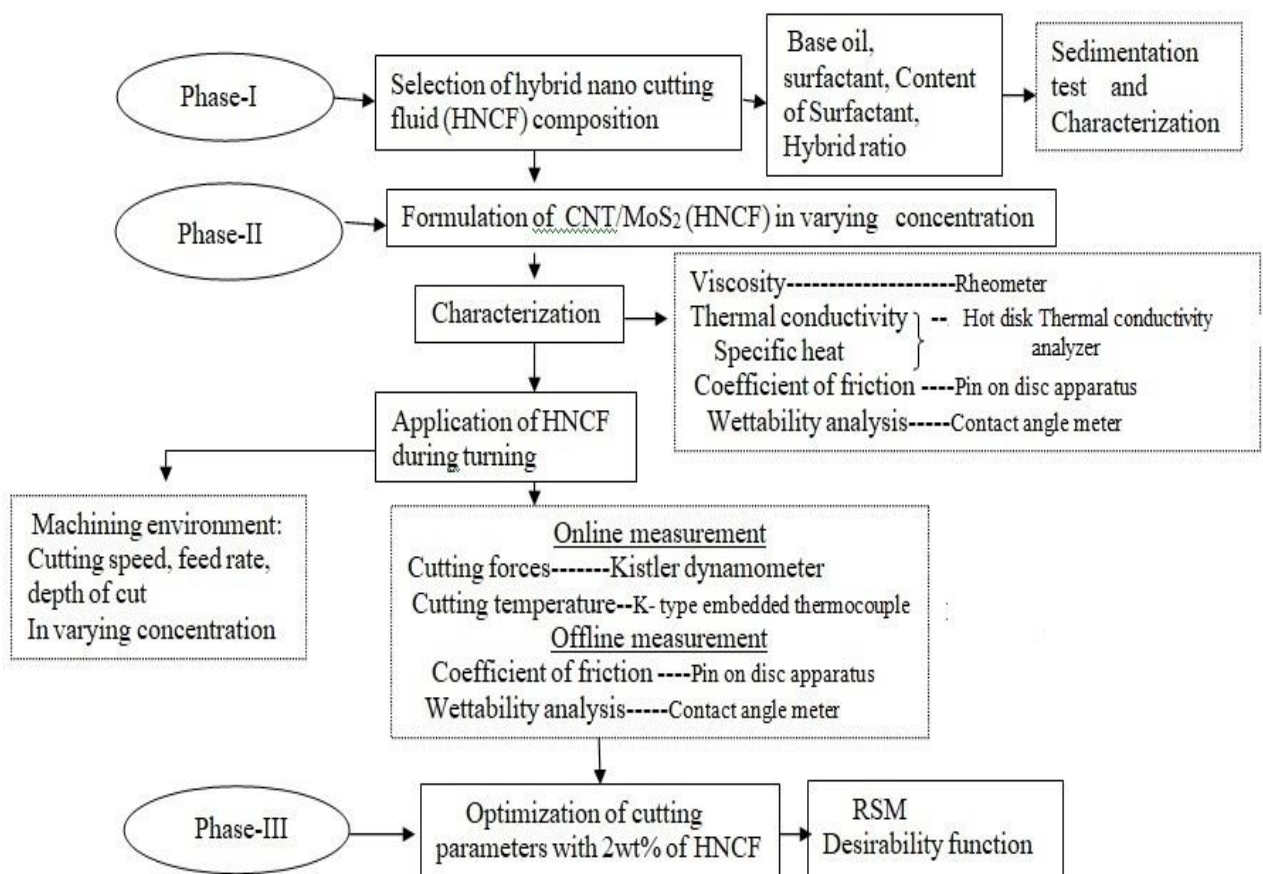


Fig.3.20 Schematic representation of experimentation

3.9 Summary

Thus, in the present study, at first stability analysis through sedimentation test and zeta potential analysis was carried out and followed by evaluation of basic properties of hybrid nano cutting fluids. Comparative assessment is made with hybrid nanocutting fluid during turning of AISI1040 steel under various lubrication environments. Measurement of machining responses is done by tracking cutting forces, cutting temperature, surface roughness and tool flank wear of machined workpiece online and offline.

Chapter- 4

Formulation of hybrid nano cutting fluids with optimum composition for stability (base oil, surfactant, hybrid ratio and content of surfactant)

4.1 Introduction

Nanofluids lose their potential transfer heat due to settling of nanoparticles over the time. Therefore, investigation on stability of nanofluid is essential which can alter the thermo-physical properties for application. It is very essential to analyze the influencing factors to the stability of nano fluids prior to testing their application in machining. This chapter presents the evaluation of stability of VOBHNCFs through sedimentation method and zeta potential analysis followed by basic properties. Applicability of stable hybrid nano cutting fluids is tested during turning of AISI 1040 steel at constant cutting conditions. Results are compared with dry and conventional cutting fluids.

4.2 Selection of vegetable oils

Performance of vegetable oils as cutting fluids in machining is largely depends on physical properties which include, viscosity index [99], kinematic viscosity [100], flash point [101], iodine value and density. A better lubricant should have properties of higher kinematic viscosity, high flashpoint and lower pour point. Chemical/ physical properties of vegetable oils are mainly depends on composition and structure of vegetable oils.

Vegetable oils consist of glycerol structure in which fatty acids are connected to polar hydroxyl group via ester linkages. Fatty acids in vegetable oils are saturated and unsaturated fatty acids. As explained in previous section 1.7.5, only single bonding is present between their carbon chains (-C-C-) of SFAs, where as more than one double bonding is existing in an USFAs. The fewer number of carbons in their chain up to (C_{12:0}) are the short and medium chain fatty acids. More than 16 carbons present in the chain (C_{16:0}) is the long chain fatty acids. For SFAs, surface area of a molecule in the film is 20.5A², which is unrelated to number of carbon atoms in the molecule. When the carbon number in their chain is up to 16, absorption capacity reaches to a largest value. Therefore antiwear and antifriction properties

are consistent for the fatty acids over the C₁₆. However, for USFAs, absorption film strength is poor due to unsaturated oilefinic bonds exist in the molecule [71].

Comparing saturated with unsaturated fatty acids in vegetable oils at same carbon number, USFAs posses low absorption film strength and lubricity property. But cohesive forces/ attractive forces among the unsaturated fatty acids are proportional to the carbon atom number in the molecule. The absorption film strength and lubricating property of the unsaturated fatty acids with long chain are better than unsaturated short chain fatty acids [71]. The percentage of unsaturation is varies for different types of vegetable oils, this can be determined by measuring iodine value. Higher the percentage of unsaturation, better the vegetable oil can be environmental friendly nature [102]. The general glycerol structure of vegetable oils is shown in Fig. 4.1. Unsaturated long chain fatty acids of oleic (C_{18:1}), linoleic (C_{18:1}) and Linolenic acids (C_{18:3}) in vegetable oils are potential candidates to form high strength durable layer of film on contacting surfaces. Polar long chain fatty acids in vegetable oils provide high strength of lubricant film that can interact strongly with metallic surfaces and reducing friction and wear. Hence, three vegetable oils with USFAs of long chain are selected in the present work. Typical chemical compositions of three different vegetable oils (sesame oil, neem oil and mahua oil) are depicted in Table 4.1[18, 102].

Table 4.1 Composition and structure of vegetable oil

Fatty acids	Sesame oils	Neem oils	Mahua oils	Fatty acids length
% of Saturated fatty acids in Three Vegetable oils				
Palmatic acid	7.9-12	19	23.7-24.7	C16:0(Long chain)
Stearic acid	3.9-6.7	20.42	19.3-29	C18:0(Long chain)
Arachidic acid		3.59	2	C20:0(Long chain)
% of Unsaturated fatty acids in Three Vegetable oils				
Oleic acid	35.9-43.7	20.46	36.3-43.3	C18:1(Long chain)
Linoleic acid	38.6-48.9	34.69	11.6-15.8	C18:2(Long chain)
Linolenic acid	Max.0.6	0.44		C18:3(Long chain)

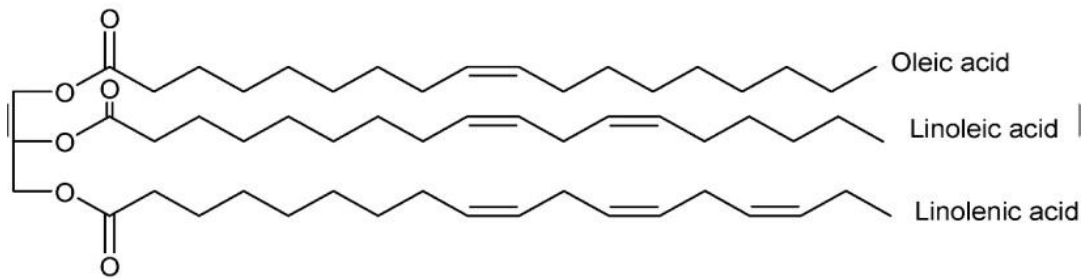


Fig. 4.1 Structure of vegetable oil [102]

4.3 Experimental design

During experimentation CNT/BA, CNT/MoS₂ hybrid nanoparticles are coded as (p:q), (p:r) respectively. For example (1:1) presents mass ratio of CNT, BA or CNT, MoS₂. Nanofluids are formulated as per L₉ orthogonal array by taking 4 factors such as base oil, surfactant, concentration of surfactant (% nanoparticles weight) and hybrid ratio at 3 levels each as shown in Table 4.2. Basic properties such as density, kinematic viscosity of these nine hybrid nanofluids are examined and stability analysis is carried out with sedimentation test and zeta potential test. Machining experiments are conducted at constant cutting conditions by applying best dispersion characteristics of hybrid nano cutting fluids with MQL technique.

Based on “Orthogonal array” experiments Taguchi has developed a method, which gives less variance and optimal control factors for the minimum number of experiments. Being logarithmic functions of the desired output Taguchi’s Signal-to-Noise (S/N) ratio used as objective function for optimization. As per quality characteristic parameters, there are 3 categories of the S/N ratios for optimization namely: (a) Smaller – the – better (b) Nominal the best (c) Larger- the better. In the present work Zeta potential value is the response or output parameter for optimization. The zeta potential value is to be maximum for stable hybrid nanofluids. Hence larger the better criterion is considered for Zeta potential value.

Larger – the – better

$$\text{S/N ratio } (\eta) = -10 \log_{10} \left(\frac{1}{n} \sum_{i=1}^n \frac{1}{y_{ij}^2} \right) \quad \text{----- (4.1)}$$

Where ‘ y ’ is the response parameter and ‘n’ is the number of replications of each trial ‘i’.

ANOVA is the statistical technique to find the significant factor. It gives the clear picture of the effect of each factor on machining response.

Table 4.2. Factors and levels

Factors	Levels		
	1	2	3
Base oil	SS	Neem	Mahua
Surfactant(SF)	Tritonx100	SDS	Tween80
Con.of SF (% of np wt.)	5	10	15
Hybrid ratio	1:1	1:2	2:1

4.4 Basic properties

Density is the one of the vital parameters which is used to calculate the specific heat and heat transfer properties of the nanofluids. Viscosity is a rheological property of the fluids, which resist the flow of fluid. The phenomenon of the development of the friction between the sliding surfaces and consistent layer of lubricant to separate contacting surfaces are depends on kinematic viscosity of the lubricant being supplied. The basic property of the viscosity is used to assess the behavior of the nanofluid more prominently when they are used as cutting fluids in machining applications.

The kinematic viscosity and density of CNT/BA and CNT/MoS₂ hybrid nano cutting fluids are measured by using redwood viscometer-I and hydrometer as per ASTM standards. Corresponding results of both hybrid nano cutting fluids are presented in Table 4.3 and Table 4.4 respectively. The enhancement in density of both CNT/BA and CNT/MoS₂ hybrid nano cutting fluids is found with Mahua oil among three base oils. This may be due to molecular weight and chemical composition of Mahua oil compared to sesame and neem oils [103].

The Mahua oil with CNT/BA and CNT/MoS₂ hybrid nanoparticles resulted in maximum kinematic viscosity to that of sesame oil and neem oil based hybrid nanofluids. The inner molecular structure of mahua oil, external forces of the fluid substance and ambient conditions (temperature, pressure) are favored for this. It can be seen that kinematic viscosity of both the hybrid nano cutting fluids is decreased with increase in temperature. The molecules of liquid are tightly bonded together due to high intermolecular forces at low temperature. Therefore, kinematic viscosity of the hybrid nano cutting fluids is large at low temperature. The weakening of intermolecular forces with increase in temperature tends to rise the movement of the particle in liquids and causes for the enhancement in kinetic thermal energy of the particle in sollution [104]. Therefore, kinematic viscosity is reduced. Low

kinematic viscosity of the nanofluid at high temperature enhances the heat dissipation, thus improves the film forming capability between contacting surfaces.

Table 4.3 Kinematic viscosity and density of CNT/BA hybrid nanofluid

S.No	Factors			Kinematic Viscosity ($10^{-6} \text{ m}^2/\text{s}$)			Density g/cc	
	Base oil	SF	(Con. of SF wt.% np.)	Hybrid ratio	40°	50°		
1	SS oil	Triton x100	5	1:1	52.87	39.2	31.72	0.922
2	SS oil	SDS	10	1:2	51.63	41.69	31.72	0.92
3	SS oil	Tween 80	15	2:1	51.13	35.72	28.22	0.921
4	Neem oil	Triton x100	10	2:1	50.14	39.2	28.72	0.921
5	Neem oil	SDS	15	1:1	54.11	39.11	29.22	0.922
6	Neem oil	Tween 80	5	1:2	48.65	33.72	26.2	0.92
7	Mahua oil	Triton x100	15	1:2	59.07	46.67	34.22	0.926
8	Mahua oil	SDS	5	2:1	64.02	47.9	35.47	0.932
9	Mahua oil	Tween 80	10	1:1	50.39	47.9	34.97	0.931

Table 4.4 Kinematic viscosity and density of CNT/MoS₂ hybrid nano cutting fluid

S.No	Factors			Kinematic Viscosity ($10^{-6} \text{ m}^2/\text{s}$)			Density g/cc	
	Base oil	SF	(Con. of SF wt.% np.)	Hybrid ratio	40°	50°		
1	SS oil	Triton x100	5	1:1	49.15	37.71	30.47	0.93
2	SS oil	SDS	10	1:2	46.67	35.47	29.22	0.925
3	SS oil	Tween 80	15	2:1	55.36	40.45	29.22	0.926
4	Neem oil	Triton x100	10	2:1	49.15	37.21	28.73	0.922
5	Neem oil	SDS	15	1:1	51.63	37.96	23.72	0.924
6	Neem oil	Tween 80	5	1:2	51.13	31.97	22.89	0.92
7	Mahua oil	Triton x100	15	1:2	50.39	42.93	29.73	0.926
8	Mahua oil	SDS	5	2:1	56.8	42.93	29.73	0.933
9	Mahua oil	Tween 80	10	1:1	55.35	41.69	29.22	0.925

From table 4.3 and table 4.4, it is observed that sesame oil and neem oil based hybrid nano cutting fluids resulted in moderate properties of kinematic viscosity and density compared to mahua oil based hybrid nano cutting fluids. The sesame oil based CNT/MoS₂ hybrid nano cutting fluid resulted in slightly improved properties of kinematic viscosity and density at the temperature of 40° C compared to CNT/ BA hybrid nano cutting fluid. This may be due to high amount of Oleic and Linoleic fatty acids in the chemical composition of sesame oil, external forces of the fluid substance and ambient conditions (temperature, pressure).

Both neem oil based CNT/BA and CNT/MoS₂ hybrid nano cutting fluids have shown moderate properties such as kinematic viscosity and density than mahua oil based hybrid nano cutting fluids at the temperature of 40°C (Table 4.3 and 4.4) . Lower amount of cohesive forces in the chemical composition of neem oil are the reason for this.

4.5 Stability of hybrid nano cutting fluid

Stability analysis of both CNT/BA, CNT/MoS₂ hybrid nano cutting fluids is carried out by using sedimentation test and zeta potential test. Taguchi's orthogonal array is used in designing the experiments by varying vegetable oils, surfactant and its content and hybrid ratio of nanoparticle.

The sedimentation results of CNT/BA hybrid nano cutting fluids after 156 hours of sedimentation time is presented in Table 4.5. The sesame oil based nanofluids with sample 1 show that moderate sedimentation whereas sample 2 and sample 3 showed more sedimentation. Neem oil based nanofluids with sample 4 and sample 6 noticed more sedimentation whereas sample 5 noticed that moderate sedimentation. The mahua oil based nanofluids with sample 7, sample 8 and sample 9 showed no more sedimentation. Some samples among the nine samples noticed very less or moderate sedimentation for the period of 156 hours due to addition of surfactants along with nanoparticle dispersion in base oil. Among the three vegetable oils, mahua oil based nanofluids has showed no sedimentation but solid form of bubbles/particles is observed on top surface of the fluids. This may be due to suspended particles of boric acid in mahua oil and saturated fatty acids in mahua oil.

The zeta potential value of CNT/BA hybrid nano cutting fluid is measured by using nano partica SZ100 series nanoparticle analyzer and corresponding results are presented in Table 4.6. Sedimentation results are in good agreement with the Zeta potential values for all tested samples. Samples with no sedimentation are given highest Zeta potential values in the

range of ± 50 mv and above. Samples with sesame oil and neem oil based nanofluids have given lesser zeta potential value than required range. This may be due to higher attractive forces between nanoparticles which are more advanced to repulsion force which leads to agglomeration and settling of nanoparticle [18]. Mahua oil based nanofluids has given required range of zeta potential values [105, 106]. Hence these samples are said to be stable.

The status of sedimentation for CNT/MoS₂ hybrid nano cutting fluid is presented in Table 4.7. From the results it is observed that sesame oil based nanofluids with sample 2 and sample 3 noticed no sedimentation for entire period of 156 hours, whereas sample 1 showed very less sedimentation. Neem oil based nanofluids with samples 4, 5 and 6 noticed more sedimentation. The strong attractive wander wall forces between the particles present in the base oil could be the reason for settling of nanoparticle at bottom surface of the beaker as shown in Fig. 4.2 [107]. From the mahua oil based nanofluids it is observed that the sample 9 is stable and uneven dispersion is observed in sample 7 and sample 8. This is due to mahua oil, which is worsening with longer storage time [19].

The zeta potential values of the CNT/MoS₂ hybrid nanofluids are presented in Table 4.8. The results of zeta potential values of hybrid nano cutting fluids are in good agreement with literature [108,109]. Surfactants of SDS and Tween 80 with concentration of 10%, 15% by weight of CNT/MoS₂ nanoparticles in sesame oil shown maximum value of the zeta potential among all cases. This shows excellent stability. These results also good agreements with sedimentation test results. Neem oil based nanofluids with samples 4, 5 and 6 has given very less zeta potential values, which means that hybrid nanoparticles in base oils are unstable. Samples 7, 8 and 9 with mahua oil nanofluids also given satisfactory zeta potential values.

Comparing CNT/MoS₂ and CNT/BA hybrid nano cutting fluids, CNT/MoS₂ hybrid nano cutting fluids has given magnitude of larger zeta potential values. Sesame oil based CNT/MOS₂ hybrid nano cutting fluids with sample 2 and sample 3 has given magnitude of highest zeta potential values (96.1 mV, 105.4 mV) compared to mahua oil based CNT/MOS₂ hybrid nano cutting fluids. This may be due to the interface bonding between the nanoparticle and base fluid supported by the surfactant and minimum agglomeration of nanoparticles. [110]. A surfactant can coat the nanoparticles and stop them from aggregation by reducing interfacial tensions or causing repulsive force between nanoparticles [111].

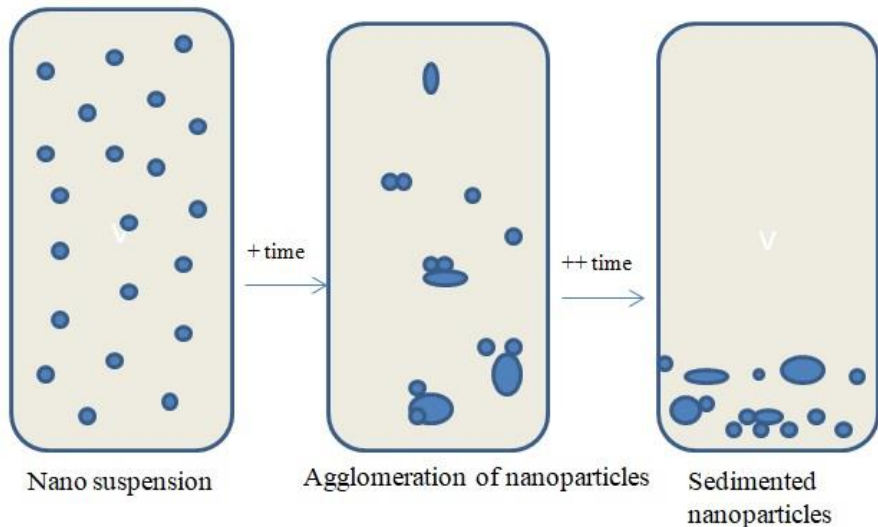


Fig. 4.2 Schematic representation of sedimentation of nanofluid over time

Table 4.5 Results of sedimentation test for CNT/BA hybrid nano cutting fluid (156 hr)

Image of the sample	Observed sedimentation level
	<ol style="list-style-type: none"> 1. Moderate sedimentation 2. More sedimentation 3. More sedimentation
	<ol style="list-style-type: none"> 4. More sedimentation 5. Moderate sedimentation 6. More sedimentation
	<ol style="list-style-type: none"> 7. Very less sedimentation. But foaming is observed on top surface which leads to degradation. 8. No sedimentation. But foaming is observed on top surface which leads to degradation. 9. No sedimentation. But foaming is observed on top surface which leads to degradation.

Table 4.6 Zeta potential values of CNT/BA hybrid nano cutting fluid

Experime ntal run	Base oil	SF	Factors		Zeta potential Value (mv)
			Con. Of SF(% np wt.)	Hybrid ratio	
1	SS oil	Triton x100	5	1:1	36.4
2	SS oil	SDS	10	1:2	31.7
3	SS oil	Tween 80	15	2:1	28.6
4	Neem oil	Triton x100	10	2:1	32.3
5	Neem oil	SDS	15	1:1	41.8
6	Neem oil	Tween 80	5	1:2	29.5
7	Mahua oil	Triton x100	15	1:2	57.1
8	Mahua oil	SDS	5	2:1	64.7
9	Mahua oil	Tween 80	10	1:1	53.9

Table 4.7 Results of sedimentation test for CNT/MoS₂ hybrid nano cutting fluid (156 hr)

Image of the sample	Observed sedimentation level
	<p>1. Moderate sedimentation</p> <p>2. No sedimentation</p> <p>3. No sedimentation</p>
	<p>4. More sedimentation</p> <p>5. More sedimentation</p> <p>6. More sedimentation</p>
	<p>7. Very less sedimentation. But foaming is observed on top surface which leads to degradation.</p> <p>8. No sedimentation. But foaming is observed on top surface which leads to degradation.</p> <p>9. No sedimentation. But foaming is observed on top surface which leads to degradation.</p>

Table 4.8 Zeta potential values of CNT/MoS₂ hybrid nano cutting fluid

Experime ntal run	Base oil	SF	Factors		Zeta potential Value (mv)
			Con. of SF(% npi wt.)	Hybrid ratio	
1	SS oil	Triton x100	5	1:1	-77.2
2	SS oil	SDS	10	1:2	96.1
3	SS oil	Tween 80	15	2:1	105.4
4	Neem oil	Triton x100	10	2:1	22.5
5	Neem oil	SDS	15	1:1	-42.7
6	Neem oil	Tween 80	5	1:2	-37.7
7	Mahua oil	Triton x100	15	1:2	-106.8
8	Mahua oil	SDS	5	2:1	-67.6
9	Mahua oil	Tween 80	10	1:1	-54.4

Further analysis is carried out using Taguchi's S/N ratio technique by perceiving larger the better criterion for finding optimized conditions and its influence on zeta potential value. Table 4.9 presents the responses for S/N ratio on zeta potential values of CNT/MoS₂ hybrid nano cutting fluid. From the results, it is found that the base oil has more influence on zeta potential value and followed by concentration of surfactant, hybrid ratio and type of surfactant. The optimized parameters on zeta potential values are found to be peak values of Fig 4.3, which are sesame oil, SDS, 15% concentration of SDS and the hybrid ratio (1:2). The ANOVA analysis is used in finding the significant effect of each parameter on zeta potential value. From ANOVA, it is found that the order of contribution on zeta potential value is the base oil (77%), concentration of surfactant (15.3%), hybrid ratio (6.5%) and surfactant (1.2%) (Table 4.10).

Table 4.9 Analysis of mean for S/N ratios for Zeta potential value

Level	Base oil (A)	SF(B)	Con. Of SF (% of npi wt) (C)	Hybrid ratio(D)
1	39.34	35.12	35.29	35.02
2	30.39	36.29	33.80	37.25
3	37.29	35.62	37.94	34.76
Max-Min	8.95	1.16	4.13	2.49
Rank	1	4	2	3
Optimum	A ₁	B ₂	C ₃	D ₂

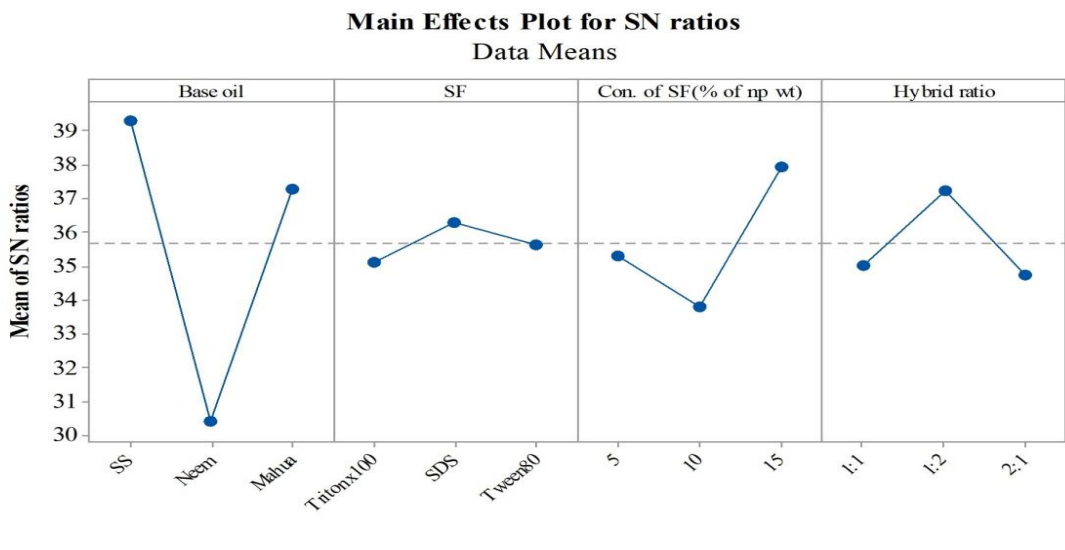


Fig.4.3 Main effect plot for zeta potential values of CNT/MoS₂ hybrid nano cutting fluid

Table 4.10 ANOVA for Zeta potential values (S/N data) of CNT/MoS₂ hybrid nano cutting fluid

Source	Degrees of freedom	Sum of squares	Mean squares	% contribution
Base oil	2	131.969	65.9847	77
SF	2	2.049	1.0245	1.2
Con. Of SF (% of npi wt)	2	26.285	13.1423	15.3
Hybrid ratio	2	11.249	5.6246	6.5
Residual error	0			
Total	8	171.552		100

Confirmation test has been done using sedimentation test and zeta potential test with obtained optimal parameters (sesame oil, SDS, 15% concentration of SDS and hybrid ratio (1:2)) from Taguchi analysis. 80 mL net quantity of CNT/MoS₂ hybrid nano cutting fluid at 1 wt % is used for confirmation test. Status of the sedimentation test after 156 hours of sedimentation time is shown in Fig. 4.2(a), zeta potential test result is shown in Fig. 4.4(b). No sedimentation has been observed for 156 hours time and highest zeta potential value is observed to be 107.5mv. Result obtained by both zeta potential test and sedimentation test is in good agreement with literature [112]. Therefore, it is said to be excellent stability.

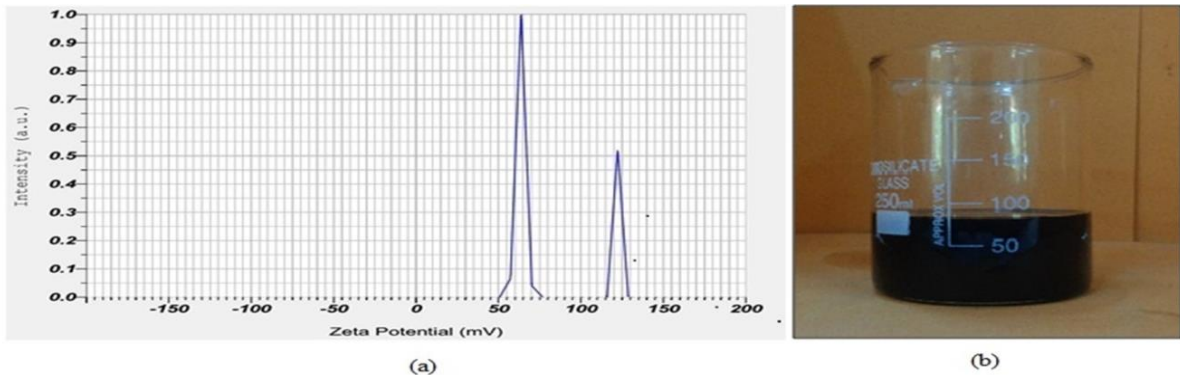


Fig. 4.4 (a)- Zeta potential report of CNT/MoS₂ hybrid nano cutting fluid

(Zeta potential at peak 1 is 122.0mv; at peak2 is 63.4mv; mean value is 107.5 mv
Electrophoretic mobility mean: 0.000831 cm² /vs)

(b) - Sedimentation of confirmation sample after 156 hours of sedimentation time.

4. 6. Selection of cutting fluids

Mahua oil based hybrid nano cutting fluid is shown improvement in kinematic viscosity and density than sesame and neem oil based fluids. However, it has shown poor stability compared to sesame oil based hybrid nano cutting fluids. The results of kinematic viscosity and density of sesame oil based hybrid nano cutting fluids are also closer to the mahua oil based hybrid nano cutting fluids and it is found to be stable for the longer duration of time 156 hours. In the present work, our primary concern in selection of hybrid nano cutting fluid is the stability for prior testing of their application in machining. Hence, based on the study of stability and these basic properties, we have chosen sesame oil based CNT/MoS₂ hybrid nano cutting fluid for the further analysis.

4.7 Machining performance

Machining is carried out at constant cutting conditions ($V = 80$ m/min, $f = 0.161$ mm/rev and $d = 0.5$ mm) with dry, CCF and HNCF environments. 1 wt% concentration of sesame oil based HNCF with 1:2 CNT/MoS₂ hybrid nanoparticles ratio, at 15% concentration of SDS surfactant by weight of nano particles is used in machining under MQL condition, based on stability analysis. Flow rate of MQL is maintained at 10 mL/min. The cutting force, cutting temperature, tool flank wear and surface roughness are measured to evaluate the performance of the HNCF in machining.

4.7.1 Cutting force (F_z)

Cutting force influences the power and specific energy consumption in machining process. The main cutting force is measured online for all considered conditions of the lubrication in machining. Fig. 4.5 represents the main cutting force values while machining with different lubrication environments. High cutting force (352.8 N) is observed in dry machining followed by conventional cutting fluid (330 N) and hybrid nano cutting fluid (265.4 N). The percentage reduction in main cutting force by the application of hybrid nano cutting fluid (1% of CNT+MoS₂ (1:2), 15% SDS, sesame oil) is 20% and 25% respectively compared to CCF and dry machining.

Vegetable oils contain polar atoms such as S, O, N, P or polar groups of COO, COOH, COR and OH in molecular structure as shown in Fig.4.6. These polar atoms/ groups are having high affinity to the workpiece surface to adsorb molecule on workpiece surface through intermolecular forces to form physical adsorption film [71]. This is mostly found in vegetable oils due to unsaturated type fatty acids. The more number of carbons in the chain provides more strength to the film [113]. High percentage of unsaturated long chain oilic and linoleic fatty acids present in sesame oil helps to form physical adsorption film. This enable to reduce the coefficient of friction on contacting surfaces thereby reduced cutting force [18]. Layered structure of the MoS₂ nanoparticles can easily adsorbed and forms consistent film on contact surfaces due to weak bonding between the layers and strong bonding within the layer. This phenomenon along with kinematic viscosity of the base oil is helped to reduce the coefficient of friction and thereby reduced the cutting force. The mechanism of MoS₂ solid lubricant during film formation on contacting surfaces is shown in Fig. 4.7. MQL supplies the aerosolization of coolant into the exact cutting zone with high pressure, which can penetrate into the cutting zone and enables to increase the shear plane angle thus reduce the cutting force [92]. Hence, reduction in cutting force is attributed to combined effect of CNT and MoS₂ hybrid nanoparticle in sesame oil and MQL technique [8].

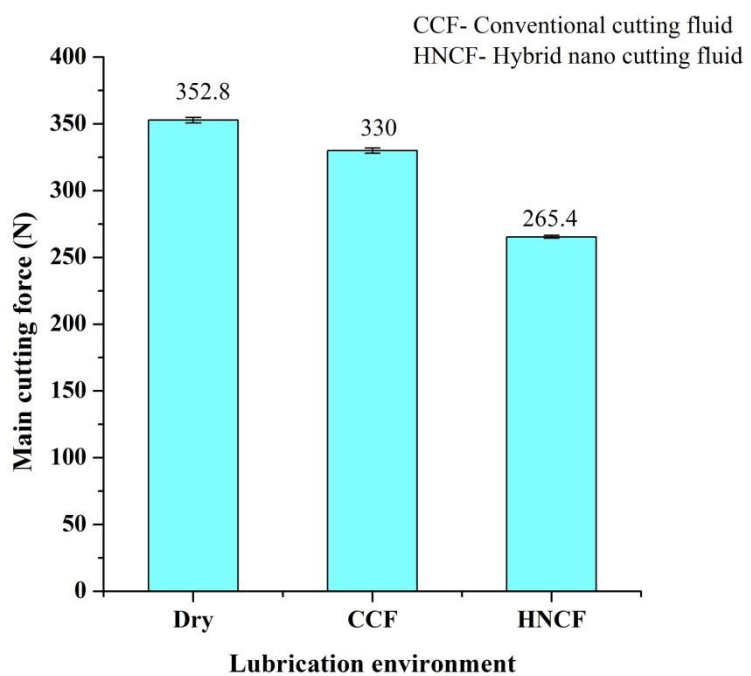


Fig.4.5 Variation of Main cutting force in dry, conventional and hybrid nano cutting fluid (Cutting conditions: $V=80$ m/min, $f=0.161$ mm/rev, $d=0.5$ mm and $t=5$ min)

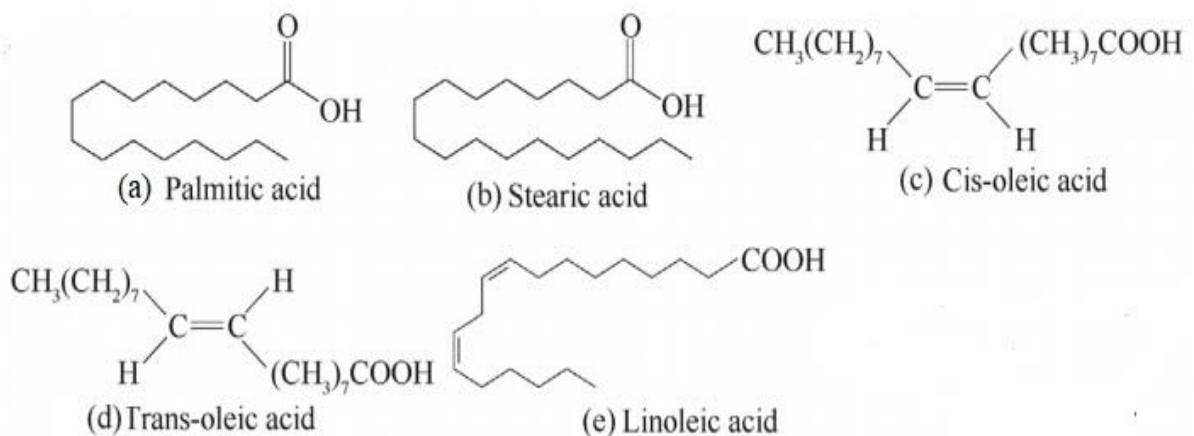


Fig. 4.6 Structures of various types of fatty acids [71]

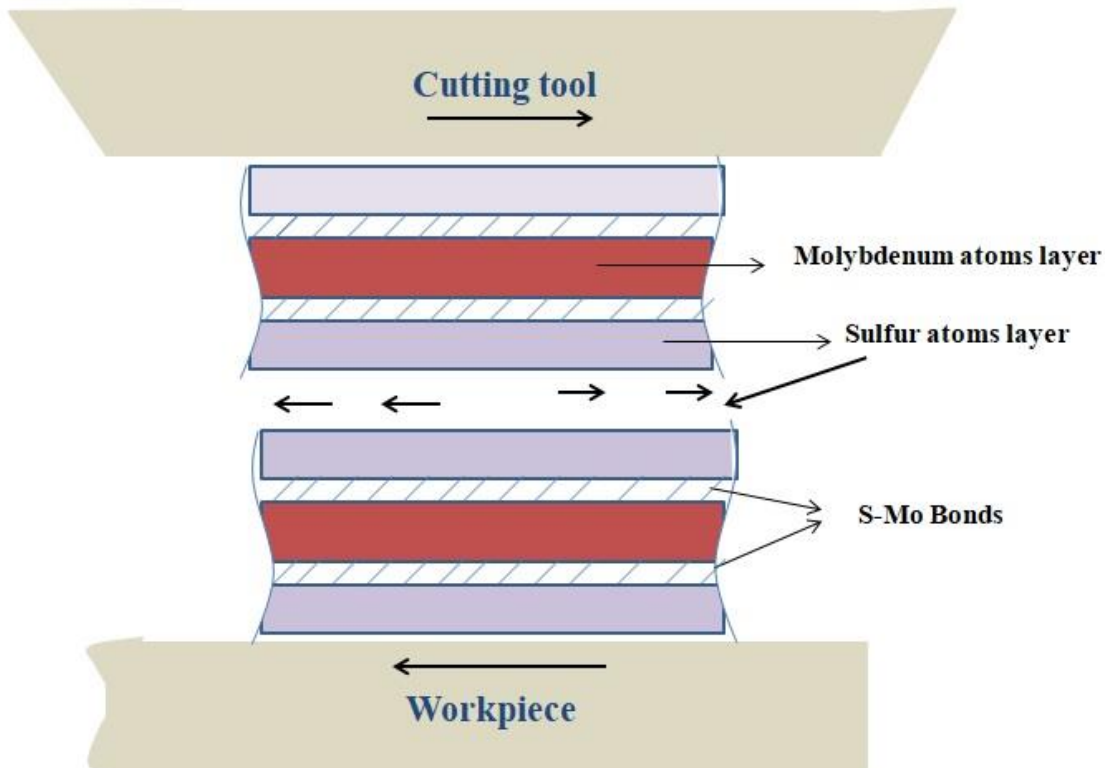


Fig. 4.7 Mechanism of MoS₂ [15]

4.7.2 Cutting temperature

The variation of the nodal temperature in cutting zone for dry, CCF and HNCFs during turning operation is presented in Fig 4.8. Due to the application of hybrid nano cutting fluid, the cutting temperature is reduced to 151°C which was 180 °C and 230°C when CCF and dry machining are used respectively. The percentage reduction in nodal temperature in cutting zone with HNCF by using MQL is recorded to be 16% and 34% when compared to CCF and to dry machining respectively. As discussed in previous section 4.2.1, vegetable oil composition, nanoparticle structure and hybridizing effect of nanoparticle in base oil are the influencing factors for forming film. The phenomenon of strong film formation on contacting surface with sesame oil is because of unsaturated long chain fatty acids, which separate the surfaces in contact by forming durable layer of adsorption film. This adsorption film along with kinematic viscosity of the base oil minimizes the heat generation by reducing friction between tool and workpiece, thus help in reducing the cutting temperature [114].

The structure of nanoparticles is one of the major reasons for improved performance of hybrid nano cutting fluids. Both nanoparticles MWCNT and MoS₂ are having different crystal structure and different shapes. MoS₂ is solid lamellar layered structure in hexagonal shape. The Mo atom is sandwiched between two sulfur atoms as discussed in previous section

(4.6.1). Structure of MWCNT is like tube with high carbon content. CNT is sandwiched between the MoS₂ nanoparticles by mixing with 1:2 proportions. This is also called physical encapsulation as shown in Fig. 4.9, thus avoids particle aggregation and prevents failure of lubricant [15].

During sliding movement, the sulfur layer of MoS₂ solid lubricant has an affinity to the metal substrate, creating an adhesion with base oil, which reduces the coefficient of friction at machining zone and tend to minimize the heat generation in machining zone. Also, at elevated temperature, high aspect ratio of CNT increases the heat transfer capacity of hybrid nanofluid [18]. Other hand sizes, shape, large surface to volume ratio of nanoparticles and Brownian motion of nanofluids improve the heat transfer rate of the hybrid nano cutting fluids than nanofluids [115]. Thus helps in enhancement of heat dissipation during turning operation and controlling temperature in cutting zone [8,18].

Application of CNT/ MoS₂ hybrid nano fluid in MQL with high pressure is another reason to reduce the cutting temperature by effective cooling and lubrication due to synergistic effect of CNT and MoS₂ and rolling effect of MoS₂ nanoparticles as shown in Fig. 4.11. Synergistic effect is an effect arising between two or more nanoparticles or substances that produce an effect greater than the sum of their individual effect. In the mixture of CNT/ MoS₂ hybrid nano cutting fluid, MoS₂ reduces the coefficient of friction between the contact surfaces, CNT nanoparticle improve the heat transfer rate. Synergistic effect of CNT and MoS₂ nanoparticle at 1:2 hybrid ratio, could integrate the advantages of individual nanoparticle in lubrication and prevent their disadvantages. In particularly the low shear force plane of MoS₂ molecular layer reduce the friction force and coefficient of friction between sliding surfaces of tool and workpiece [15]. The high strength and aspect ratio (l/d) of CNT could resist the friction and reducing the cutting temperature in machining. The combined effect of all the above factors leads to reduce the cutting temperature compared to dry and conventional cutting fluids.

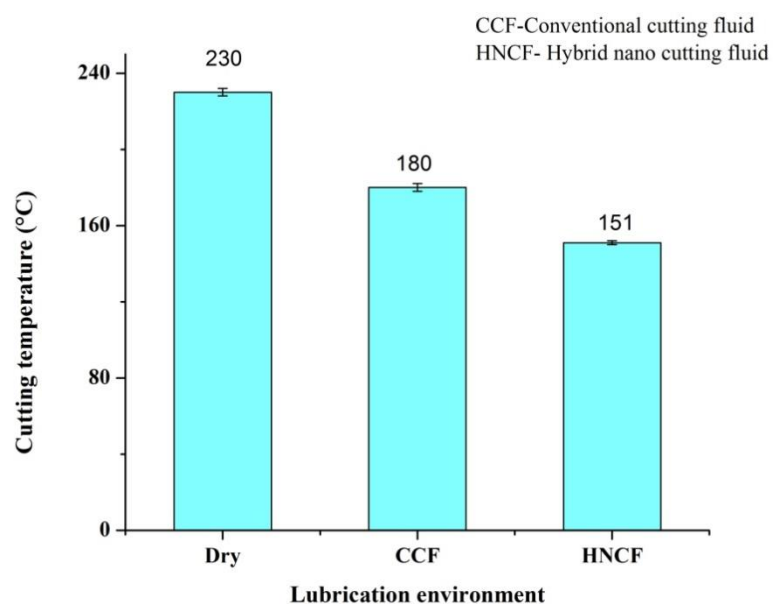


Fig. 4.8 Variation of cutting temperature in dry, conventional and hybrid nano cutting fluid (Cutting conditions: $V = 80$ m/min, $f = 0.161$ mm/rev, $d = 0.5$ mm, $t = 5$ min)

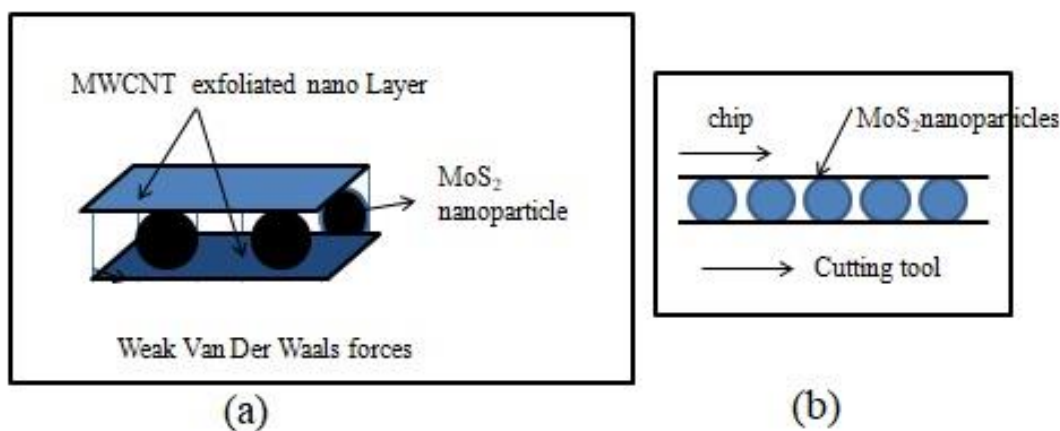


Fig. 4.9 (a) Synergistic effect of CNT/ MoS₂ hybrid nanoparticles (b) Rolling effect of MoS₂

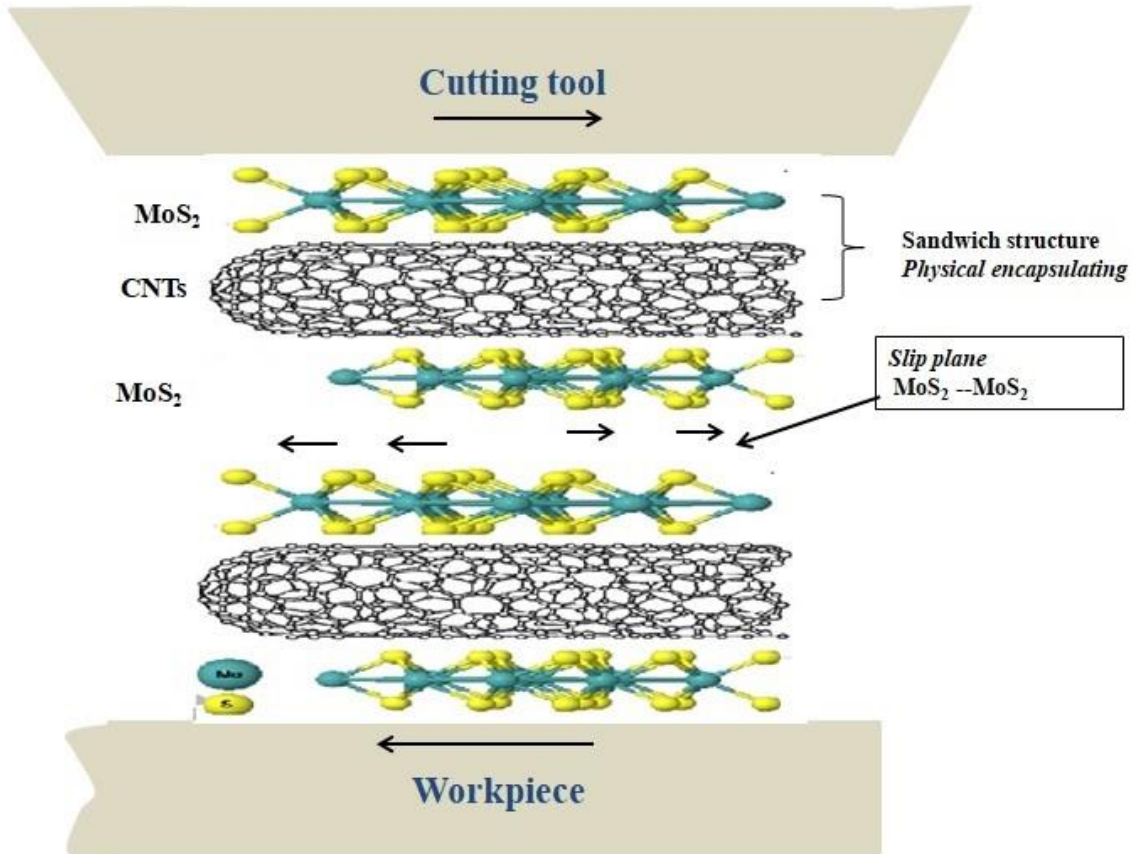


Fig. 4.10 Physical encapsulation of CNT and MoS₂ nanoparticle

4.7.3 Surface Roughness (R_a)

The surface roughness is the main response parameter to get the qualitative end product from machining. R_a for dry machining has given highest value (2.8 μm), followed by CCF (2.45 μm) and HNCF (1.7 μm) with MQL mode (Fig 4.11). The Surface roughness value is reduced to be 31% and 39% by the application of HNCF than CCF and dry machining respectively. The combination of long chain unsaturated fatty acid profiles in sesame oil and fullerene related structure of nano MoS₂ provides stable film on sliding surfaces of tool and workpiece resulting in reduced friction. Low resistance to shear property of hexagonal structure of nano MoS₂ has high chemical affinity to metallic workpiece surface, it tends to cover all the valleys between the asperity contacts and produce smoothness on machined product [12]. As discussed in previous section 4.6.2, rolling effect of nanoparticle in base oil helps to reduce the uneven nature of machined surface which leads to improve the surface finish of machined surface [116]. Combining CNT and MoS₂ nanoparticles at 1:2 proportions in sesame oil enhances the capacity of heat dissipation due to improved properties of heat transfer than base oil/ nanofluid, thus reduced cutting temperature.

Reductions in main cutting force, cutting temperature were resulted in better surface quality of the workpiece.

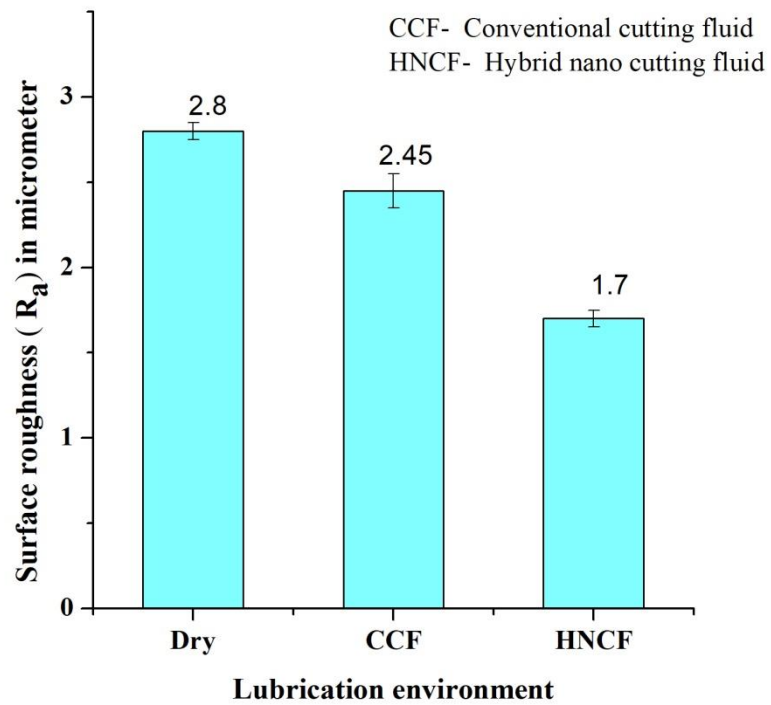


Fig.4.11 Variation of Surface roughness (R_a) in dry, conventional and hybrid nano cutting fluid (Cutting conditions: $V = 80$ m/min, $f = 0.161$ mm/rev, $d = 0.5$ mm and $t = 5$ min)

4.7.4 Tool flank wear

The temperature developed in primary and secondary shear zone leads to flank wear of the cutting tool. The variation in tool flank wear for dry, wet and hybrid nanofluid environment is presented in Fig 4.12. Due to high heat generation and severe plastic deformation the maximum tool flank wear (225 μ m) is observed in dry machining, followed by CCF (170 μ m) and HNCF (61 μ m). The percentage reduction in tool flank wear by the application of HNCF is observed to be an extent of 64% and 73% compared to CCF and dry machining respectively. This improvement may be because of less heat generation in machining zone and reduced plastic contacts between the chip and tool interface [22]. This may be achieved due to the stable film formation and low friction property of the lamellar structure of MoS_2 solid lubricant in sesame oil [117].

The weak Van der Waals forces between MWCNT nanoparticles easily shed from a surface in scales or layers because of shearing action of chip over the tool [109]. This leads to film formation between work and tool that reduces the plastic contact at contacting zone and thus reduces the friction thereby reduced cutting temperature and tool flank wear [18]. Synergistic effect of CNT and MoS₂ nanoparticles and ball bearing effect of MoS₂ nanoparticle shown in Fig. 4.13 could be other reason for reducing tool flank wear.

Very fine particles of CNT/MoS₂ in MQL vegetable oils are easily spread on exact cutting area through MQL device with use of compressed air and resulting in a very fine mist (Fig. 4.14). This mist is penetrating into workpiece and tool interfacing zone and forms Tribo film. This Tribo film is helpful to decrease in generated heat in machining zone and reduce coefficient of friction between tool and workpiece, thus reduce the cutting temperature and tool flank wear. Consequently improves the cooling and lubrication functions and maintained tool hardness for longer time [118]. Therefore, MQL nanofluid showed better improvement in reducing the tool flank wear compared to dry machining and CCF.

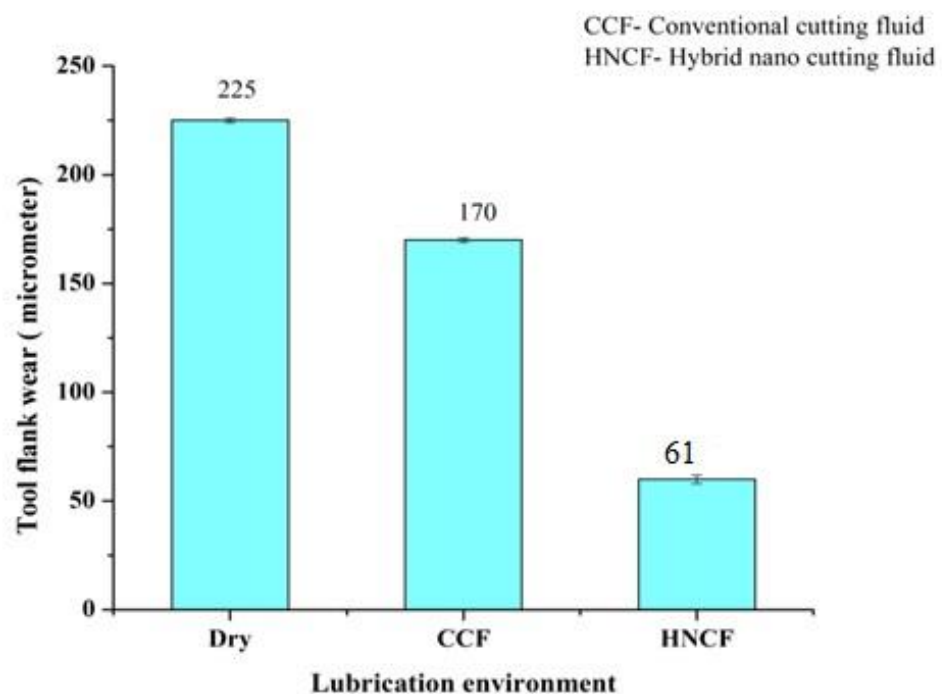


Fig. 4.12 Variation of tool flank wear in dry, conventional and hybrid nano cutting fluid
(Cutting conditions: $V=80$ m/min, $f=0.161$ mm/rev, $d=0.5$ mm and $t=5$ min)

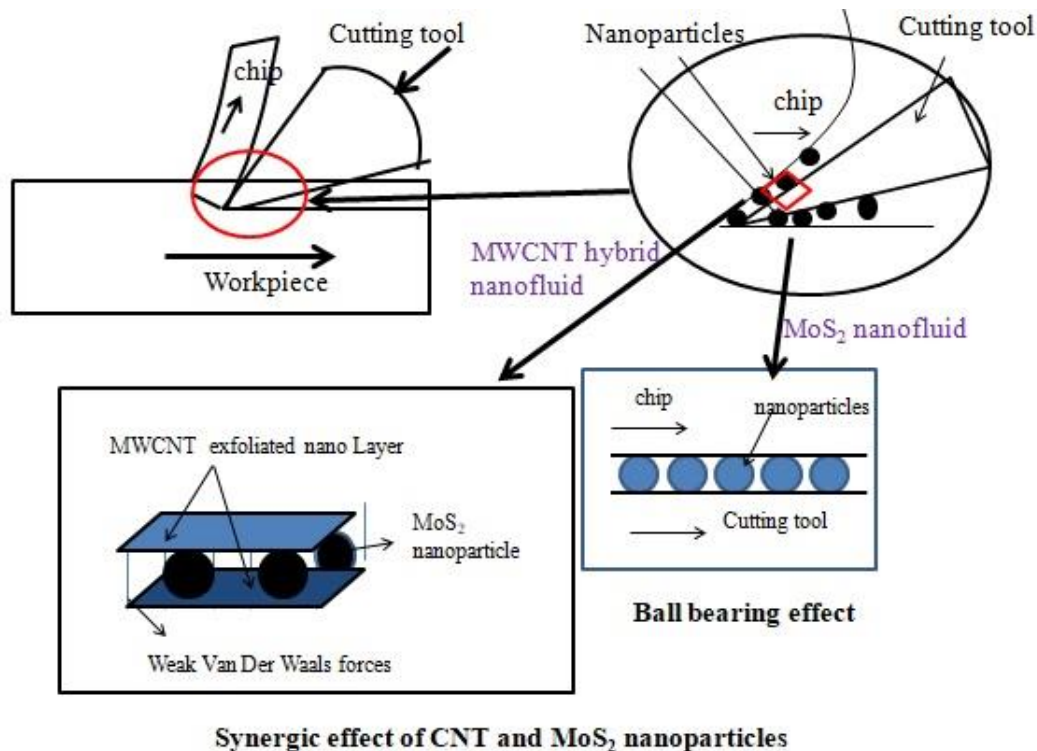


Fig. 4.13 Synergistic effect of CNT and MoS₂ and ball bearing effect of MoS₂ nanoparticles [98]

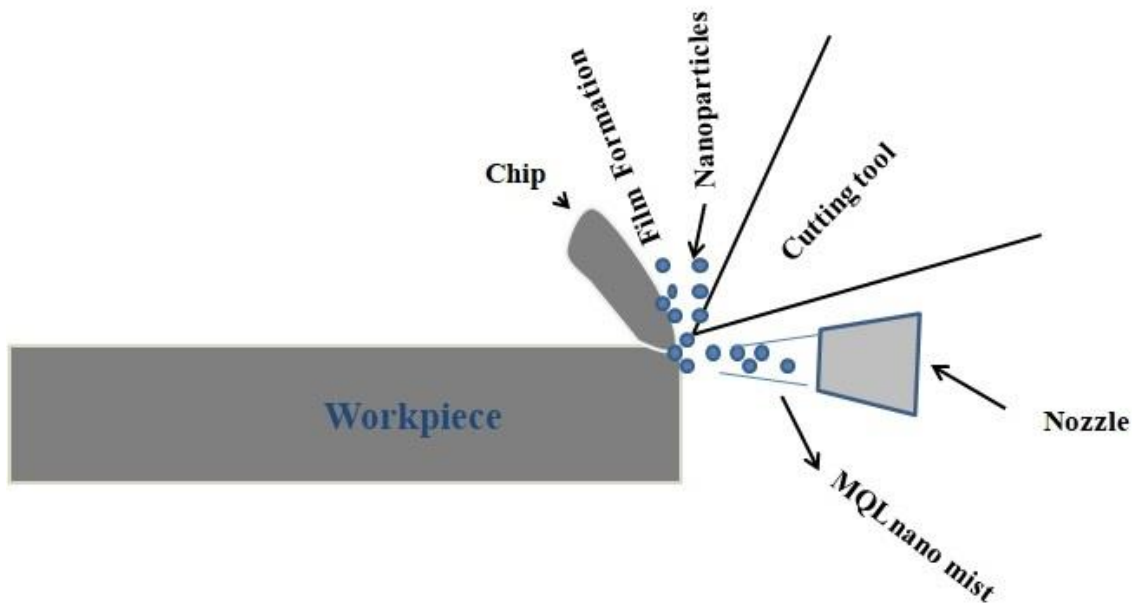


Fig. 4.14 MQL nanomechanism [118]

4.8 Summary

It is found that density and Kinematic viscosity are high for Mahua oil based CNT/BA and CNT/MoS₂ HNCFs and observed to decrease with raise in temperature. Sesame oil based CNT/MoS₂ HNCFs are proved to be stable based on sedimentation test and Zeta potential values. Sesame oil based CNT/MoS₂ HNCF with SDS surfactant at 15% concentration of nanoparticle by weight in base oil and (1:2) hybrid ratio is optimum for better stability of the nanofluid from taguchi analysis. HNCF applied as MQL in machining improved performance compared to CCF and dry machining by reducing the cutting force, cutting temperature, surface roughness and tool flank wear. Basic properties in varying concentration of CNT/MoS₂ in sesame oil, lubrication property and machining performance are discussed in next chapter.

Chapter-5

Evaluation of basic properties and machining performance of hybrid nano cutting fluids in varying concentration of nanoparticle for machining

5.1 Introduction

This chapter deals with evaluation of effectiveness of the CNT/MoS₂ (1:2) HNCFs in machining as cutting fluids by evaluating basic properties, followed by coefficient of friction on contacting surfaces by varying concentration of CNT/MoS₂ nanoparticle in base oil. Dynamic viscosity, thermal conductivity and volumetric heat capacity of formulated fluids are evaluated. Results of coefficient of friction are presented and discussed. Cutting forces, cutting temperature, surface roughness and tool flank wear are examined by supplying CNT/MoS₂ HNCFs under MQL mode in concentrations of 0 to 3 wt%.

5.2 Sedimentation test results

Sedimentation test results of hybrid nano cutting fluids are shown in Fig. 5.1. It is observed that after 72 hours, minimum sedimentation is observed at concentration of 0.5 wt% of CNT/MoS₂ nanoparticle in sesame oil sample1 among all the concentrations which gives more stability. However, 2 wt% (sample 4) also shown less sedimentation compared to other samples. Concentration of 2.5 wt% (sample 5) and 3 wt% (sample 6) have shown maximum sedimentation. There are two reasons for settling of nanoparticles during sedimentation test. The primary reason is the augment in density and viscosity with rise in nanoparticle concentration due to which agglomeration starts at higher concentration and ensuring uneven dispersion. Influence of repulsion and Van der Waals force of attraction when nanoparticles are attracted to each other being the second one [18]. Hence, for combination of base oil and surfactant, 0.5 wt% and 2wt% of CNT/MoS₂ nanoparticles (1:2) is observed to be the more stable among the selected fluids.

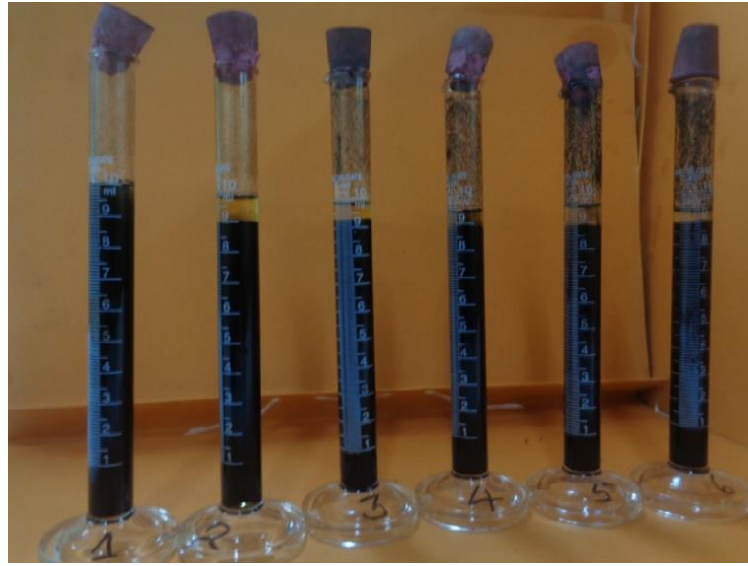


Fig. 5.1 Sedimentation test results after 72 hours

5.3 Basic properties of CNT/MoS₂ hybrid nanofluid

To assess the effectiveness of the VOBHNCFs in machining, basic properties such as viscosity, thermal conductivity and volumetric heat capacity are evaluated as per ASTM standards.

5.3.1 Dynamic viscosity

Dynamic viscosity is a rheological property of the fluid due to which fluid offers a internal resistance to flow. Development of the sliding friction between contacting surfaces and film forming capability of lubricant to separate surfaces are mainly dependent on viscosity of the lubricant. Thus dynamic viscosity is the important property to assess the behavior of the hybrid nano cutting fluids in machining when supply as cutting fluids. Dynamic viscosity of CNT/MoS₂ hybrid nano cutting fluids is measured in 30°C- 60°C temperature range at 100 to 1000 s⁻¹ shear rate. The dynamic viscosity of the CNT/MoS₂ hybrid nano cutting fluid is measured by using Rheometer and presented in Fig 5.2. Improvement in dynamic viscosity of hybrid nanocutting fluid is observed when compared to base oil for particle concentration of 0.5 to 3 wt%. Dynamic viscosity of the CNT/MoS₂ hybrid nanofluid is observed to be increased with particle concentration due to increase in particle loading. This property is gradually reduced with increase in temperature. The weaker inter molecular force of attraction between the particles at high temperature leads to reduction in dynamic viscosity, while molecular forces tend to be high with increase in nanoparticle concentration and thus help in enhancement of dynamic viscosity [18]. Low dynamic

viscosity of the fluid at high temperature is easily penetrating between sliding surfaces when supply as coolant through MQL condition. When this property is low, heat dissipation property of the nanofluid is high and ability of film formation on contact zone improves, thus helps for reducing friction [119].

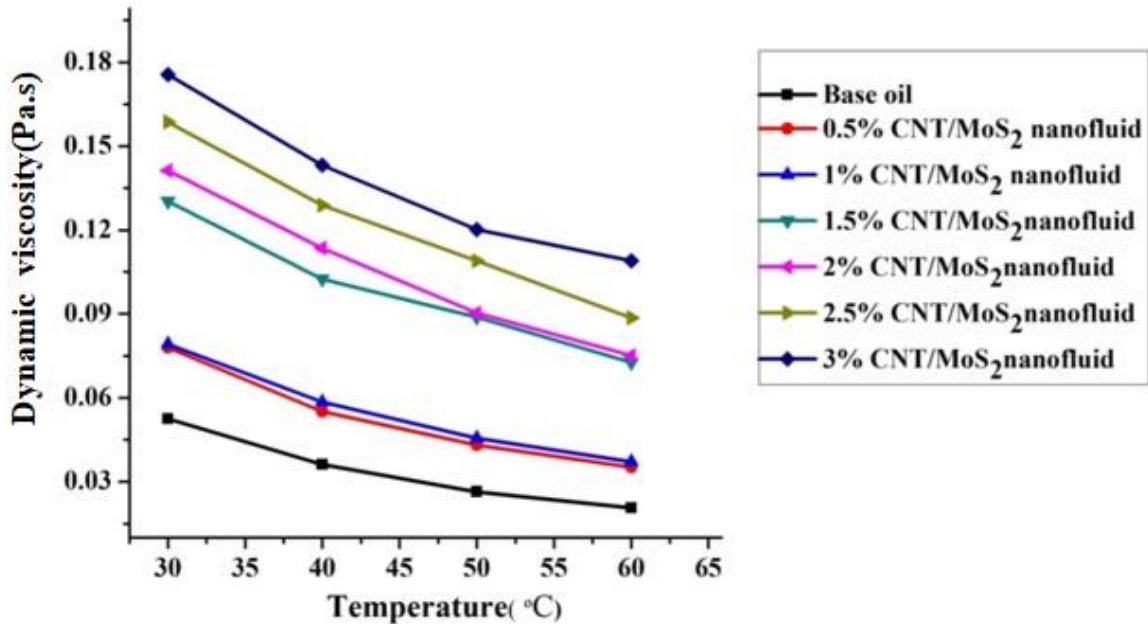


Fig. 5.2 Dynamic viscosity of nanofluids with respect to temperature

5.3.2 Thermal conductivity

Thermal conductivity of base oil and CNT/MoS₂ hybrid nano cutting fluids are measured by using hot disk thermal conductivity analyzer at temperatures 30°C, 40°C and 50°C up to 3 wt% concentration of hybrid nanoparticle. The values of thermal conductivity versus temperature of various concentration of CNT/MoS₂ hybrid nano cutting fluids are shown in Fig 5.3. Thermal conductivity of CNT/MoS₂ hybrid nano cutting fluids is increased with nano particle concentration (wt %) and temperature. This trend shows the enhancement in thermal conductivity by adding the nanoparticles and thus, gets enhanced heat transfer rate. Enhancement in thermal conductivity with CNT/MoS₂ hybrid nano cutting fluid is found to be 28.31% for the particle concentration of 3 wt% at 30°C compared to base oil. This is due to collision between the nanoparticles and increasing Brownian motion of nanoparticles with temperature [23]. Size, shape and large surface area of the nanoparticle could be another reason for enhancing the heat transfer rate of the hybrid nano cutting fluids than base oil.

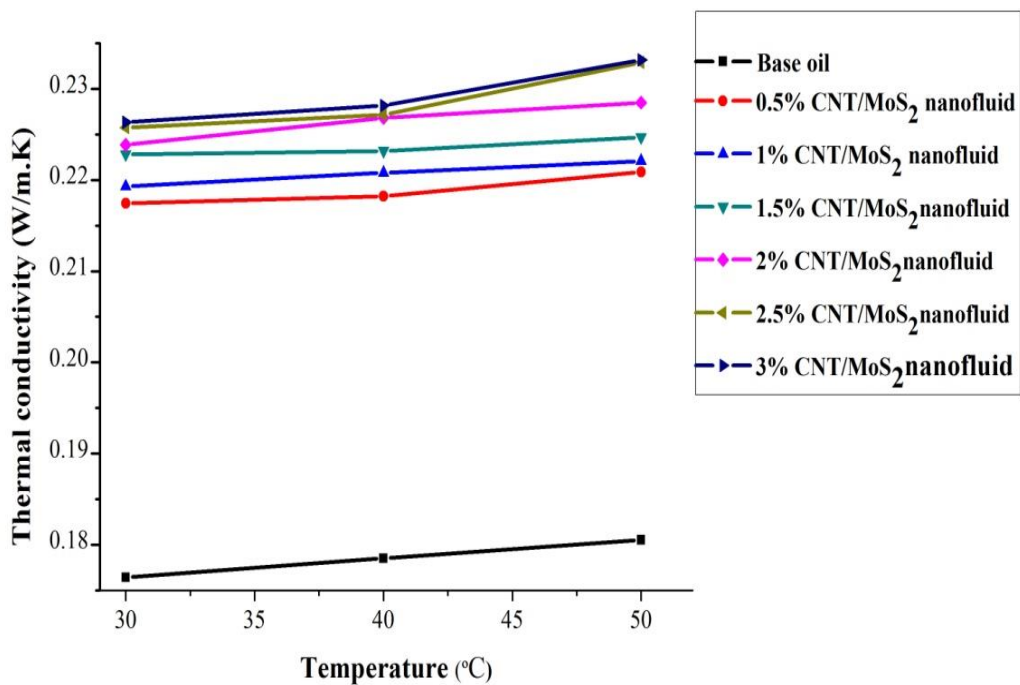


Fig. 5.3 Thermal conductivity versus temperature

5.3.3 Volumetric heat capacity

Volumetric heat capacity ($\text{J/m}^3 \text{ K}$) of CNT/MoS₂ hybrid nano cutting fluids with varying particle concentration (wt %.) is measured with hot disk thermal conductivity analyzer. Results of volumetric heat capacity by varying nanoparticle concentration are shown in Fig. 5.4. It is noticed that the volumetric heat capacity is increased from the nanoparticle concentration of 0.5 wt% to 3wt% and at temperature range of 30° to 50°. Significant improvement in volumetric heat capacity is observed to be 10.98% at 3wt% of CNT/MoS₂ hybrid nano cutting fluid compared to base oil. The presence of film as increase in nanoparticle concentration is the reason for enhancement of the volumetric heat capacity. It is helpful to calculate the specific heat by dividing the density. The improvement in thermal conductivity and specific heat help in enhancement of heat dissipation capability of hybrid nano cutting fluid. This removes more amount of heat in contacting zone and helps to reduce temperature.

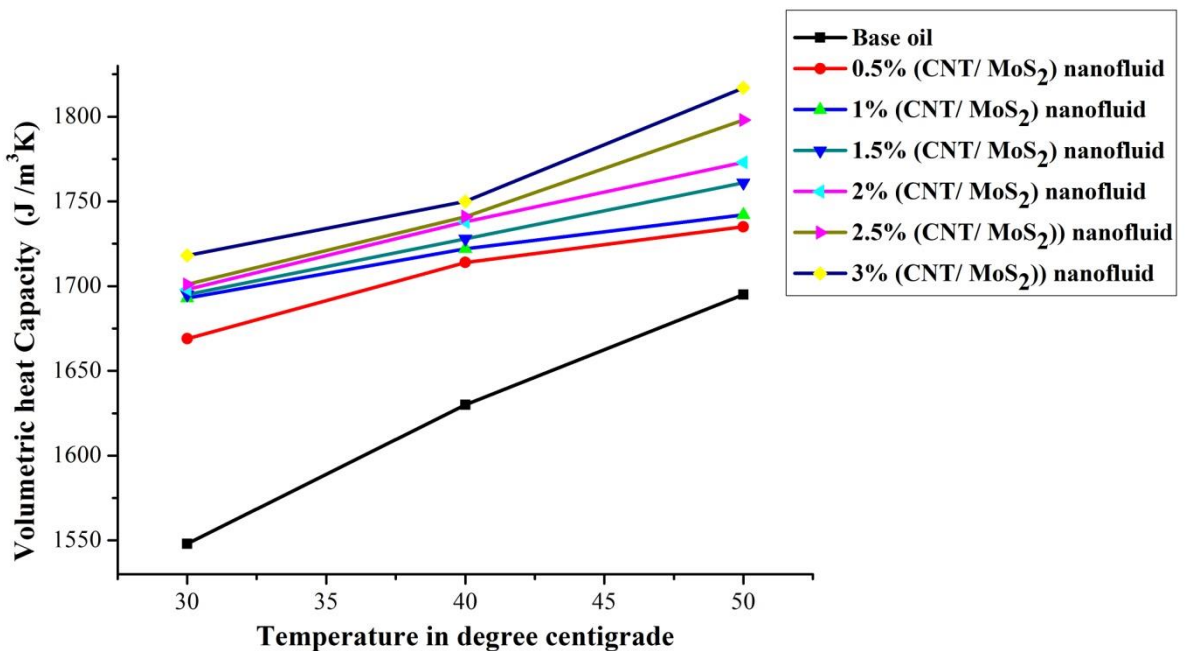


Fig. 5.4 Volumetric heat capacity of CNT/MoS₂ hybrid nano cutting fluids with variation in temperature

5.4 Coefficient of friction

The coefficient of friction for all the concentration of the hybrid nano cutting fluids is shown in Fig. 5.5. The results of coefficient of friction for six concentration of CNT/MoS₂ hybrid nano cutting fluids are NCF1 (0.5%) = 0.22, NCF2 (1%) = 0.135, NCF3 (1.5%) = 0.047, NCF4 (2%) = 0.038, NCF5 (2.5%) = 0.076 and NCF6 (3%) = 0.105. Coefficient of friction values under dry condition and with base oil are 0.61 and 0.223. The trend of coefficient of friction is gradually decreased up to 2% nanoparticle concentration and then slightly increased. At first, coefficient of friction is decreased from 0.22 (0.5wt %) to 0.038 (2 wt %) reaches the minimum level. Then the coefficient of friction is gradually increased beyond the 2 wt % with continues increase in nanoparticle concentration and reaches the maximum value 0.105 at 3wt %, which is higher than the 0.038 at (2 wt %).

After analyzing experimental results, we can conclude that before 2wt% of nanoparticle concentration, the coefficient of friction is inversely proportional to nanoparticle concentration. This reflects that the lubrication performance of hybrid nano cutting fluids is improved gradually. After the 2 wt%, coefficient of friction is proportional to nanoparticle concentration, which reflects that lubrication performance of the hybrid nano cutting fluid is decreased gradually. The reason could be the agglomeration of nanoparticle at higher

concentration which is observed in sedimentation results (Fig 5.1). The reduction in coefficient of friction with hybrid nano cutting fluid at the concentration of 2 wt% is observed to be 93.77% compared to dry condition and 82.9% compared to base oil. As discussed in previous section (1.7.4), shape, size, and crystal structure of the CNT and MoS₂ nanoparticles are the influencing factors for improving lubrication performance of hybrid nano cutting fluids [115].

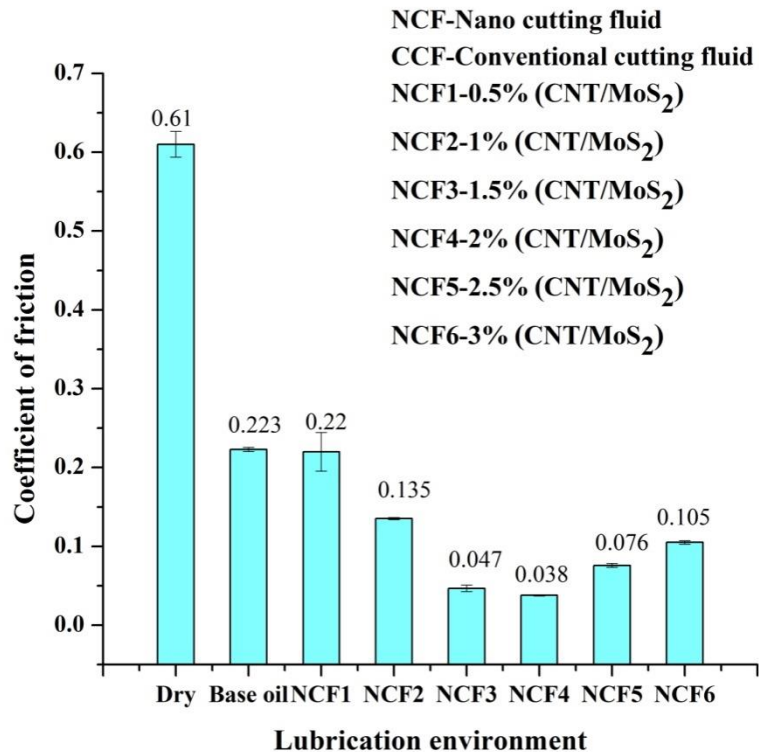


Fig. 5.5 Coefficient of friction with respect to nanoparticles concentration

In addition to that, combination of CNT and MoS₂ nanoparticles at 1:2 ratio possess good “physical synergistic effect” indicates that MoS₂ and CNT nanoparticle develop their advantages in lubrication and prevent the failure of lubricant. Low resistance to shear property of MoS₂ solid lubricant reduces coefficient of friction on contacting surfaces. The high strength of CNT could serve as similar bearings and prevent the failure of lubricant under high pressure and temperature. This effect is resulted in reduction of coefficient of friction between the sliding surfaces. When compared to base fluid, hybrid nanoparticles enriched cutting fluids improved the lubrication performance in reducing friction due to their ball bearing effect as explained in section (4.6.4) [15]. This improvement is also attained by the formation of thin physical Tribo- film between sliding surfaces, which reduces wear and friction, when applied as coolant on contacting surfaces [120]. The phenomenon of formation

of thin physical Tribo film between the contacting surfaces is shown in Fig.5.6. Furthermore, presence of long chain unsaturated fatty acids in sesame oil with conjunction of nanoparticles improve the strength of the film that can reduce coefficient of friction compared to base oil and dry condition respectively [22].

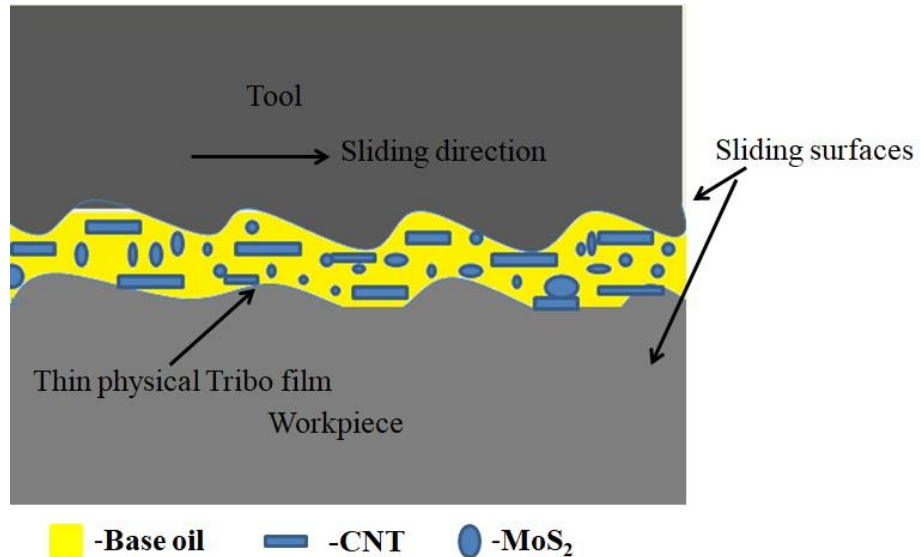


Fig. 5.6 Thin Tribo film between sliding surfaces [120]

5.5 Machining performance

After examining basic properties of CNT/MoS₂ hybrid nano cutting fluid, their applicability is evaluated during turning of AISI1040 steel under MQL flow rate of 10 mL/min by varying concentration of CNT/MoS₂ nanoparticles. Constant cutting conditions are chosen for machining which is cutting speed: 80 m/min, feed rate 0.161 mm/rev, depth of cut: 0.5 mm and machining time 5 min. Corresponding machining responses in terms of cutting force, cutting temperature, surface roughness and tool flank wear are discussed in varying concentration of nanoparticles.

5.5.1 Cutting forces

Cutting forces are influenced by coefficient of friction in machining. Therefore this can be reduced by minimizing the friction in chip tool interface. Thrust force (F_x), feed force (F_y) and cutting force (F_z) are measured online with six component Piezo electric dynamometer on lathe at constant cutting conditions. Figure 5.7 represents the values of the cutting forces in x, y and z directions at varied lubrication conditions. The force F_z is referred to as main cutting forces or tangential component of the force, which is used to calculate the

power required to perform machining operation. F_x accounts vary little for power consumption and it is least significant. F_y feed force does not accounts power consumption at all but leads to dimensional inaccuracy and vibration during turning. It is noticed that decrease in all the forces with increase in particle concentration up to 2 wt% and beyond that slightly increased. Hybrid nano cutting fluid with concentration of 2 wt% reduced all the components of forces and more than 2wt% leads to increase in forces. Film thickness between the tool and workpiece surface is increased up to certain level with increase in nanoparticle concentration due to increase in viscosity and thus reduced the cutting force. Cutting forces are observed to increase at higher concentration due to settling of nanoparticles. This is due to forming dense or slurry layer at higher concentrations, therefore cutting force will increase with increase in nanoparticle concentration [121].

The intermolecular force of attraction between the nanoparticles dominates the repulsion forces with increase in nanoparticle concentration, which tends to aggregate the nanoparticles and causes for poor lubrication effect. Thrust force is observed to reduce by 22% and 11.2%, feed force is observed to reduce by 28.3% and 13.8% and main cutting force is observed to reduce by 32% and 27.3% with 2 wt% of CNT/MoS₂ hybrid nano cutting fluid than that of dry machining and conventional cutting fluid respectively. Results obtained with hybrid nano cutting fluids are in good agreement with literature [22].

Long chains, polar fatty acid in sesame oil gives high strength lubricant film that interact with metallic workpiece surfaces, reducing both friction and wear [16,118]. As explained in previous section 4.6.1, chemical composition of sesame oil [102], MoS₂ solid lubricants, MQL conditions are the reasons for reduction in cutting forces. This is also evident from coefficient of friction results (Fig. 5.5) and increase in viscosity of CNT/MoS₂ hybrid nano cutting fluid. This viscosity is another factor for maintaining consistent film between workpiece and tool with nanofluid. The formation of strong film at the contacting surfaces reduces the friction thereby reduces cutting forces. All the above discussed affirmative factors help in reducing the cutting forces.

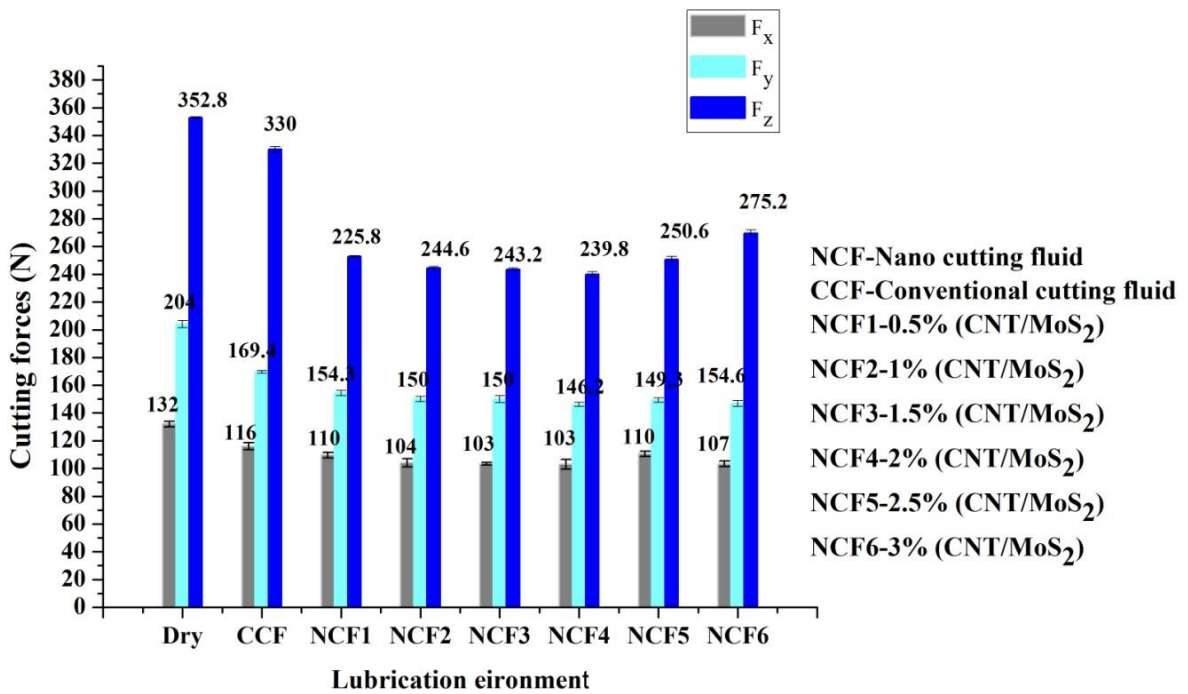


Fig. 5.7 Variation of cutting forces in different lubrication environment

(Cutting conditions: $V = 80$ m/min, $f = 0.161$ mm/rev, $d = 0.5$ mm and $t = 5$ min)

5.5.2 Cutting temperature

Cutting temperature is influenced by amount of heat generated at chip-tool interface. To assess the performance of CNT/MoS₂ hybrid nano cutting fluids under MQL machining, the nodal temperature at a remote point on tool, i.e. 5 mm below the cutting edge is recorded with embedded thermocouple technique. The Variation of cutting temperatures with respect to different lubrication conditions are depicted in Fig. 5.8. Cutting temperature under the machining with dry condition and application of CCF is observed to be 230° C and 180° C. Cutting temperature for the varying concentration of CNT/MoS₂ are NCF1 (0.5%) = 167° C, NCF2 (1%) = 160° C, NCF3 (1.5%) = 143° C, NCF4 (2%) = 140° C, NCF5 (2.5%) = 133° C and NCF6 (3%) = 130° C. The application of CNT/MoS₂ HNCF resulted in low cutting temperatures compared to dry and CCF. It may be noticed that the cutting temperatures are observed to decrease from (167°C) at 0.5 wt% to (130 °C) at 3 wt% and reaches the minimum level with increase in CNT/MoS₂ concentration. The possible reduction in cutting temperature is found to be 43.4% and 28% with CNT/MoS₂ hybrid nano cutting fluid at 3 wt% than that of dry machining and CCF respectively. As discussed in section 4.6.2, the synergistic effect of

both CNT and nano MoS₂ at 1:2 mixing ratio is improved the performance of HNCF. Thus reduces the heat generation in machining process.

Cutting temperatures may be reduced because of more heat dissipation also. This improvement is due to increase in thermal conductivity of hybrid nano cutting fluid with increase in hybrid nanoparticle concentration. The increment in thermal conductivity and heat transfer coefficient improves the heat dissipation capability of CNT/MoS₂ hybrid nano cutting fluid and thus reduces the temperature in cutting zone.

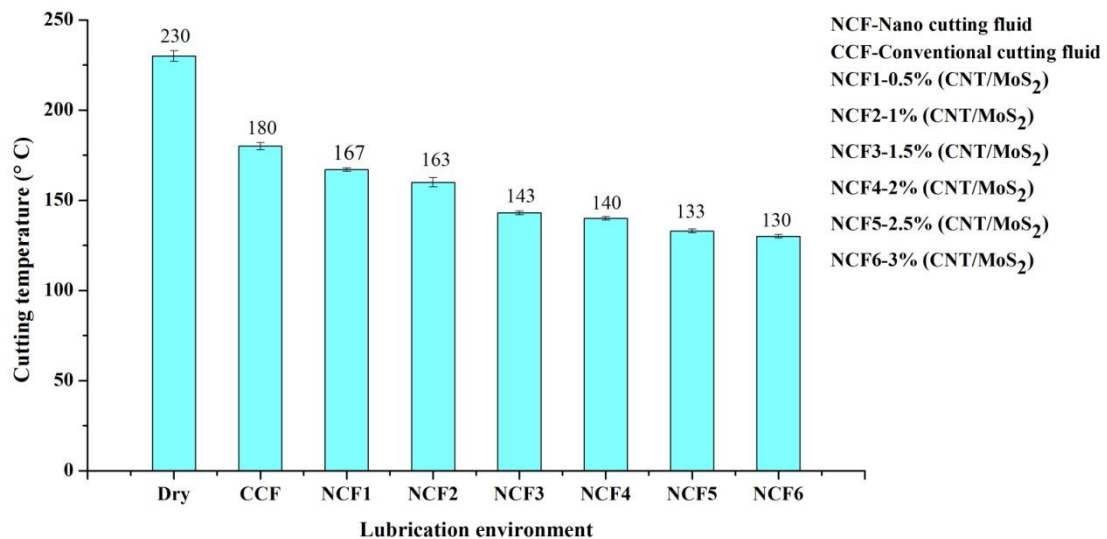


Fig. 5.8 Variation of cutting temperature in different lubrication environment

(Cutting conditions: $V = 80$ m/min, $f = 0.161$ mm/rev, $d = 0.5$ mm and $t = 5$ min)

5.5.3 Surface roughness (R_a)

The quality of the machined product is assessed by its surface finish. The effectiveness of the hybrid nano cutting fluid in machining is evident by minimizing the surface roughness. The surface roughness (R_a) of the machined product is determined at regular interval by using surface roughness tester. Results of surface roughness (R_a) in different lubrication conditions are presented in Fig 5.9. It is seen that the values of surface roughness (R_a) under dry machining and conventional cutting fluids are $2.8\mu\text{m}$ and $2.45\mu\text{m}$. Surface roughness (R_a) values for varying concentration of CNT/MoS₂ are NCF1 (0.5%) = $2.13\mu\text{m}$, NCF2 (1%) = $2.1\mu\text{m}$, NCF3 (1.5%) = $2.03\mu\text{m}$, NCF4 (2%) = $2\mu\text{m}$, NCF5 (2.5%) = $2.1\mu\text{m}$ and NCF6 (3%) = $2.11\mu\text{m}$. Surface roughness (R_a) value is decreased from $2.13\mu\text{m}$ at 0.5 wt% nanoparticle

concentration to 2 μm at 2wt% nanoparticle concentration and again increase in trend is observed for further nanoparticle concentration.

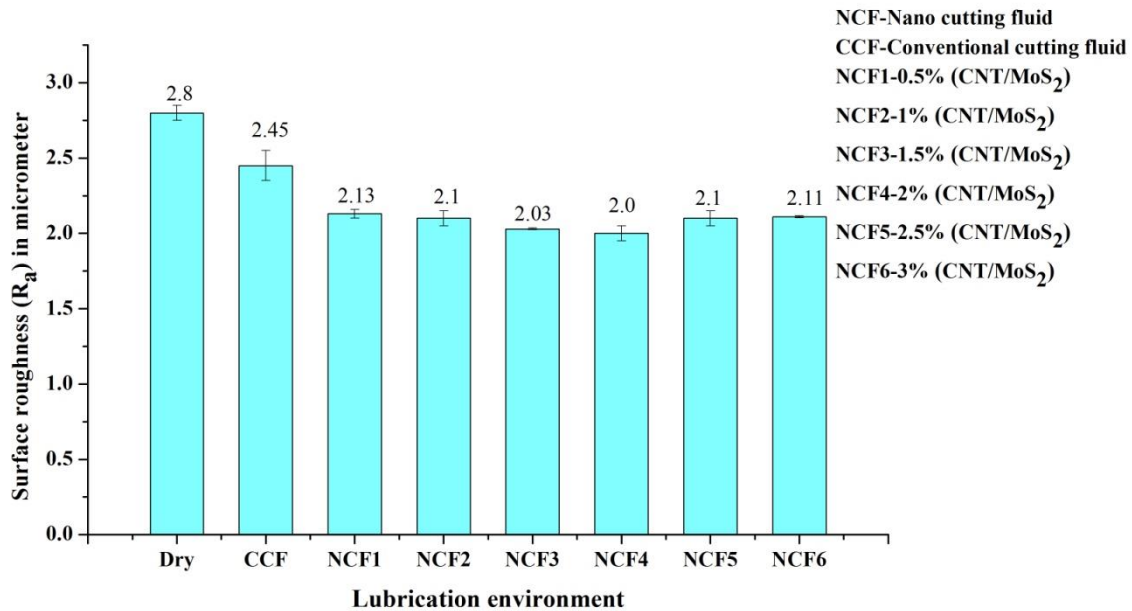


Fig. 5.9 Variation of surface roughness (R_a) in different lubrication environment

(Cutting conditions: $V = 80 \text{ m/min}$, $f = 0.161 \text{ mm/rev}$, $d = 0.5 \text{ mm}$ and $t = 5 \text{ min}$)

This may be due to agglomeration of nanoparticle beyond the concentration of 2 wt%. Surface roughness (R_a) is found to reduce by 28.5% and 18.3% with 2 wt% of CNT/MoS₂ hybrid nano cutting fluid compared to dry machining and CCF respectively. As discussed in previous section 4.6.3, structure of MoS₂ and CNT nano particles and MQL mechanism is the reason for obtaining low surface roughness (R_a) value with CNT/ MoS₂ hybrid nano cutting fluid. Furthermore Nano MoS₂ easily covers all valleys of workpiece surface which forms strong thin film between tool and workpiece and results in low shear resistance between the contact surfaces and thus reduced coefficient of friction [71]. Reduction in all the components of forces at 2 wt% nanoparticle concentrations and reduction in cutting temperature with increase in nanoparticle concentration imparts better surface quality of the machined surface. All the above discussed facts resulted in lower cutting force, cutting temperature and tool wear and thus achieved good surface finish.

5.5.4 Tool flank wear

The life of tool is improved indirectly by minimizing the tool wear. The results with different lubrication conditions are presented in Fig. 5.10. Tool flank wear by varying concentration of CNT/MoS₂ are NCF1 (0.5%) = 0.072 mm, NCF2 (1%) = 0.064 mm, NCF3(1.5%) = 0.053 mm, NCF4 (2%) = 0.05 mm, NCF5 (2.5%) = 0.045 mm and NCF6(3%) = 0.042 mm. From the Fig. 5.10, it is noticed that tool flank wear obtained by varying CNT/MoS₂ hybrid nano cutting fluids is lower than that of dry machining (0.225 mm) and CCF (0.170 mm). Trend of tool flank wear is observed to decrease with increase in nanoparticle concentration. Increase in thermal conductivity of CNT/MoS₂ hybrid nano cutting fluid with increase in concentration and temperature is favored for this improvement. Tool flank wear is found to reduce by 81.3% and 75% at concentration of 3wt% with CNT/MoS₂ hybrid nano cutting fluid than that of dry machining and CCF respectively.

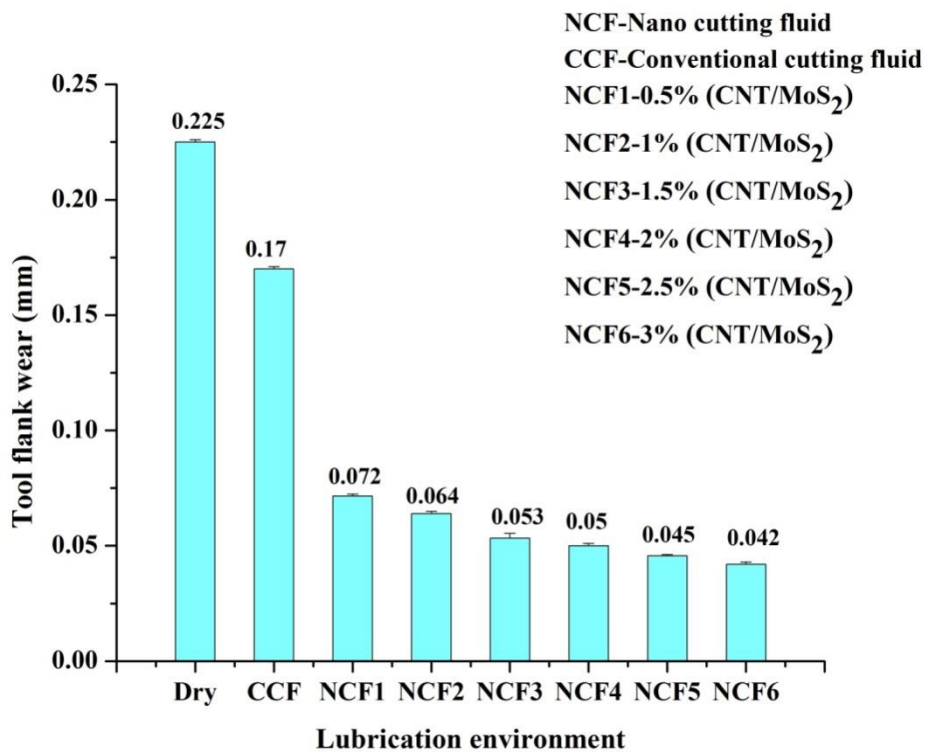


Fig. 5.10 Variation of tool flank wear in different lubrication environment
(Cutting conditions: V= 80 m/min, f= 0.161 mm/rev, d= 0.5 mm and t = 5 min)

As discussed in previous section (4.6.4) synergistic effect of CNT and MoS₂ nanoparticles and ball bearing effect of MoS₂ could be other reason for reducing tool flank wear [15]. High thermal conductivity of hybrid nano cutting fluids reduced the nodal

temperature at chip-tool interface by providing effective lubrication and cooling actions at higher concentration of nanoparticle. Hence, tool flank wear is reduced with hybrid nano cutting fluids by reducing cutting temperature.

5.6 Comparing machining performance of HNCF with nanofluids at (2 wt %.)

5.6.1 Main cutting force (F_z)

The magnitude of main cutting force during machining with different lubrication environment is presented in Fig. 5.11. From the experimental results, Main cutting force (F_z) is observed for NCF1 (2%) = 308 N for pure CNT nanofluid, NCF2 (2%) = 290 N for pure MoS₂ nanofluid and HNCF (2%) = 239.8 N for CNT/MoS₂ (1:2) hybrid nano cutting fluid. Main cutting force (F_z) is observed under dry condition is 352.8N and under CCF is observed to be 330 N. It is observed that the main cutting force is found to be lower with hybrid nano cutting fluid compared to pure CNT and pure MoS₂ nanofluid at same mass concentration due to synergistic effect of CNT and MoS₂ [20,122]. This improvement is due to enhanced physical and thermal properties of hybrid nanofluids compared to single nanoparticle enriched cutting fluids and base fluid.

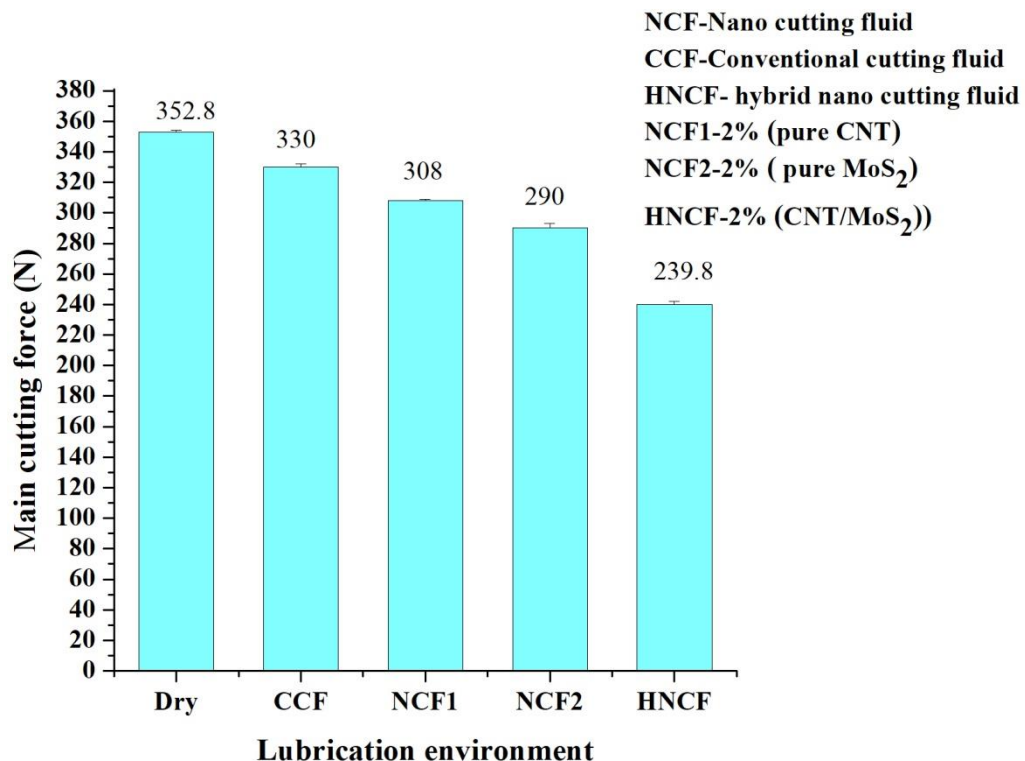


Fig. 5.11 Variation of main cutting force with different lubrication environment
(Cutting conditions: $V = 80$ m/min, $f = 0.161$ mm/rev, $d = 0.5$ mm and $t = 5$ min)

5.6.2 Cutting temperature (T ° C)

Cutting temperature observed during machining with different lubrication environment is presented in Fig. 5.12. These are only representative of nodal temperature but not exact cutting tip temperature. High cutting temperature (230°C) is observed in dry machining followed by CCF (180°C), pure CNT nanofluid (152°C), pure MoS₂ nanofluid (160°C) and hybrid nano cutting fluid (140°C) respectively. The temperature in cutting zone is observed to reduce by 43.4%, 28%, 8% and 12.5% with 2 wt% of CNT/MoS₂ (1:2) hybrid nano cutting fluid compared to dry, CCF, 2 wt% of pure CNT and pure MoS₂ nanofluids respectively. This may be due to low coefficient of friction of MoS₂ and high thermal conductivity property of CNT nanoparticle which reduces the heat generation and improves the heat transfer rate of CNT/MoS₂ hybrid nanofluid effectively compared to pure nanofluids. The increase in thermal conductivity at 2 wt% concentration enhances the heat dissipation capability of CNT/MoS₂ hybrid nanofluid and resulted in lower cutting temperature.

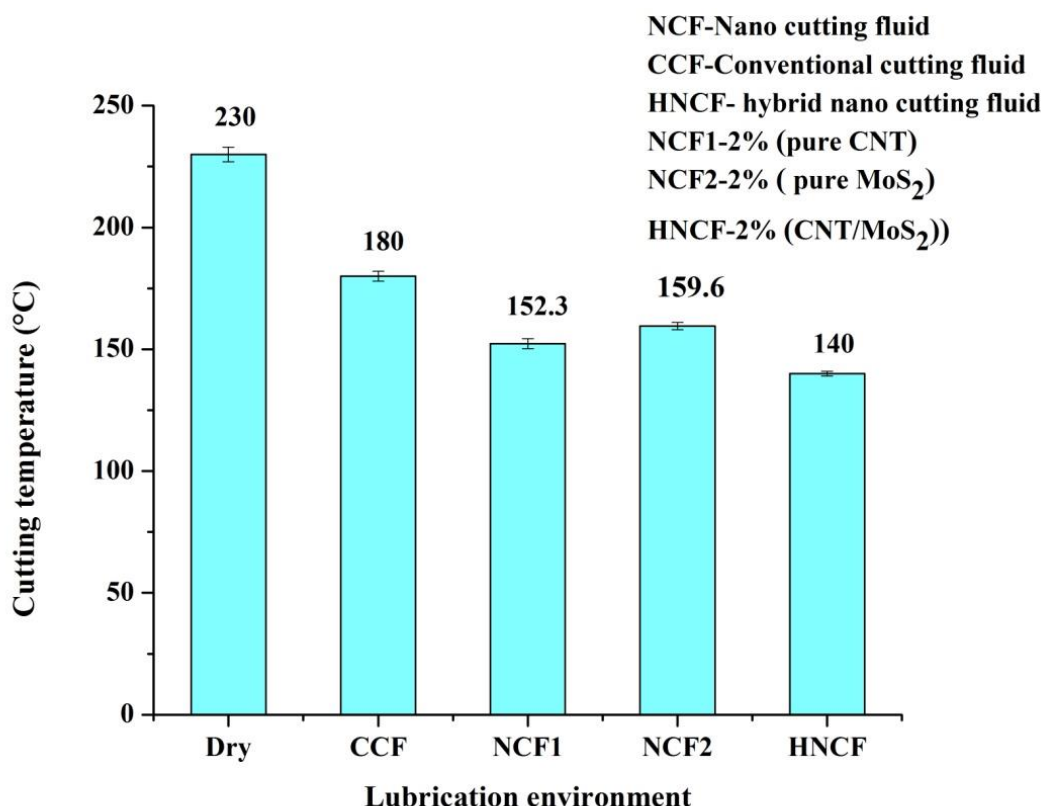


Fig. 5.12 Variation of cutting temperature with different lubrication environment
(Cutting conditions: V= 80 m/min, f = 0.161 mm/rev, d = 0.5 mm and t = 5 min)

5.6.3. Surface roughness (R_a)

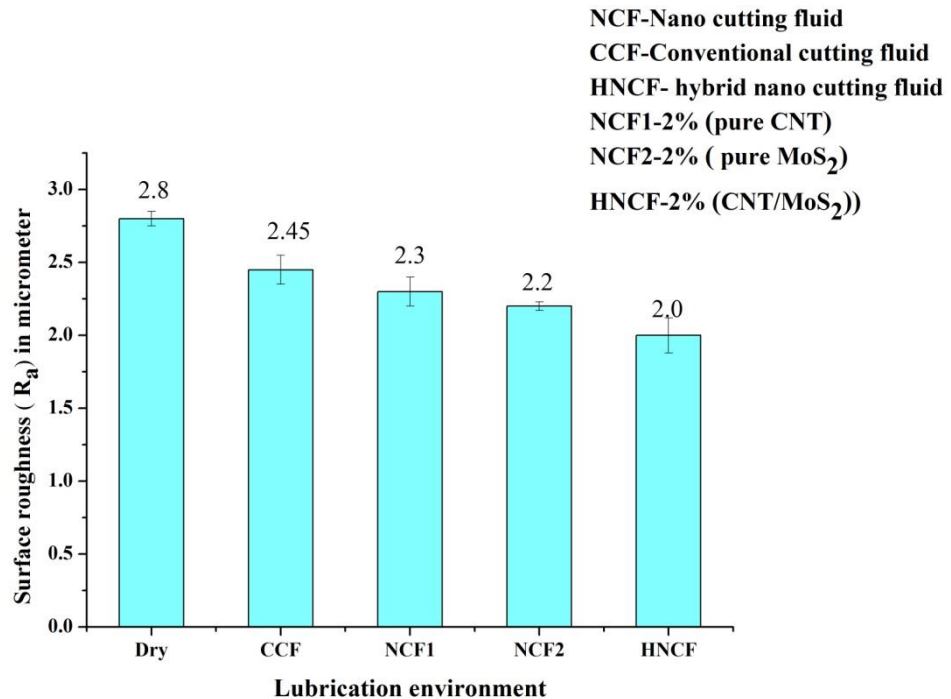


Fig. 5.13 Variation of surface roughness (R_a) with different lubrication environment

(Cutting conditions: $V = 80$ m/min, $f = 0.16$ mm/rev, $d = 0.5$ mm and $t = 5$ min)

Fig. 5.13 presents the R_a values under different lubrication environment. The R_a value is observed for NCF1 (2%) = 2.3 for pure CNT nanofluid, NCF2 (2%) = 2.2 for pure MoS_2 nanofluid and HNCF (2%) = 2 for CNT/ MoS_2 (1:2) hybrid nano cutting fluid. R_a value is observed under dry condition is 2.8 μm followed by CCF 2.45 μm . R_a value is found to reduce by 28.5 %, 18.3 %, 13 % and 9 % with the use of 2wt% of CNT/ MoS_2 (1:2) hybrid nano cutting fluid compared to dry, CCF, pure CNT and pure MoS_2 nanofluids. This may be due to consistent film on contact surfaces which reduces the coefficient of friction thereby reducing the main cutting force [84]. The reduced main cutting force and cutting temperature imparts better surface finish.

5.6.4 Tool flank wear (V_b)

Tool flank wear during machining with different lubrication environment is shown in Fig. 5.14. It is noticed that maximum tool flank wear is found with dry machining (0.225 mm) and least with 2 wt% of CNT/ MoS_2 (1:2) hybrid nano cutting fluids (0.05 mm). The possible reduction in tool flank wear is found to reduce by 77.8%, 70.5%, 63% and 65% with 2 wt% of

CNT/MoS₂ (1:2) hybrid nano cutting fluid compared to dry, CCF, 2 wt% of pure CNT and pure MoS₂ nanofluids respectively. The weaker bonding between the structures of MoS₂ nanoparticle easily forms slicing layers due to shearing action of chip on cutting tool. This provides better film formation on sliding surfaces thus reduce the plastic contacts and resulting reduction in tool flank wear [22]. Hybrid nanofluids are penetrating into the contacting surfaces with compressed air in a MQL system by mist generation when applied as cutting fluid in machining and thus reduced coefficient of friction. High thermal conductivity of the CNT nanoparticle in base fluid improves the heat dissipation property of the fluid. The synergistic effect of both CNT and MoS₂ nanoparticles enriched hybrid nano cutting fluid has given much reduced tool flank wear than pure nanofluids.

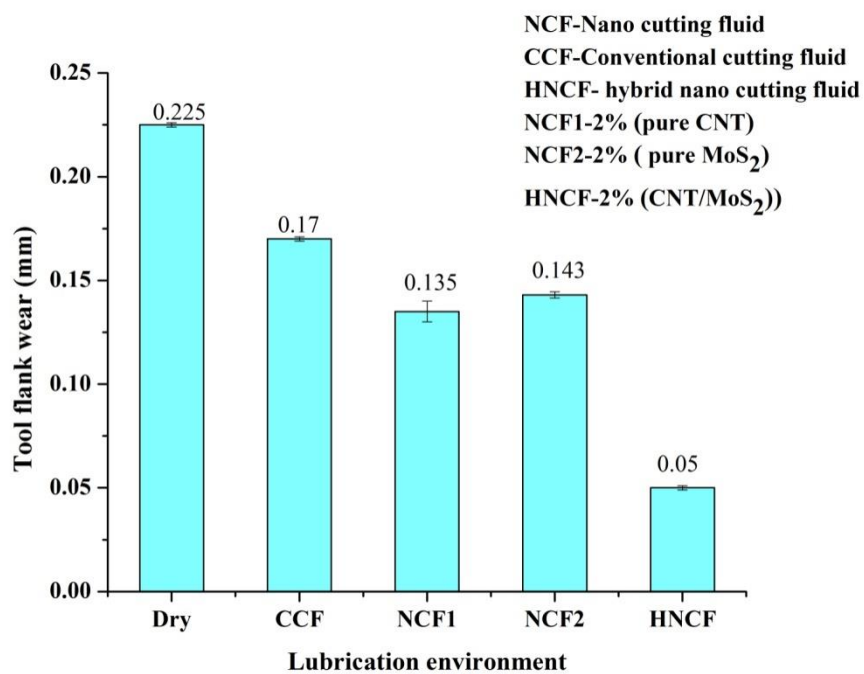


Fig. 5.14 Variation of V_b with different lubrication environment
(Cutting conditions: V= 80 m/min, f = 0.161mm/rev, d =0.5 mm and t = 5 min)

5.7 Summary

It is noticed that the samples of 0.5 wt% and 2 wt% of CNT/MoS₂ hybrid nano cutting fluids are obtained minimum sedimentation among all the samples. Viscosity of CNT/MoS₂ of nano cutting fluid increased with concentration of nanoparticle in base oil and decreased with temperature. Thermal conductivity and volumetric heat capacity of CNT/MoS₂ hybrid nano cutting fluid is seen to increase with particle concentration and temperature. Coefficient of friction is found to decrease up to particle concentration 2wt% then slightly increased.

Machining performance also discussed in this chapter by conducting turning experiments on lathe and comparative assessment is made under different lubrication environment in terms of cutting forces, cutting temperature, surface roughness and tool flank wear. The performance of 2 wt% of CNT/MoS₂ hybrid nano cutting fluid among the other samples is found to better compared to dry machining and CCF respectively.

Chapter-6

Evaluation of optimal machining parameters using hybrid nano cutting fluids for better performance in turning

6.1 Introduction

The aim of this chapter is to present the optimal machining parameters using hybrid nano cutting fluids for maximum machining performance in terms of minimum main cutting force (F_z), cutting temperature (T), surface roughness (R_a) and tool flank wear (V_b) in varying cutting conditions. Turning of AISI 1040 steel with variable cutting conditions is performed by using Response Surface Methodology (RSM). The experimental plan is adopted with Box Behnken design in RSM. Analysis of variance is applied to study the effect of each individual cutting parameters and their interaction effect on the main cutting force, cutting temperature, surface roughness, and tool flank wear. Regression models and significant input factors on machining output parameters are discussed.

6.2 Design of experiments

RSM is one of the best statistic techniques used for creating model build up relationship between experimental input and output parameters. RSM has the two important functions in statistics one is the establishing the correlation between several independent input factors and one or more response variable, second is to evaluate the response variable by changing the different input factors. Each and every response (y) is influenced by different input factors (x_i, x_j, \dots). The established correlation between independent input factors and response variable is presented with the following polynomial equation (6.1).

$$y = f(x_1, x_2, x_3, \dots, x_k) \quad (6.1)$$

The first order model is not used for optimization due to lack of fit. Second order model improves optimization for response variable due to more interaction effects of the several independent input factors. A general form of second order model is represented as

$$y = a_0 + \sum_{i=1}^n a_i x_i + \sum_{i=1}^n a_{ii} x_i^2 + \sum_{i=1}^n \sum_{j=1}^n a_{ij} x_i x_j : i < j \quad (6.2)$$

where a_0 constant

a_i, a_{ii}, a_{ij} are the coefficients for the quadratic model

x_i, x_j are the input factors

Cutting parameters are optimized with Box-Behnken design in RSM tool to get desired response value. Levels chosen in Box-Behnken design are low, medium and high which coded as -1, 1 and 1. Total of 15 experimental runs are considered in this design with three centre points. The independent input factors with their values and levels chosen in the present work are presented in Table 6.1 and response variables noted during machining are presented in Table 6.2. For experimental design and building of the model design expert software is used. The regression analysis of experimental data also carried out by using the same. The quality of the fit for second order model is checked with the value of R^2 and R^2 adjusted. The point optimization is used for multiple response parameters and values of optimal setting parameters are found.

Table 6.1 Factors and levels chosen

Factors	Units	Levels		
		-1	0	+1
Cutting speed	(m/min)	60	80	100
Feed rate	(mm/rev)	0.131	0.161	0.191
Depth of cut	(mm)	0.5	0.75	1

6.3 Optimization using desirability approach

Selecting optimal combination of process parameter for desired response parameters is challenging task in machining because of large number of input parameters. Derringer and Suich illustrated a method for optimization of multiple responses is called desirability [123]. This method is widely used in industry for optimization of multiple responses to get optimal process parameters for improved response variable. The objective function of this method is called desirability function denoted by $D(X)$. The objective form of the desirability function is the geometric mean of all the responses. A range of the desirability is 0 to 1 the value near to 1 is most desirable and ideal case, the value 0 indicates that the responses are outside the limits. The optimal combination for multiple responses is selected based on combined

desirability which considered to be maximum. The geometric mean of individual desirability gives the overall desirability (D).

$$D = (d_1 y_1 \cdot d_2 y_2 \dots d_k y_k)^{1/k} \quad (6.3)$$

Where K is the number of response parameters, y is the response variable

6.4 Machining performance with variable cutting conditions

Main cutting force, cutting temperature, surface roughness are measured online and offline during and after turning of AISI1040 steel under MQL mode of 2wt% of CNT-MoS₂ hybrid nano cutting fluid and tabulated in Table 6.2.

Table 6.2 Machining input cutting conditions and four response parameters

Run order	Input machining parameters			Response variable			
	V (m/min)	f mm/rev	D (mm)	F _z (N)	T °C	R _a (μm)	V _b (mm)
1	60	0.131	0.75	145	95	2.1	0.071
2	80	0.131	1	692	125	1.4	0.087
3	60	0.191	0.75	539	102	2.3	0.081
4	80	0.191	1	828	130	1.6	0.092
5	80	0.161	0.75	813	125	2.07	0.080
6	100	0.161	1	823	137	2.17	0.107
7	100	0.131	0.75	453	130	1.4	0.102
8	80	0.191	0.5	815	134	1.93	0.103
9	100	0.191	0.75	726	145	2.2	0.113
10	80	0.131	0.5	263	109	1.33	0.078
11	80	0.161	0.75	810	123	2.15	0.08
12	80	0.161	0.75	807	123	2.05	0.083
13	60	0.161	0.5	333	97	2.4	0.078
14	100	0.161	0.5	548	134	1.93	0.103
15	60	0.161	1	522	100	2.21	0.079

6.4.1 Effect of cutting parameters on main cutting force (F_z)

It is noticed from Fig. 6.1 (a-c) that the main cutting force is found to increase and then slightly decrease with increase in cutting speed. Continuous increase in trend is found with increase in feed rate and depth of cut. This is due to higher area of chip tool interface during machining processes. The least main cutting force is recorded with $V= 60$ m/min and $f = 0.131$ mm/rev feed rate at $d = 0.75$ mm.

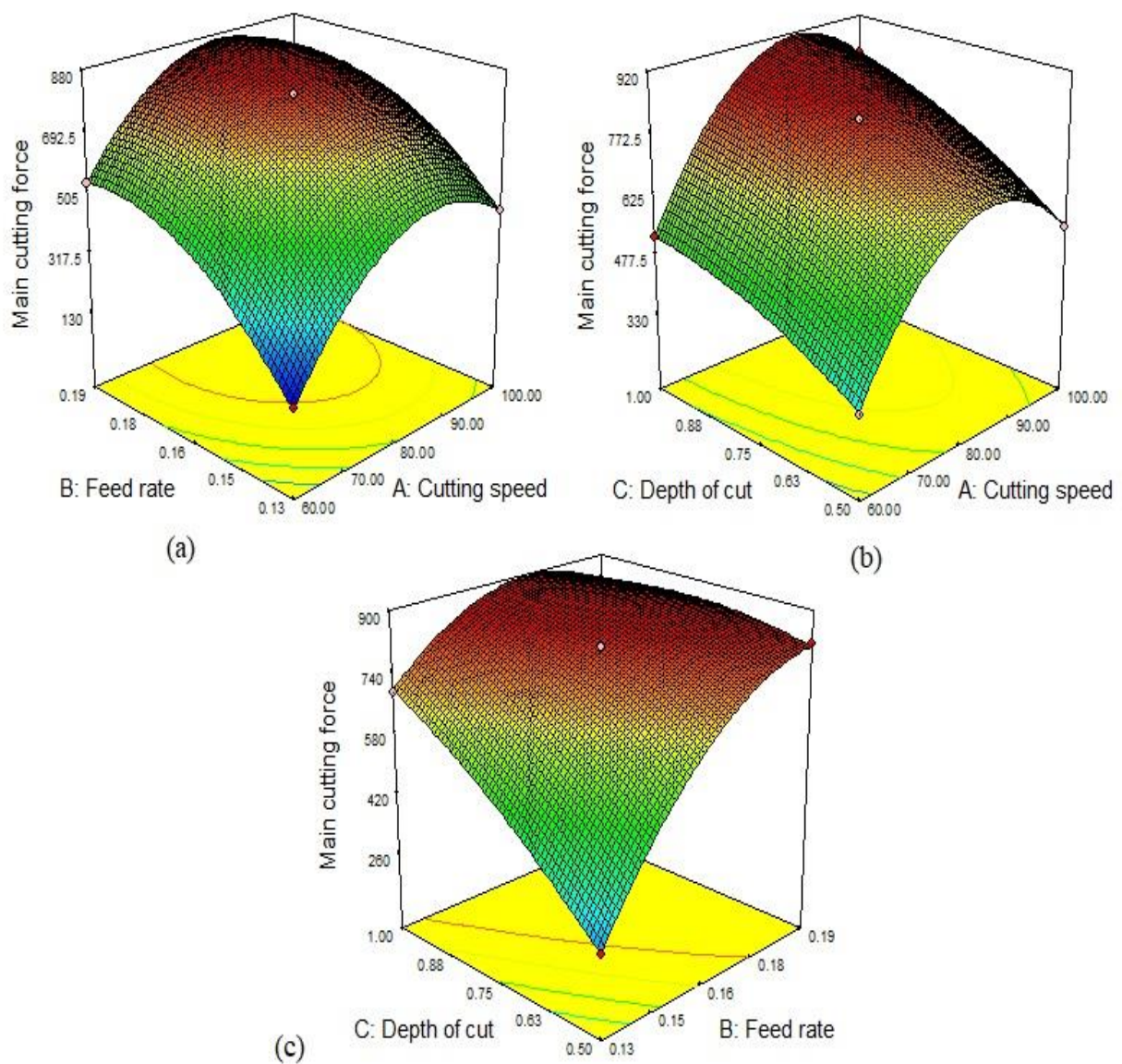


Fig. 6.1 (a-c) Esteemed response surface plot for main cutting force

The ANOVA for main cutting force is performed at 95% (5% significance) level which is summarized in Table 6.3. The developed quadratic model for main cutting force is

found to be significant and lack of fit is found to be non significant. From the ANOVA results, P value of the model is 0.0001. Hence the model and its terms V, f and d are statistically significant on main cutting force [124]. The regression model values of R^2 and R^2 adjusted for main cutting force are equal to 0.9997 and 0.9993. The values of R^2 predicted and adequate precision are equal to 0.9962 and 137.218. From the adequate precision value it is understood that the model is better fitted. The regression model for main cutting force is as follows.

$$\text{Main cutting force} = -10440.01042 + 98.66083 \times V + 65025.000 \times f + 3178.534 \times d + 50.41667 \times v \times f + 4.300 \times v \times d - 13866.66667 \times f \times d - 0.54656 \times V^2 - 1.39583E + 005 \times f^2 - 558.000 \times d^2 \quad (6.4)$$

Table 6.3 ANOVA for main cutting force (F_z)

Source	Sum of Square	DF	MS	F-Value	P-Value	Remarks
Model	7.295E+005	9	81055.07	2147.15	< 0.0001	Significant
A-V	1.278E+005	1	1.278E+005	3384.51	< 0.0001	
B-f	2.295E+005	1	2.295E+005	6079.55	< 0.0001	
C-d	1.026E+005	1	1.026E+005	2718.00	< 0.0001	
AB	3660.25	1	3660.25	96.96	0.0002	
AC	1849.00	1	1849.00	48.98	0.0009	
BC	43264.00	1	43264.00	1146.07	< 0.0001	
A^2	1.765E+005	1	1.765E+005	4674.99	< 0.0001	
B^2	58270.67	1	58270.67	1543.59	< 0.0001	
C^2	4490.83	1	4490.83	118.96	0.0001	
Residual	188.75	5	37.75			
Lack of fit	170.75	3	56.92	6.32	0.1396	not significant
Pure error	1700.667	2	850.3333			
Cor total	786434.9	14				
	DF= Degrees of freedom; MS= Mean square					

6.4.2 Effect of cutting parameters on cutting temperature (T°C)

Figure 6.2 (a-c) shows that increase in cutting temperature with increase in cutting parameters of V, f and d due to generation of heat in deformation zone. The lowest cutting temperature is found at lower values of V, f and d. The results of ANOVA for cutting temperature are presented in Table 6.4. The value P for developed regression model is less than 0.05 which indicates that the terms of the model have significant effect on response. The R^2 value of regression model is 0.9952 and the value of adjusted R^2 is 0.9865. The predicted R^2 value 0.9333 is as close as to the R^2 - adjusted value. The adequate precision value 33.71 in this case is more than 4. Hence, the developed regression model for cutting temperature is desirable. The regression model for cutting temperature is as follows.

$$\text{Cutting temperature} = -111.21565 + 3.04667 \times V + 122.03704 \times f + 118.33333 \times d + 3.3333 \times v \times f + 0.0000 \times v \times d - 666.66667 \times f \times d - 0.01645 \times V^2 + 1018.51852 \times f^2 - 1.33333 \times d^2 \quad (6.5)$$

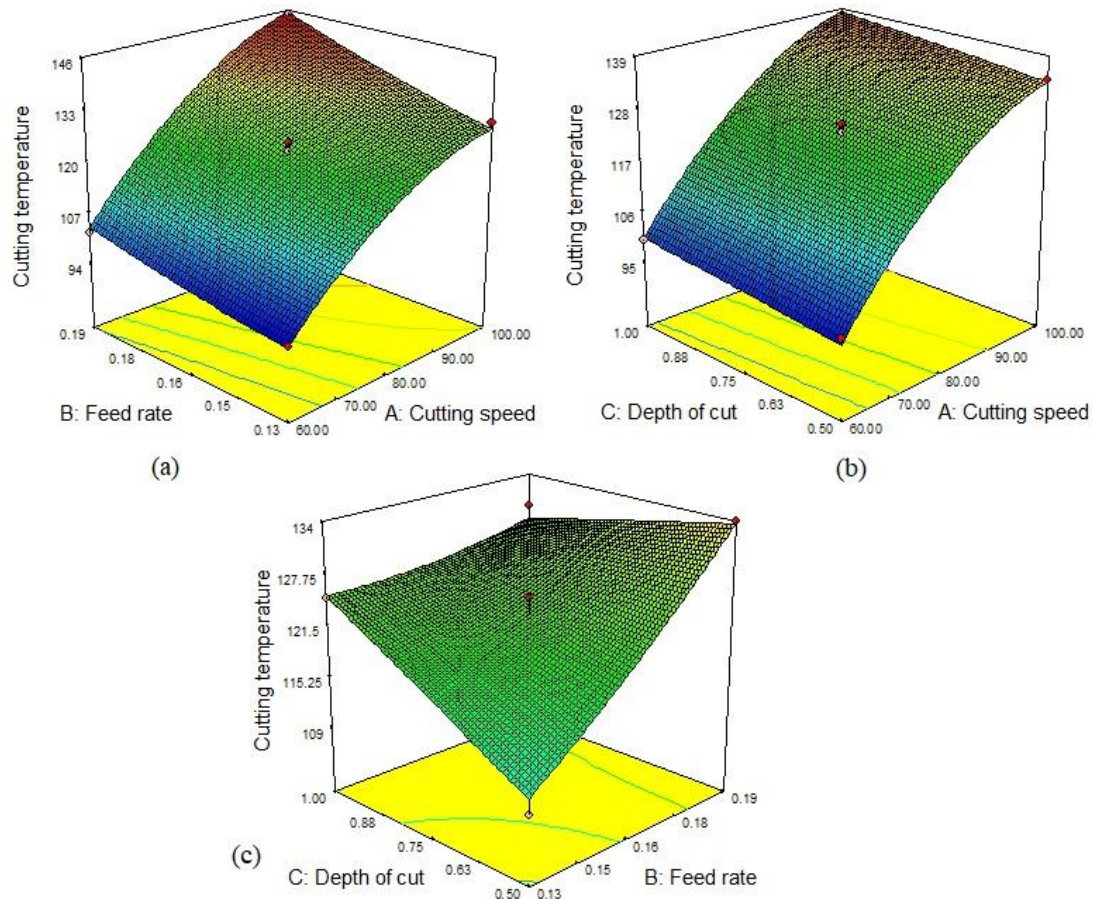


Fig. 6.2 (a-c) Esteemed response surface plot for cutting temperature

Table 6.4 ANOVA table for cutting temperature (T° C)

Source	Sum of Square	DF	MS	F-Value	P-Value	Remarks
Model	3550.43	9	394.49	114.90	< 0.0001	Significant
A-V	2888.00	1	2888.00	841.17	<0.0001	
B-f	338.00	1	338.00	98.45	0.0002	
C-d	40.50	1	40.50	11.80	0.0185	
AB	16.00	1	16.00	4.66	0.0833	
AC	0.000	1	0.000	0.000	1.000	
BC	100.00	1	100.00	29.13	0.0029	
A ²	160.03	1	160.03	16.61	0.0010	
B ²	3.10	1	3.10	0.90	0.3855	
C ²	0.026	1	0.026	7.468E-003	0.9345	
Residual	17.17	5	3.43			
Lack of fit	14.50	3	4.83	3.63	0.2237	not significant
Pure error	2.67	2	1.33			
Cor total	3567.60	14				

6.4.3 Effect of cutting parameters on surface roughness (R_a)

The influence of cutting parameters V, f and d by using 2wt% of CNT-MoS₂ (1:2) hybrid nano cutting fluid on R_a is illustrated with Fig. 6.3(a-c). R_a value is observed to decrease and then increase with the cutting parameter V due to vanishing of built up edge on tool tip at high speed. R_a value is increases with increase in f and d due to axial movement of tool and rigidity effect of machine. The lowest R_a value is achieved with interaction of f = 0.131 mm /rev and d = 0.5 mm at middle level of V. Increase in V causes easier plastic deformation and chip flow during machining which reduces the built up edge formation on tool and improves the surface quality of the machined part [82]. The results of ANOVA are depicted in Table 6.5. P-value of the model is 0.0009 which is less than 0.05 indicate that model is significant. The model terms V and f are significant where as d is not significant on R_a value. The non significant terms are not counted in building of the models. The regression model R_a with the values of R² and R² adjusted are equal to 0.9806 and 0.9455. R² predicted value is 0.7340 and adequate precision value is 18.188. The R² predicted value is in good

agreement with the value of adjusted R^2 . From the R^2 value and adequate precision value, it is understood that the developed model is desirable for prediction of R_a value. The regression model for R_a is as follows.

$$\text{Surface roughness } (R_a) = -2.98389 - 0.16906 \times V + 123.16944 \times f + 4.49167 \times d + 0.25000 \times v \times f + 0.021500 \times v \times d - 13.33333 \times f \times d + 6.653125E - 004 \times V^2 - 390.1018.27778 \times f^2 - 2.78000 \times d^2 \quad (6.6)$$

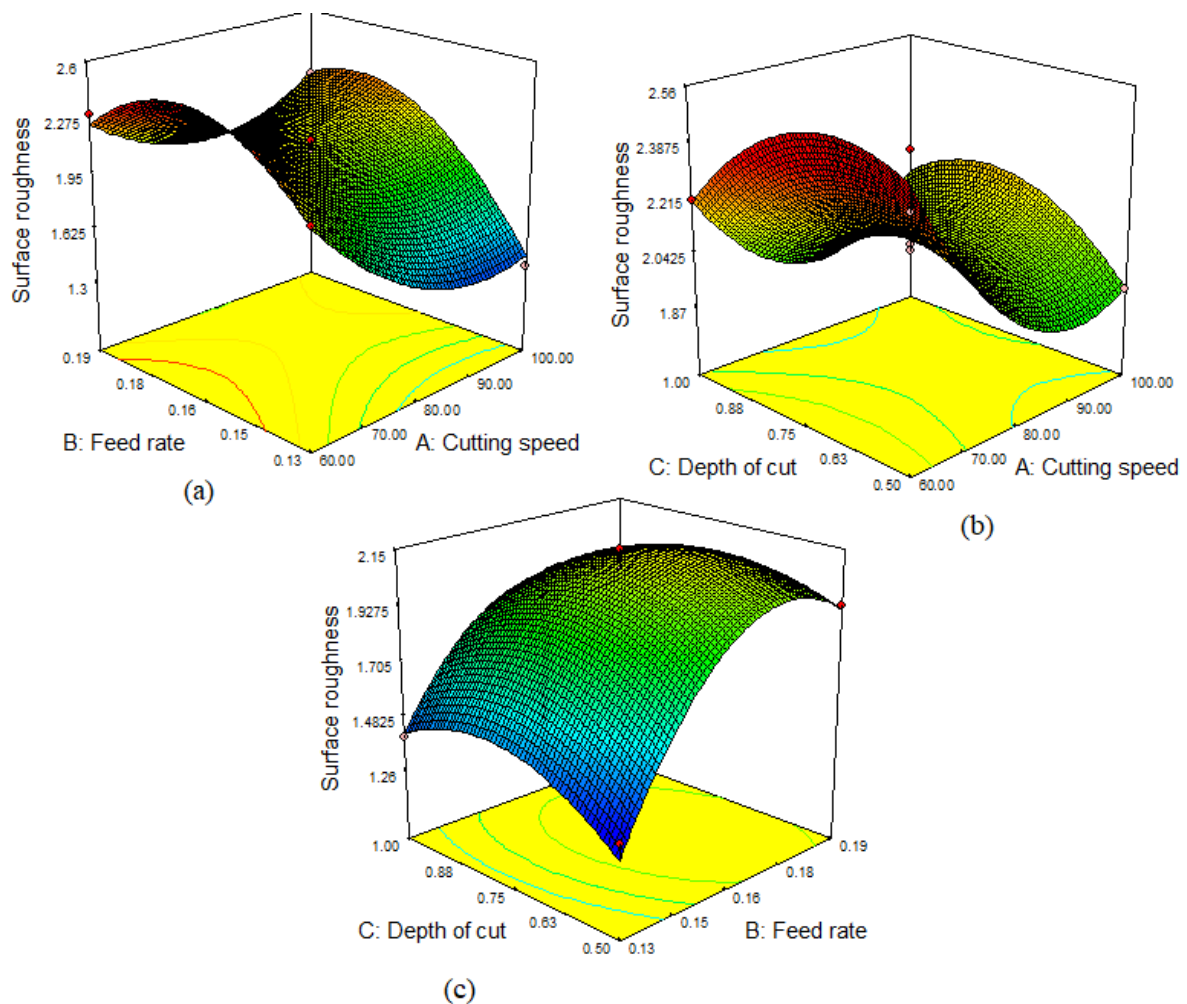


Fig. 6.3 (a-c) Esteemed response surface plot for surface roughness (R_a)

Table 6.5 ANOVA table for surface roughness (R_a)

Source	Sum of Square	DF	MS	F-value	P-value	Remarks
Model	1.67	9	0.19	28.01	0.0009	Significant
A-V	0.21	1	0.21	32.38	0.0023	
B-f	0.40	1	0.40	61.13	0.0005	
C-d	5.513E-003	1	5.513E-003	0.83	0.4035	
AB	0.090	1	0.090	13.58	0.0142	
AC	0.046	1	0.046	6.98	0.0459	
BC	0.040	1	0.040	6.04	0.0574	
A^2	0.25	1	0.25	38.04	0.0016	
B^2	0.46	1	0.46	68.76	0.0004	
C^2	0.11	1	0.11	16.83	0.0093	
Residual	0.033	5	6.625E-003			
Lack of fit	0.028	3	9.175E-003	3.28	0.2425	not significant
Pure error	5.600E-003	2	2.800E-003			
Cor total	1.70	14				

6.4.4 Effect of cutting parameters on tool flank wear (V_b)

Figure 6.4 (a-c) shows the response surface plot for tool flank wear and it is observed to increase with increase in cutting parameters V , f and d due to formation of built up edge on tool face which causes failure of tool. The lowest tool flank wear is found with the combination of $V = 60$ m/min, $f = 0.131$ mm/rev at $d=0.75$ mm. Results of ANOVA for tool flank wear are depicted in Table 6.6. P-value of the model for tool flank wear is 0.0005 which denotes that model and its terms are significant on response value. The cutting parameters V and f are significant on tool flank wear and d is not significant. The regression model values R^2 and R^2 adjusted are equal to 0.9855 and 0.9595. The value of predicted R^2 is 80.29 which is very near to the value of adjusted R^2 . Adequate precision value is 9.396 which is greater than 4. Hence, the developed regression model is better fitted for predicting tool flank wear.

The regression model for tool flank wear is as follows.

$$\begin{aligned} \text{Tool flank wear } (V_b) = & +0.19163 - 1.95458E - 003 \times V - 0.93083 \times f - \\ & 0.011167 \times d + 4.16667E - 004 \times v \times f + 1.50000E - 004 \times v \times d - 0.66667 \times f \times \\ & d + 1.56250E - 005 \times V^2 + 5.0000 \times f^2 + 0.072000 \times d^2 \end{aligned} \quad (6.7)$$

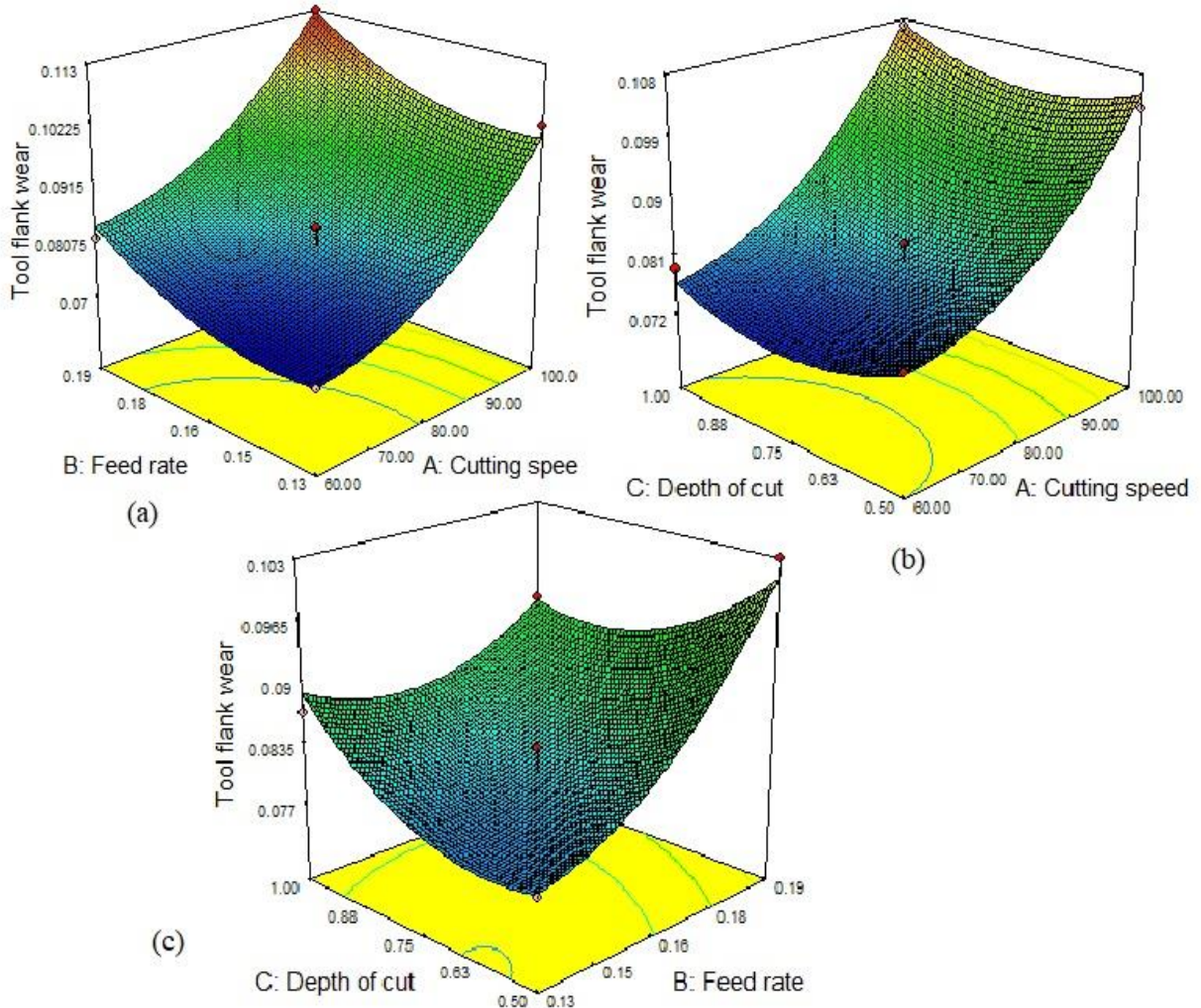


Fig. 6.4 (a-c) Esteemed response surface plot for tool flank wear

Table 6.6 ANOVA table for tool flank wear (V_b)

Source	Sum of Square	DF	MS	F-value	P-Value	Remarks
Model	2.367E-003	9	2.630E-004	37.84	0.0005	Significant
A-V	1.682E-003	1	1.682E-003	242.01	< 0.0001	
B-f	3.251E-004	1	3.251E-004	46.78	0.0010	
C-d	1.125E-006	1	1.125E-006	0.16	0.7041	
AB	2.500E-007	1	2.500E-007	0.036	0.8570	
AC	2.250E-006	1	2.250E-006	0.32	0.5940	
BC	1.000E-004	1	1.000E-004	14.39	0.0127	
A ²	1.442E-004	1	1.442E-004	20.75	0.0061	
B ²	7.477E-005	1	7.477E-005	10.76	0.0220	
C ²	7.477E-005	1	7.477E-005	10.76	0.0220	
Residual	3.475E-005	5	6.950E-006			
Lack of fit	2.875E-005	3	9.583E-006	3.19	0.2475	not significant
Pure error	6.000E-006	2	3.000E-006			
Cor total	2.402E-003	14				

6.5 Optimization using desirability function

In optimization, desired goals are chosen for each cutting parameter and response parameter. Low and high level values are set to each cutting parameter of V, f and d and goal is set in that range. The possible goals for each response parameter like main cutting force, cutting temperature, surface roughness and tool flank wear are set as per quality characteristics which are considered to be minimization for four responses. The goals of the multiple response parameters are combined into an overall desirability objective function that ranges from 0 to 1 by using developed models for response parameters in design expert software and optimization is carried out.

The combination of optimal setting parameters of V, f and d for the four machining response parameters are in the order of 70.25 m/min, 0.13 mm /rev and 0.5 mm, which are obtained by using desirability function, is shown in Table 6.7 and Fig. 6.9. Desirability value

for this combination is 0.907. Machining responses are predicted from the developed model at this optimum values and confirmation experiment is conducted at the same optimum values. The predicted values and experimental values of machining responses using optimal setting parameters are also shown in Table 6.7. Maximum error between the values of experimental and predicted responses is found to be 8%. Hence, the developed models in RSM are fit to the present problem and the optimum machining parameters obtained from the same models gives the best response values for the selected hybrid nanofluid.

Table 6.7 Optimized and experimental values

Input parameters			Response parameters							
			Predicted value				Experimental value			
V (m/min)	f (mm/rev)	D (mm)	F _z (N)	T (°C)	R _a (μm)	V _b (mm)	F _z (N)	T (°C)	R _a (μm)	V _b (mm)
70.25	0.131	0.5	145	100.89	1.53	0.073	158	105	1.6	0.081

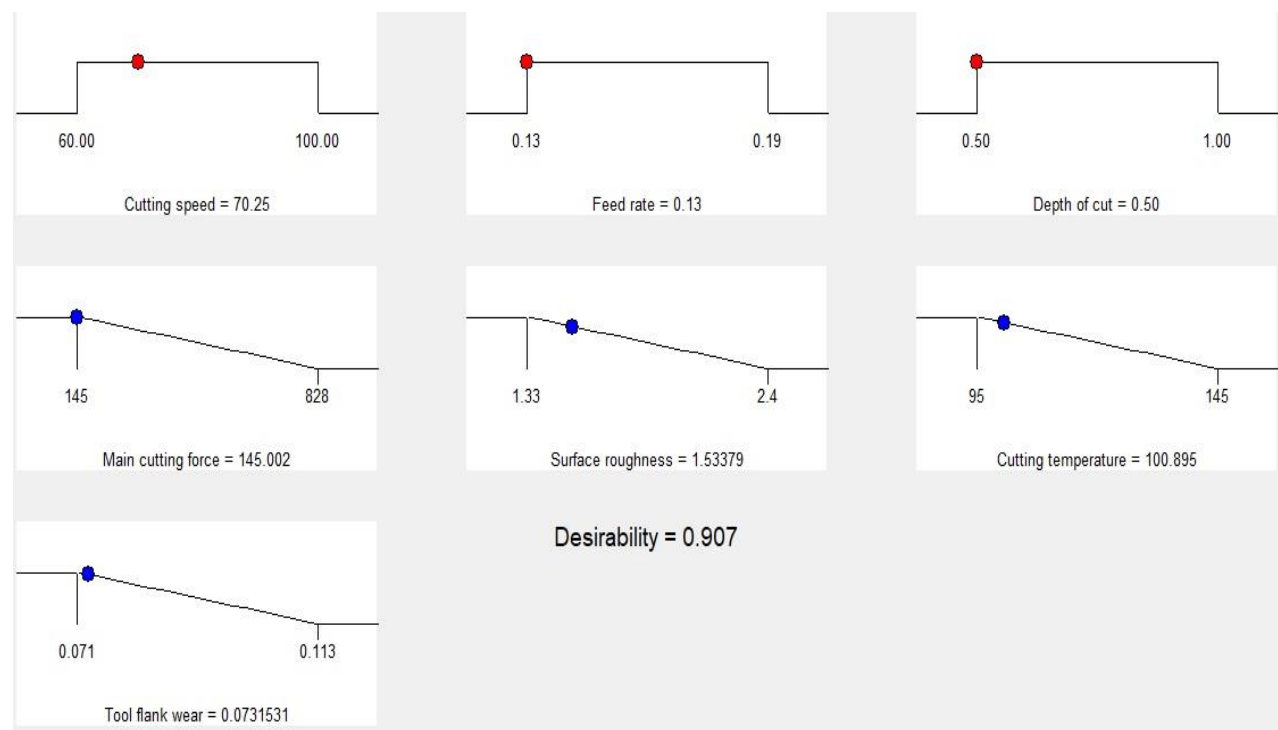


Fig. 6.5 Ramp function graph of desirability

6.6 Machining performance obtained with optimal cutting parameters

After obtaining optimal cutting parameters using desirability approach, turning experiments are conducted on lathe with the same input parameters. Machining performance in terms of main cutting force, cutting temperature, surface roughness (Ra) and tool flank wear are examined for the lubrication environments of dry machining, conventional cutting fluid and 2 wt% of CNT/MoS₂ hybrid nano cutting fluid.

6.6.1 Main cutting force (F_z)

Results of main cutting force using dry machining, CCF and hybrid nano cutting fluid with optimal cutting parameters is shown in Fig. 6.6. Main cutting force is obtained to be 230 N under dry machining, followed by CCF (210 N) and hybrid nano cutting fluid (158 N). The percentage reduction in main cutting force using hybrid nano cutting fluid is found to be 31% and 25% compared to dry machining and CCF respectively.

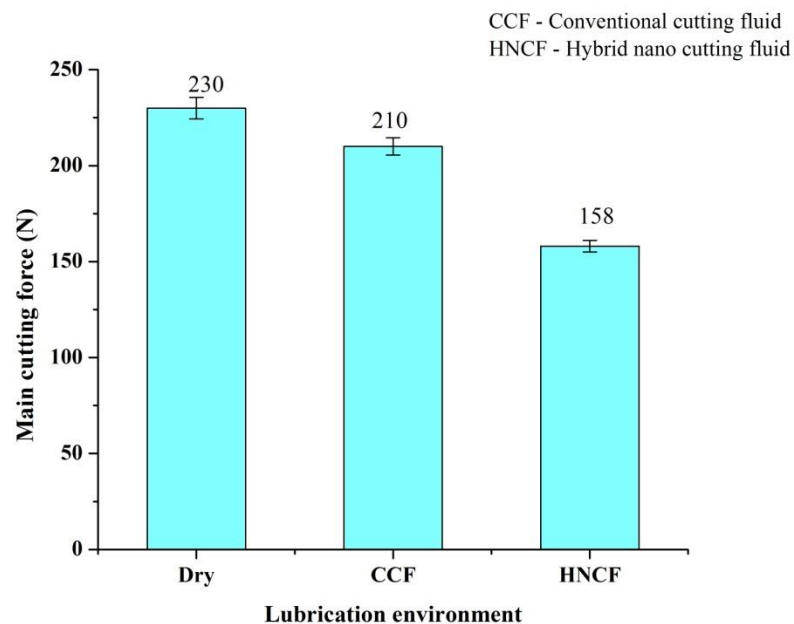


Fig. 6.6 Variation of main cutting force with different lubrication environment
(Cutting conditions: V=70.25 m/min, f = 0.13 mm/rev, d = 0.5 mm and t = 5 min)

6.6.2 Cutting temperature

Results of cutting temperature versus different lubrication environment with optimal cutting parameters are presented in Fig. 6.7. Maximum cutting temperature is found to be (200 C) under dry machining and least cutting temperature (105°C) is obtained using hybrid nano cutting fluid under MQL condition. The cutting temperature is reduced by 47 % and 27 % with use of hybrid nano cutting fluid than that of dry and CCF.

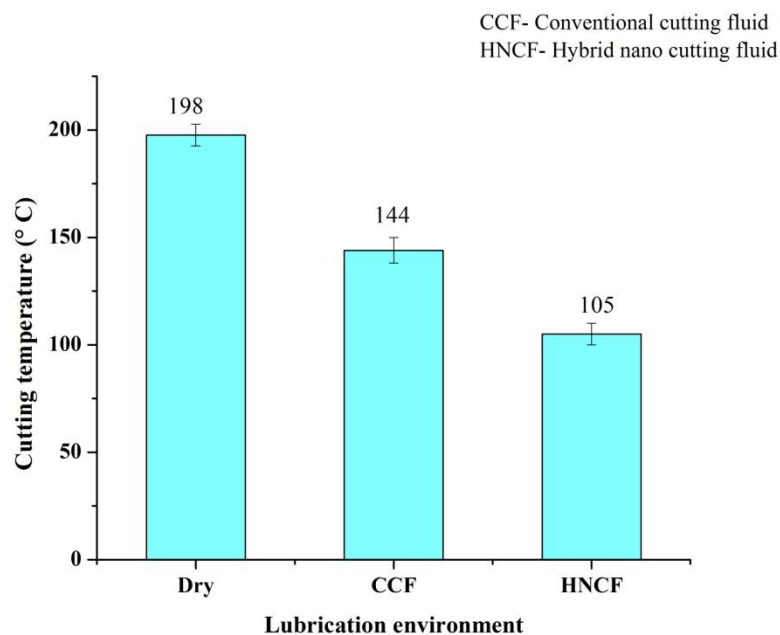


Fig. 6.7 Variation of cutting temperature with different lubrication environment
(Cutting conditions: $V=70.25$ m/min, $f = 0.13$ mm/rev, $d = 0.5$ mm and $t = 5$ min)

6.6.3 Surface roughness (R_a)

Figure 6.8 presents the average surface roughness (R_a) of machined surface in different lubrication environments with optimal cutting parameters. From Fig. 6.8, it is noticed that maximum surface roughness (R_a) value is found to be 2.3 μm under dry machining, followed by using CCF (2 μm) and least surface roughness (R_a) value is found to be 1.6 μm with use of hybrid nano cutting fluid. Surface roughness (R_a) value is found to reduce by 30% and 20% with use of hybrid nano cutting fluid compared to dry machining and CCF respectively. The reduction main cutting force and cutting temperature as explained in

section (4.6.3) is the reason for improvement of surface finish of the machined surface by the application of hybrid nano cutting fluid.

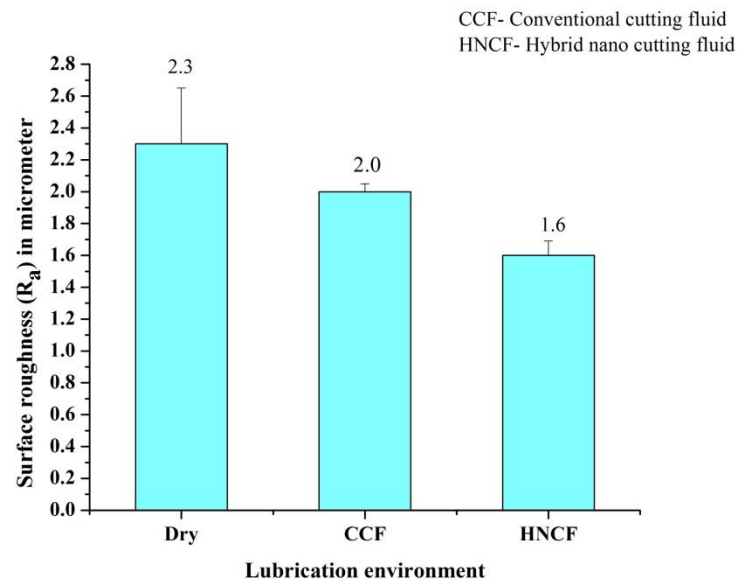


Fig. 6.8 Variation of the surface roughness with different lubrication environment
(Cutting conditions: $V=70.25$ m/min, $f = 0.13$ mm/rev, $d = 0.5$ mm and $t = 5$ min)

6.6.4 Tool flank wear

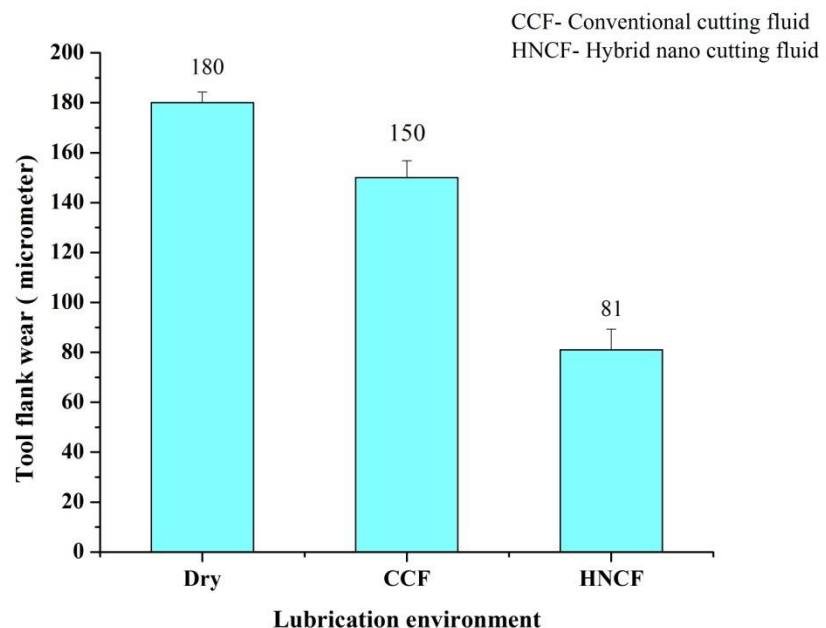


Fig. 6.9 Variation of tool flank wear with different lubrication environment
(Cutting conditions: $V=70.25$ m/min, $f = 0.13$ mm/rev, $d = 0.5$ mm and $t = 5$ min)

Tool flank wear is measured after the each turning operation using Tool maker's microscope. Figure 6.9 represents the results of the tool flank wear in different lubrication environment with optimal cutting parameters. From the experimental results maximum tool flank wear is found to be 180 micrometer under dry machining, 150 micrometer is obtained using CCF and 81 micrometer is obtained with use of hybrid nano cutting fluid. Tool flank wear is found to reduce by 55% and 46% with use of hybrid nano cutting fluid compared to dry machining and CCF respectively.

6.7 Summary

The significant reduction in main cutting force, cutting temperature, surface roughness and tool flank wear is found with use of 2 wt% of CNT1MoS₂ (1:2) hybrid nano cutting fluid compared to Dry, CCF, pure CNT and pure MoS₂ nanofluid. Machining performance obtained with variable cutting conditions also discussed. Single combination of optimal setting parameters of V, f and d for main cutting force, cutting temperature, surface roughness and tool flank wear are found to 70.25 m/min, 0.13 mm/rev and 0.5 mm at desirability value of 0.907.

Chapter-7

Conclusions

7.1 Conclusions

Experimental investigations are carried out to examine the performance of vegetable oil based hybrid nano cutting fluids during turning of AISI1040 steel. In the present work, stability of different vegetable oil based hybrid nano cutting fluids is studied and their applicability in machining under MQL mode is evaluated. Thermo physical properties are evaluated by preparing CNT/MoS₂ stable hybrid nano cutting fluids at 1:2 proportions in 0.5%, 1%, 1.5%, 2%, 2.5% and 3% concentrations. Machining performance is examined at different concentration of nano particles at stable composition. Experimental results are compared for dry, CCF, pure CNT, pure MoS₂ nanofluids and CNT/MoS₂ (1:2) hybrid nano cutting fluids at constant cutting conditions and optimum cutting conditions are evaluated by observing the machining performance at variable cutting conditions.

Overall observations from the present work are as follows:

- Sedimentation and zeta potential test confirms that sesame oil based CNT/MoS₂ hybrid nanofluid is found to be stable compared to CNT/BA hybrid nanofluid.
- Sesame oil based CNT/MoS₂ hybrid nanofluid with SDS surfactant at 15% concentration of nanoparticle weight in base oil and (1:2) hybrid ratio is optimum for better stability of the nanofluid. This may be due to the interface bonding between the nanoparticle and base fluid supported by the surfactant and minimum agglomeration of nanoparticles.
- Application of vegetable oil based hybrid nano cutting fluids under MQL conditions improved machining performance by reducing cutting force, cutting temperature, surface roughness and tool flank wear compared to dry machining and CCF. This may be due to formation of durable layer of lubricant film on contacting surfaces and effectiveness of MQL.
- From sedimentation test it is found that 0.5 wt% and 2 wt% of CNT/MoS₂ (1:2) hybrid nano cutting fluids showed minimum sedimentation among all the samples.

- Thermal conductivity, volumetric heat capacity and viscosity of CNT/MoS₂ (1:2) hybrid nano cutting fluids increased with increase in nanoparticle concentration in base oil and temperature.
- Enhancement in thermal conductivity of CNT/MoS₂ (1:2) hybrid nano cutting fluid is found to be 28.31% at 3wt% compared to base oil. Nanoparticle size, shape and brownian motion are the reasons for this improvement.
- Coefficient of friction is decreased up to 2wt% particle concentration and then slightly increased. The reduction in coefficient of friction is 93.77% compared to dry and 82.9% compared to base oil at 2wt%.of CNT/MoS₂ (1:2) hybrid nano cutting fluids respectively.
- Machining performance is improved by reduction in cutting force, cutting temperature, surface roughness and tool flank wear with the application of 2 wt% of CNT/MoS₂ hybrid nano cutting fluid compared to pure CNT and pure MoS₂ nanofluids. This may due to synergistic effect of CNT and MoS₂ nanoparticles, ball bearing effect of MoS₂ and stable form of nanofluid.
- Significant reductions of cutting force, cutting temperature, surface roughness and tool flank wear with hybrid nano cutting fluids in machining are quantified as follows.
 - i. Thrust force is found to reduce by 22% and 11.2%, feed force is found to reduce by 28.3%, 13.8% and main cutting force is found to reduce by 32%, 27.3% at 2 wt% of CNT/MoS₂ hybrid nano cutting fluid compared to dry machining and CCF respectively.
 - ii. Cutting temperature is reduced by 43.4% and 28%, tool flank wear is reduced by 81.3% and 75% with CNT/MoS₂ (1:2) hybrid nano cutting fluid at 3wt% than that of dry machining and CCF respectively.
 - iii. Surface roughness is reduced by 28.5% and 18.3% at 2 wt% of CNT/MoS₂ (1:2) hybrid nano cutting fluid compared dry machining and CCF respectively.
- Significant factors on cutting force and cutting temperature are cutting speed, feed and depth of cut. However, depth of cut is not significant on surface roughness and tool flank wear whereas parameters cutting speed and feed are significant.
- The value of predicted R² and adjusted R² are almost same for all the output responses. All the models are significant.

- Desirability test confirms that optimal setting parameters of cutting speed, feed and depth of cut for four response parameters are found to be 70.25 m/min, 0.13 mm/rev and 0.5mm at desirability value of 0.907.
- Maximum error between the values of experimental and predicted responses is found to be 8%.

7.2 Future scope

Present work can be extended in the following directions:

- Application of vegetable oil based hybrid nano cutting fluids may be studied in machining process like milling, grinding and drilling etc.
- Effect of nozzle orientation in MQL may be studied for different machining processes by supplying hybrid nano coolant.
- Cost analysis may be carried out for vegetable oil based nanofluid.
- Residual stresses may be analyzed for with hybrid nano cutting fluid under MQL mode.

References

- [1] R. Padmini, P. Vamsi Krishna, and G. Krishna Mohana Rao, “Performance assessment of micro and nano solid lubricant suspensions in vegetable oils during machining,” *Proc. Inst. Mech. Eng. Part B J. Eng. Manuf.*, vol. 229, no. 12, pp. 2196–2204, 2015.
- [2] M. Amrita, R. R. Srikant, A. V. Sitamaraju, M. Prasad, and P. V. Krishna, “Preparation and characterization of properties of nanographite-based cutting fluid for machining operations,” *Proc. Inst. Mech. Eng. Part J J. Eng. Tribol.*, vol. 228, no. 3, pp. 243–252, 2014.
- [3] M. Bacci and J. Wallbank, “Cutting temperature: prediction and measurement methods — a review,” *J. Mater. Process. Technol.*, vol. 88, pp. 195–202, 1999.
- [4] Y. Huang and S. Y. Liang, “Cutting forces modeling considering the effect of tool thermal property—Application to CBN hard turning,” *Int. J. Mach. Tools Manuf.*, vol. 43, no. 3, pp. 307–315, 2003.
- [5] G. Byrne, “Thermoelectric signal characteristics and average interfacial temperatures in the machining of metals under geometrically defined conditions,” *Int. J. Mach. Tools Manuf.*, vol. 27, no. 2, pp. 215–224, 1987.
- [6] T. Yashiro, T. Ogawa, and H. Sasahara, “Temperature measurement of cutting tool and machined surface layer in milling of CFRP,” *Int. J. Mach. Tools Manuf.*, vol. 70, pp. 63–69, 2013.
- [7] S. W. M. A. I. Senevirathne, “Effect of Air and Chilled Emulsion Minimum Quantity Lubrication (ACEMQL) in Machining Hard to Cut Metals,” no. February, pp. 76, 2015.
- [8] M. Amrita, R. R. Srikant, A. V. Sitamaraju, M. M. S. Prasad, and P. V. Krishna, “Experimental investigations on influence of mist cooling using nanofluids on machining parameters in turning AISI 1040 steel,” *Proc. Inst. Mech. Eng. Part J J. Eng. Tribol.*, vol. 227, no. 12, pp. 1334–1346, 2013.
- [9] R. Padmini, P. Vamsi Krishna, and G. Krishna Mohana Rao, “Experimental evaluation of nano-molybdenum disulphide and nano-boric acid suspensions in vegetable oils as prospective cutting fluids during turning of AISI 1040 steel,” *Proc. Inst. Mech. Eng. Part J J. Eng. Tribol.*, vol. 230, no. 5, pp. 493–505, 2015.
- [10] Y. Yildiz and M. Nalbant, “A review of cryogenic cooling in machining processes,”

Int. J. Mach. Tools Manuf., vol. 48, no. 9, pp. 947–964, 2008.

[11] M. Hadi and R. Atefi, “Effect of Minimum Quantity Lubrication with Gamma-Al₂O₃ Nanoparticles on Surface Roughness in Milling AISI D3 Steel,” *Indian J. Sci. Technol.*, vol. 8, no. 3, pp. 296–300, 2015.

[12] A. Erdemir, “Solid lubricants and self-lubricating films,” in *Modern Tribology Handbook: Volume One: Principles of Tribology*, 2000, pp. 787–825.

[13] S. Shaji and V. Radhakrishnan, “Investigations on the application of solid lubricants in grinding,” vol. 216, no. 10, pp. 1325–1343, 2002.

[14] M. Pushpavanam and S. R. Natarajan, “Nickel-boron nitride electrocomposites,” *Met. Finish.*, vol. 93, no. 6, pp. 97–99, 1995.

[15] Y. Zhang, C. Li, D. Jia, D. Zhang, and X. Zhang, “Experimental evaluation of the lubrication performance of MoS₂/CNT nanofluid for minimal quantity lubrication in Ni-based alloy grinding,” *Int. J. Mach. Tools Manuf.*, vol. 99, pp. 19–33, 2015.

[16] J. Van Gerpen, B. Shanks, R. Pruszko, D. Clements, and G. Knothe, “Biodiesel Production Technology,” *Natl. renewable energy Lab.*, vol. 1617, no. July, pp. 80401–3393, 2004.

[17] Y. M. Shashidhara and S. R. Jayaram, “Vegetable oils as a potential cutting fluid-An evolution,” *Tribol. Int.*, vol. 43, no. 5–6, pp. 1073–1081, 2010.

[18] R. Padmini, P. Vamsi Krishna, and G. Krishna Mohana Rao, “Effectiveness of vegetable oil based nanofluids as potential cutting fluids in turning AISI 1040 steel,” *Tribol. Int.*, vol. 94, pp. 490–501, 2016.

[19] A. Suhane, A. Rehman, and H. K. Khaira, “Tribological Investigation of Mahua Oil Based Lubricant for Maintenance Applications,” *Int. J. Eng.*, vol. 3, no. 4, pp. 2367–2371, 2013.

[20] S. Gugulothu and V. K. Pasam, “Testing and Performance Evaluation of Vegetable-Oil – Based Hybrid Nano Cutting Fluids,” *J. Test. Eval.*, vol. 48 no.5, 2018.

[21] A. M. Elias and M. P. Saravanakumar, “A review on the classification, characterisation, synthesis of nanoparticles and their application,” *IOP Conf. Ser. Mater. Sci. Eng.*, vol. 263, no. 3, 2017.

[22] R. K. Singh, A. K. Sharma, A. R. Dixit, A. K. Tiwari, A. Pramanik, and A. Mandal, “Performance evaluation of alumina-graphene hybrid nano-cutting fluid in hard turning,” *J. Clean. Prod.*, vol. 162, pp. 830–845, 2017.

[23] A. K. Sharma, R. K. Singh, A. R. Dixit, and A. K. Tiwari, “Novel uses of alumina-

MoS₂ hybrid nanoparticle enriched cutting fluid in hard turning of AISI 304 steel,” *J. Manuf. Process.*, vol. 30, pp. 467–482, 2017.

[24] S. A. Lawal, “A review of application of vegetable oil-based cutting fluids in machining non-ferrous metals,” *Indian J. Sci. Technol.*, vol. 6, no. 1, pp. 3951–3956, 2013.

[25] S. A. Lawal, I. A. Choudhury, and Y. Nukman, “Application of vegetable oil-based metalworking fluids in machining ferrous metals - A review,” *Int. J. Mach. Tools Manuf.*, vol. 52, pp. 1–12, 2012.

[26] A. E. Diniz and R. Micaroni, “Cutting conditions for finish turning process aiming : the use of dry cutting,” *Int. J. Mach. Tools Manuf.*, vol. 42, pp. 899–904, 2016.

[27] A. E. Diniz and A. J. De Oliveira, “Optimizing the use of dry cutting in rough turning steel operations,” *Int. J. Mach. Tools Manuf.*, vol. 44, no. 10, pp. 1061–1067, 2004.

[28] A. Alok and M. Das, “Multi-objective optimization of cutting parameters during sustainable dry hard turning of AISI 52100 steel with newly develop HSN² - coated carbide insert,” *Measurement*, vol. 133, pp. 288–302, 2019.

[29] F. Pusavec, P. Krajnik, and J. Kopac, “Transitioning to sustainable production - Part I: application on machining technologies,” *J. Clean. Prod.*, vol. 18, no. 2, pp. 174–184, 2010.

[30] Z. Z. Shane Y. Hong, “Thermal aspects, material considerations and cooling strategies in cryogenic machining,” *Clean Prod. Process.*, vol. 1, pp. 107–116, 1999.

[31] Z. Y. Wang and K. P. Rajurkar, “Wear of CBN tool in turning of silicon nitride with cryogenic cooling,” *Int. J. Mach. Tools Manuf.*, vol. 37, no. 3, pp. 319–326, 1997.

[32] D. G. Thakur, B. Ramamoorthy, and L. Vijayaraghavan, “Optimization of Minimum Quantity Lubrication Parameters in High Speed Turning of Superalloy Inconel 718 for Sustainable Development,” *World Acad. Sci. Eng. Technol.*, vol. 54, pp. 224–226, 2009.

[33] Chetan, B. C. Behera, S. Ghosh, and P. V. Rao, “Application of nanofluids during minimum quantity lubrication: A case study in turning process,” *Tribol. Int.*, vol. 101, pp. 234–246, 2016.

[34] A. Uysal, F. Demiren, and E. Altan, “Applying Minimum Quantity Lubrication (MQL) Method on Milling of Martensitic Stainless Steel by Using Nano MoS₂ Reinforced Vegetable Cutting Fluid,” *Procedia - Soc. Behav. Sci.*, vol. 195, pp.

2742–2747, 2015.

[35] S. Pervaiz, I. Deiab, A. Rashid, and M. Nicolescu, “Minimal quantity cooling lubrication in turning of Ti6Al4V: Influence on surface roughness, cutting force and tool wear,” *Proc. Inst. Mech. Eng. Part B J. Eng. Manuf.*, vol. 231, no. 9, pp. 1542–1558, 2017.

[36] D. Setti, M. K. Sinha, S. Ghosh, and P. Venkateswara Rao, “Performance evaluation of Ti-6Al-4V grinding using chip formation and coefficient of friction under the influence of nanofluids,” *Int. J. Mach. Tools Manuf.*, vol. 88, pp. 237–248, 2015.

[37] S. B. Kedare, D. R. Borse, and P. T. Shahane, “Effect of Minimum Quantity Lubrication (MQL) on Surface Roughness of Mild Steel of 15HRC on Universal Milling Machine,” *Procedia Mater. Sci.*, vol. 6, pp. 150–153, 2014.

[38] M. Amrita, R. R. Srikant, and A. V. S. R. Raju, “Performance Evaluation and Economic Analysis of Minimum Quantity Lubrication with Pressurized / Non-Pressurized Air and Nanofluid Mixture,” *Int. J. Mech. Aerospace, Ind. Mechatron. Manuf. Eng.*, vol. 9, no. 6, pp. 1012–1017, 2015.

[39] A. Marques, C. Guimarães, R. Batista, C. Fonseca, W. F. Sales, and Á. R. Machado, “Surface Integrity Analysis of Inconel 718 after Turning with Different Solid Lubricants Dispersed in Neat Oil Delivered by MQL,” in *44th Proceedings of the North American Manufacturing Research Institution of SME*, 2016, vol. 5, pp. 609–620.

[40] S. Roy and A. Ghosh, “High Speed Turning of AISI 4140 Steel Using Nanofluid through Twin Jet SQL System,” in *proceedings of the ASME2013 Internationa Manufacturing Science and Engineering Conference MSEC2013*, 2013, no. June 2013, pp. 1–6.

[41] S. Shaji and V. Radhakrishnan, “An investigation on surface grinding using graphite as lubricant,” *Int. J. Mach. Tools Manuf.*, vol. 42, pp. 733–740, 2002.

[42] A. V. Gopal and P. Venkateswara Rao, “Performance improvement of grinding of SiC using graphite as a solid lubricant,” *Mater. Manuf. Process.*, vol. 19, no. 2, pp. 177–186, 2004.

[43] U. M. R. Paturi, Y. R. Maddu, R. R. Maruri, and S. K. R. Narala, “Measurement and Analysis of Surface Roughness in WS2 Solid Lubricant Assisted Minimum Quantity Lubrication (MQL) Turning of Inconel 718,” *Procedia CIRP*, vol. 40, pp. 138–143, 2016.

[44] B. Rahmati, A. A. D. Sarhan, and M. Sayuti, “Morphology of surface generated by end milling AL6061-T6 using molybdenum disulfide (MoS_2) nanolubrication in end milling machining,” *J. Clean. Prod.*, vol. 66, pp. 685–691, 2014.

[45] K. Sanjeev, S. Dilbag, and K. N.S, “Study the Performance of Solid Lubricants during Machining of Variable Hardened AISI 4340 Steel Using Grey-Fuzzy Approach,” *Int. J. Curr. Trends Sci. Technol.*, vol. 7, no. 10, pp. 20367–20380, 2017.

[46] R. K. Gunda and S. K. R. Narala, “Evaluation of friction and wear characteristics of electrostatic solid lubricant at different sliding conditions,” *Surf. Coatings Technol.*, vol. 332, no. July, pp. 341–350, 2017.

[47] P. Vamsi Krishna, R. R. Srikant, and D. Nageswara Rao, “Experimental investigation on the performance of nanoboric acid suspensions in SAE-40 and coconut oil during turning of AISI 1040 steel,” *Int. J. Mach. Tools Manuf.*, vol. 50, no. 10, pp. 911–916, 2010.

[48] N. Suresh Kumar Reddy and P. Venkateswara Rao, “Experimental investigation to study the effect of solid lubricants on cutting forces and surface quality in end milling,” *Int. J. Mach. Tools Manuf.*, vol. 46, pp. 189–198, 2005.

[49] D. N. Rao, P. V. Krishna, and R. R. Srikant, “Surface model and tool-wear prediction model for solid lubricant-assisted turning,” *Proc. Inst. Mech. Eng. Part J J. Eng. Tribol.*, vol. 222, no. 5, pp. 657–665, 2008.

[50] S. J. Ojolo, M. O. H. Amuda, O. Y. Ogunmola, and C. U. Ononiwu, “Experimental determination of the effect of some straight biological oils on cutting force during cylindrical turning,” *Rev. Matéria*, vol. 13, no. 4, pp. 650–663, 2008.

[51] M. A. Xavior and M. Adithan, “Determining the influence of cutting fluids on tool wear and surface roughness during turning of AISI 304 austenitic stainless steel,” *J. Mater. Process. Technol.*, vol. 209, no. 2, pp. 900–909, 2009.

[52] M. H. Cetin, B. Ozcelik, E. Kuram, and E. Demirbas, “Evaluation of vegetable based cutting fluids with extreme pressure and cutting parameters in turning of AISI 304L by Taguchi method,” *J. Clean. Prod.*, vol. 19, no. 17–18, pp. 2049–2056, 2011.

[53] B. S. Kumar, G. Padmanabhan, and P. V. Krishna, “Experimental investigations of vegetable oil based cutting fluids with extreme pressure additive in machining of AISI 1040 steel,” *Manuf. Sci. Technol.*, vol. 3, no. 1, pp. 1–9, 2015.

[54] C. M. Y. Wang, C. Li, Y. Zhang, M. Yang, B. Li, D. Jia, Y. Hou, "Experimental evaluation of the lubrication properties of the wheel/workpiece interface in minimum quantity lubrication (MQL) grinding using different types of vegetable oils," *J. Clean. Prod.*, vol. 127, pp. 487–499, 2016.

[55] R. R. Srikant and V. S. N. V. Ramana, "Performance evaluation of vegetable emulsifier based green cutting fluid in turning of American Iron and Steel Institute (AISI) 1040 steel - an initiative towards sustainable manufacturing," *J. Clean. Prod.*, vol. 108, pp. 104–109, 2015.

[56] B. Ozcelik, E. Kuram, M. Huseyin Cetin, and E. Demirbas, "Experimental investigations of vegetable based cutting fluids with extreme pressure during turning of AISI 304L," *Tribol. Int.*, vol. 44, no. 12, pp. 1864–1871, 2011.

[57] M. H. S. Elmunafî, D. Kurniawan, and M. Y. Noordin, "Use of castor oil as cutting fluid in machining of hardened stainless steel with minimum quantity of lubricant," *Procedia CIRP*, vol. 26, pp. 408–411, 2015.

[58] S. M. S. Murshed, K. C. Leong, and C. Yang, "Thermophysical and electrokinetic properties of nanofluids - A critical review," *Appl. Therm. Eng.*, vol. 28, no. 17–18, pp. 2109–2125, 2008.

[59] Y. Li, J. Zhou, S. Tung, E. Schneider, and S. Xi, "A review on development of nanofluid preparation and characterization," *Powder Technol.*, vol. 196, no. 2, pp. 89–101, 2009.

[60] A. Turgut, I. Tavman, and S. Tavman, "Measurement of thermal conductivity of edible oils using transient hot wire method," *Int. J. Food Prop.*, vol. 12, no. 4, pp. 741–747, 2009.

[61] B. Wei, C. Zou, and X. Li, "Experimental investigation on stability and thermal conductivity of diathermic oil based TiO₂ nanofluids," *Int. J. Heat Mass Transf.*, vol. 104, pp. 537–543, 2017.

[62] W. Yu, H. Xie, Y. Li, and L. Chen, "Particuology Experimental investigation on thermal conductivity and viscosity of aluminum nitride nanofluid," *Particuology J.*, vol. 9, no. 2, pp. 187–191, 2011.

[63] P. Krajnik, F. Pusavec, and A. Rashid, "Nanofluids : Properties , Applications and Sustainability Aspects in Materials Processing Technologies," *Adv. Sustain. Manuf.*, pp. 107–113, 2011.

[64] Y. Su, L. Gong, B. Li, and D. Chen, "An experimental investigation on thermal

properties of molybdenum disulfide nanofluids," in *International Conference on Materials, Environmental and Biological Engineering (MEBE 2015)*, 2015, pp. 881–885.

[65] B. Anil kumar naik and A. Venu Vinod, "Rheological Behavior and Effective Thermal conductivity of Non-Newtonian Nanofluids," *J. Test. Eval.*, vol. 46, no. 2, pp. 1–14, 2018.

[66] S. Suresh, K. P. Venkitaraj, P. Selvakumar, and M. Chandrasekar, "Synthesis of Al₂O₃ – Cu/water hybrid nanofluids using two step method and its thermo physical properties," *Colloids Surfaces A Physicochem. Eng. Asp.*, vol. 388, no. 1–3, pp. 41–48, 2011.

[67] T. X. Phuoc and M. Massoudi, "Experimental observations of the effects of shear rates and particle concentration on the viscosity of Fe₂O₃ – deionized water nanofluids," *Int. J. Therm. Sci.*, vol. 48, no. 7, pp. 1294–1301, 2009.

[68] S. K. Mechiri, V. Vasu, A. Venu Gopal, and R. Satish Babu, "Thermal Conductivity of Cu-Zn Hybrid Newtonian Nanofluids: Experimental Data and Modeling using Neural Network," *Procedia Eng.*, vol. 127, pp. 561–567, 2015.

[69] M. S. Kumar, V. Vasu, and A. V. Gopal, "Thermal Conductivity and Viscosity of Vegetable Oil-Based Cu, Zn, and Cu–Zn Hybrid Nanofluids," *J. Test. Eval.*, vol. 44, no. 3, pp. 1077–1083, 2016.

[70] Kalitha parash and P.Malshe A, "ribological study of nano lubricant integrated soybean oil for minimum quantity lubrication (MQL) grinding," *Trans. NAMRI/SME*, vol. 38, pp. 137–144, 2010.

[71] Y. Zhang, C. Li, D. Jia, D. Zhang, and X. Zhang, "Experimental evaluation of MoS₂nanoparticles in jet MQL grinding with different types of vegetable oil as base oil," *J. Clean. Prod.*, vol. 87, pp. 930–940, 2015.

[72] S. Khandekar, M. R. Sankar, V. Agnihotri, and J. Ramkumar, "Nano-cutting fluid for enhancement of metal cutting performance," *Mater. Manuf. Process.*, vol. 27, no. 9, pp. 963–967, 2012.

[73] R. A. Raju, A. Andhare, and N. K. Sahu, "Performance of multi-walled carbon nanotube- based nanofluid in turning operation," *Mater. Manuf. Process.*, vol. 32, no. 13, pp. 1490–1496, 2017.

[74] J. Dongzhou, M. Yan, C. Li, Y. Wang, S. Guo, and H. Cao, "Specific energy and surface roughness of minimum quantity lubrication grinding Ni- based alloy with

mixed vegetable oil-based nanofluids," *Precis. Eng.*, vol. 50, pp. 248–262, 2017.

[75] A. K. Sharma, J. K. Katiyar, S. Bhaumik, and S. Roy, "Influence of alumina/MWCNT hybrid nanoparticle additives on tribological properties of lubricants in turning operations," *Friction*, pp. 1–16, 2018.

[76] J. Nam, P.-H. Lee, and S. Won Lee, *Experimental characterization of micro-drilling process using nanofluid minimum quantity lubrication*, vol. 51. 2011.

[77] K. Park, B. Ewald, and Kwon.Patrick, "Effect of Nano-Enhanced Lubricant in Minimum Quantity Lubrication Balling Milling," *J. Tribol.*, vol. 133, no. July, pp. 1–8, 2011.

[78] V. Vasu and G. P. K. Reddy, "Effect of minimum quantity lubrication with Al_2O_3 nanoparticles on surface roughness , tool wear and temperature dissipation in machining Inconel 600 alloy," *Proc. Inst. Mech. Eng. Part N J. Nano Eng. Nano Syst.*, vol. 225, pp. 3–15, 2011.

[79] A. Zareie and M. Akbari, "Hybrid nanoparticles effects on rheological behavior of water-EG coolant under different temperatures: An experimental study," *J. Mol. Liq.*, vol. 230, pp. 408–414, 2017.

[80] M. R. Tanshen *et al.*, "Pressure distribution inside oscillating heat pipe charged with aqueous Al_2O_3 nanoparticles, MWCNTs and their hybrid," *J.Cent.South Univ.*, vol. 21, pp. 2341–2348, 2014.

[81] X. Zhang *et al.*, "Performances of $\text{Al}_2\text{O}_3/\text{SiC}$ hybrid nanofluids in minimum-quantity lubrication grinding," *Int. J. Adv. Manuf. Technol.*, vol. 86, no. 9–12, pp. 3427–3441, 2016.

[82] M. Sarikaya and A. Güllü, "Multi-response optimization of minimum quantity lubrication parameters using Taguchi-based grey relational analysis in turning of difficult-to-cut alloy Haynes 25," *J. Clean. Prod.*, vol. 91, pp. 347–357, 2015.

[83] R. Deepak Joel Johnson, K. L. D. Wins, A. Raj, and B. A. Beatrice, "Optimization of cutting parameters and fluid application parameters during turning of OHNS steel," *Procedia Eng.*, vol. 97, no. April, pp. 172–177, 2014.

[84] P. Rapeti, V. K. Pasam, K. M. Rao Gurram, and R. S. Revuru, "Performance evaluation of vegetable oil based nano cutting fluids in machining using grey relational analysis-A step towards sustainable manufacturing," *J. Clean. Prod.*, vol. 172, pp. 2862–2875, 2016.

[85] V. K. Pasam, S. B. Battula, P. Madar Valli, and M. Swapna, "Optimizing surface

finish in WEDM using the taguchi parameter design method," *J. Brazilian Soc. Mech. Sci. Eng.*, vol. 32, no. 2, pp. 107–113, 2010.

[86] P. J. Liew, A. Shaaroni, J. A. Razak, M. S. Kasim, and M. A. Sulaiman, "Optimization of cutting condition in the turning of AISI D2 steel by using carbon nanofiber nanofluid," *Int. J. Appl. Eng. Res.*, vol. 12, no. 10, pp. 2243–2252, 2017.

[87] C. J. Rao, D. N. Rao, and P. Srihari, "Influence of cutting parameters on cutting force and surface finish in turning operation," *Procedia Eng.*, vol. 64, pp. 1405–1415, 2013.

[88] M. Hemmat Esfe, M. Firouzi, H. Rostamian, and M. Afrand, "Prediction and optimization of thermophysical properties of stabilized Al₂O₃/antifreeze nanofluids using response surface methodology," *J. Mol. Liq.*, vol. 261, no. 2017, pp. 14–20, 2018.

[89] E. Montazer *et al.*, "Development of a new density correlation for carbon-based nanofluids using response surface methodology," *J. Therm. Anal. Calorim.*, vol. 132, no. 2, pp. 1399–1407, 2018.

[90] M. Hemmat Esfe, M. Kiannejad Amiri, and M. Bahiraei, "Optimizing thermophysical properties of nanofluids using response surface methodology and particle swarm optimization in a non-dominated sorting genetic algorithm," *J. Taiwan Inst. Chem. Eng.*, vol. 103, no. xxxx, pp. 7–19, 2019.

[91] M. K. Gupta and P. K. Sood, "Surface roughness measurements in NFMQL assisted turning of titanium alloys: An optimization approach," *Friction*, vol. 5, no. 2, pp. 155–170, 2017.

[92] S. Gugulothu, V. K. Pasam, and R. S. Revuru, "Machining Performance and Sustainability of Vegetable Oil based Nano Cutting Fluids in Turning," in *Proceedings of 10th international conference on Precision, Meso, Micro and Nano Engineering(COPEN)*, pp. 871–874.

[93] B. Salopek, D. Krasić, and S. Filipović, "Measurement and application of Zeta-potential," *Rud. Zb.*, vol. 4, no. 1, pp. 147–151, 1992.

[94] V. K. Pasam, R. S. Revuru, and S. Gugulothu, "Comparing the performance & viability of nano and microfluids in minimum quantity lubrication for machining AISI1040 steel," *Mater. Today Proc.*, vol. 5, no. 2, pp. 8016–8024, 2018.

[95] R. R. Srikant, M. M. S. Prasad, M. Amrita, A. V. Sitamaraju, and P. V. Krishna, "Nanofluids as a potential solution for Minimum Quantity Lubrication: A review,"

Proc. Inst. Mech. Eng. Part B J. Eng. Manuf., vol. 228, no. 1, pp. 3–20, 2014.

[96] M. Amrita, S. A. Shariq, M. Manoj, and C. Gopal, “Experimental investigation on application of emulsifier oil based nano cutting fluids in metal cutting process,” *Procedia Eng.*, vol. 97, pp. 115–124, 2014.

[97] P.V. Krishna, R.R. Srikant, and N. Parimala, “Experimental Investigation on Properties and Machining Performance of CNT Suspended Vegetable oil Nanofluids,” *International journal of Automotive and Mechanical Engineering.*, vol. 15, no.4, pp. 5957–5975, 2018.

[98] S. B. Rao, “Tool Wear Monitoring Through the Dynamics of Stable Turning,” *J. Eng. Ind.*, vol. 108, no. 3, pp. 183–190, 1986.

[99] B. Fathi-Achachlouei and S. Azadmard-Damirchi, “Milk thistle seed oil constituents from different varieties grown in Iran,” *J. Am. Oil Chem. Soc.*, vol. 86, no. 7, pp. 643–649, 2009.

[100] M. Hassan El-Mallah, S. M. El-Shami, and M. M. Hassanein, “Detailed studies on some lipids of *Silybum marianum*(L.) seed oil,” *Grasas y Aceites*, vol. 54, no. 4, pp. 397–402, 2003.

[101] A. Kamal-Eldin and R. Andersson, “A multivariate study of the correlation between tocopherol content and fatty acid composition in vegetable oils,” *J. Am. Oil Chem. Soc.*, vol. 74, no. 4, pp. 375–380, 1997.

[102] G. Karmakar, P. Ghosh, and B. Sharma, “Chemically Modifying Vegetable Oils to Prepare Green Lubricants,” *Lubricants*, vol. 5, no. 4, pp. 1–17, 2017.

[103] C. M. Rodenbush, F. H. Hsieh, and D. S. Viswanath, “Density and viscosity of vegetable oils,” *J. Am. Oil Chem. Soc.*, vol. 76, no. 12, pp. 1415–1419, 1999.

[104] C. T. Nguyen *et al.*, “Temperature and particle-size dependent viscosity data for water-based nanofluids - Hysteresis phenomenon,” *Int. J. Heat Fluid Flow*, vol. 28, no. 6, pp. 1492–1506, 2007.

[105] A. Ghadimi, R. Saidur, and H. S. C. Metselaar, “A review of nanofluid stability properties and characterization in stationary conditions,” *Int. J. Heat Mass Transf.*, vol. 54, no. 17–18, pp. 4051–4068, 2011.

[106] S. Mukherjee, “Preparation and Stability of Nanofluids-A Review,” *IOSR J. Mech. Civ. Eng.*, vol. 9, no. 2, pp. 63–69, 2013.

[107] K. Kouloulias, A. Sergis, and Y. Hardalupas, “Sedimentation in nanofluids during a natural convection experiment,” *Int. J. Heat Mass Transf.*, vol. 101, pp. 1193–1203,

2016.

- [108] M. Venkataraman, “The effect of colloidal stability on the heat transfer characteristics of nanosilica dispersed fluids,” in *M.Sc. Thesis, University of Central Florida Orlando, Florida*, 2005, pp. 1–93.
- [109] M. A. Safi, A. Ghozatloo, and A. A. Hamidi, “Preparation of MWNT/TiO₂ Nanofluids and Study of its Thermal Conductivity and Stability,” *Iran. J. Chem. Eng.*, vol. 11, no. 4, pp. 3–9, 2014.
- [110] L. Vaisman, H. D. Wagner, and G. Marom, “The role of surfactants in dispersion of carbon nanotubes,” *Adv. Colloid Interface Sci.*, vol. 128–130, pp. 37–46, 2006.
- [111] F. Niyaghi, K. R. Haapala, S. L. Harper, and M. C. Weismiller, “Stability and Biological Responses of Zinc Oxide Metalworking Nanofluids (ZnO MWnFTM) using Dynamic Light Scattering and Zebrafish Assays,” *Tribol. Trans.*, vol. 57, no. 4, pp. 730–739, 2014.
- [112] N. Ali, J. A. Teixeira, and A. Addali, “A Review on Nanofluids: Fabrication, Stability, and Thermophysical Properties,” *J. Nanomater.*, vol. 2018, pp. 1–33, 2018.
- [113] S. A. Lawal, I. A. Choudhury, and Y. Nukman, “Application of vegetable oil-based metalworking fluids in machining ferrous metals - A review,” *Int. J. Mach. Tools Manuf.*, vol. 52, no. 1, pp. 1–12, 2012.
- [114] S. Johnson and N. Saikia, “Fatty acids profile of Edible Oils and Fats in India,” *Pollut. Monit. Lab. Cent. Sci. Environ.*, pp. 1–33, 2009.
- [115] D. K. Devendiran and V. A. Amirtham, “A review on preparation, characterization, properties and applications of nanofluids,” *Renew. Sustain. Energy Rev.*, vol. 60, pp. 21–40, 2016.
- [116] S. K. Dwivedi, *Application of Nanofluid Lubrication during machining of Aeroengine grade stainless steel*. 2015.
- [117] Y. Zhang, C. Li, D. Jia, D. Zhang, and X. Zhang, “Experimental evaluation of MoS₂nanoparticles in jet MQL grinding with different types of vegetable oil as base oil,” *J. Clean. Prod.*, vol. 87, pp. 930–940, 2015.
- [118] A. Eltaggaz, H. Hegab, I. Deiab, and H. A. Kishawy, “Hybrid nano-fluid-minimum quantity lubrication strategy for machining austempered ductile iron (ADI),” *Int. J. Interact. Des. Manuf.*, vol. 12, no. 4, pp. 1273–1281, 2018.
- [119] S. Y. Hong and M. Broomer, “Economical and ecological cryogenic machining of

AISI304 austenitic stainless steel,” *Clean Prod. Process.*, vol. 2, pp. 157–166, 2000.

[120] H. Xie, B. Jiang, B. Liu, Q. Wang, J. Xu, and F. Pan, “An Investigation on the Tribological Performances of the SiO_2 / MoS_2 Hybrid Nanofluids for Magnesium Alloy-Steel Contacts,” *Nanoscale Res. Lett.*, vol. 11, no. 1, pp. 1–17, 2016.

[121] B. Shen, A. J. Shih, and S. C. Tung, “Application of nanofluids in minimum quantity lubrication grinding,” *Tribol. Trans.*, vol. 51, no. 6, pp. 730–737, 2008.

[122] Y. bin Zhang *et al.*, “Experimental study on the effect of nanoparticle concentration on the lubricating property of nanofluids for MQL grinding of Ni-based alloy,” *J. Mater. Process. Technol.*, vol. 232, no. 2016, pp. 100–115, 2016.

[123] T. A. El-tawee and S. A. Gouda, “Performance analysis of wire electrochemical turning process — RSM approach,” *Int. jour Adv. Manuf. Technol.*, vol. 53, pp. 181–190, 2011.

[124] S. Gopalakannan and T. Senthilvelan, “Optimization of machining parameters for EDM operations based on central composite design and desirability approach,” *J. Mech. Sci. Technol.*, vol. 28, no. 3, pp. 1045–1053, 2014.

Publications from the present work

1. Srinu Gugulothu, Vamsi Krishna Pasam, “Testing and Performance Evaluation of Vegetable oil Based Hybrid Nano cutting fluids,” *Journal of testing and Evaluation*, 2018, 48(5), ASTM publications (SCI).
2. Srinu Gugulothu, Vamsi Krishna Pasam, “Optimizing multi-response parameters in turning of AISI1040 steel using Desirability approach”, *International Journal of Mathematical, Engineering and Management Sciences*, 2019, 4(4), 905-921 IJMEMS publications, Scopus.
3. Srinu Gugulothu, Vamsi Krishna Pasam, “Performance evaluation of CNT/ MoS_2 hybrid nanofluids for Surface roughness in machining”, *International Journal of Automotive and Mechanical Engineering (IJAME)*, 2019, UMP publications, Scopus & ESCI (Accepted).
4. Srinu Gugulothu, Vamsi Krishna Pasam, “Experimental investigation to study the performance of CNT/ MoS_2 Hybrid nanofluid in Turning of AISI1040 steel”, *Australian Journal of Mechanical Engineering*, 2018, Taylor and Francis publications, Scopus & ESCI (Under Review).